NUREG/CR—3538
SAND83—1258
RV
Printed October 1983

The Effect of LOCA Simulation Procedures on Ethylene Propylene Rubber's Mechanical and Electrical Properties

Larry D. Bustard

Prepared by
Sandia National Laboratories
Albuquerque, New Mexico 87185 and Livermore, California 94550
for the United States Department of Energy
under Contract DE-AC04-76DP00789

Prepared for
U. S. NUCLEAR REGULATORY COMMISSION

Available from

GPO Sales Program
Division of Technical Information and Document Control
U.S. Nuclear Regulatory Commission
Washington, D.C. 20555

and

National Technical Information Service
Springfield, Virginia 22161

NUREG/CR-3538
SAND83-1258
RV

THE EFFECT OF LOCA SIMULATION PROCEDURES ON ETHYLENE PROPYLENE RUBBER'S MECHANICAL AND ELECTRICAL PROPERTIES

L. D. Bustard

Printed: October 1983

Sandia National Laboratories
Albuquerque, New Mexico 87185
Operated by
Sandia Corporation
for the
U.S. Department of Energy

Prepared for
Electrical Engineering Branch
Division of Engineering Technology
Office of Nuclear Regulatory Research
U.S. Nuclear Regulatory Commission
Washington, DC 20555
Under Interagency Agreement 40-550-75
NRC FIN No. A-1051

Abstract

Electrical and mechanical properties of several commercial ethylene-propylene rubber (EPR) materials, typically used as electrical cable insulation, have been monitored during three simulations of nuclear power plant aging and accident stresses. For one set of cables and separate tensile specimens we did a sequential test. We first performed accelerated thermal aging, then irradiated the samples to the combined aging and LOCA total dose. Finally we applied a steam exposure. For a second and third set of cables and separate tensile specimens we used simultaneous applications of elevated temperature and radiation stresses to preaccident age our specimens. We followed these aging exposures by simultaneous radiation and steam exposures to simulate a LOCA environment.

Our measurement parameters during these tests included: dc insulation resistance, ac leakage current, ultimate tensile strength, ultimate tensile elongation, percentage dimensional changes, and percentage moisture absorption. We present test results for nine EPR materials. The implications of our research results for future cable qualification testing efforts is discussed.

Contents

Preceding page blank

Contents

List of Figures

List of Figures

List of Figures

List of Tables

List of Tables

List of Tables

Acknowledgments

My appreciation is extended to all those who contributed to this research effort. John Lewin, Tim Gilmore, and Jack Bartberger ably assisted throughout the experimental program. Mike Luker and Jerry Seitz helped perform simultaneous test #2. I thank Frank Thome for his assistance during development of the thermal aging techniques and Bill Buckalew for his help with radiation mapping. Ed Salazar, Roger Clough, and Ken Gillen's polymer expertise was extremely valuable. I thank the many attendees of the IEEE-ICC meeting in Memphis, April 25-27, 1983 for their comments and suggestions concerning my research results. Finally, I extend my appreciation to Karen Palmer for typing this report.

KEYWORDS

CPE	- Chlorinated polyethylene; a jacket material employed in one of the multiconductor constructions
CSPE	- Chlorosulfonated polyethylene; a jacket material employed in several of the single conductor and multiconductor constructions
Desorbed	- To lose moisture content
e	- Ultimate tensile elongation
EPDM	- Ethylene-propylene-diene terpolymer elastomer; commonly referred to by the more generic description ethylene-propylene rubber, EPR
EPR	- Ethylene-propylene rubber. Includes ethylene-propylene copolymer, EPM, and ethylene-propylene-diene terpolymer, EPDM, as subsets.
FR-EPDM	- Ethylene-propylene-diene terpolymer elastomer which includes fire-retardant ingredients. Commonly referred to by the more generic description ethylene-propylene rubber, EPR.
HIACA	- High Intensity Adjustable Cobalt Array. A Sandia National Laboratories' irradiation facility capable of producing a simultaneous radiation, steam, and chemical spray exposure or a simultaneous radiation and elevated temperature exposure.
HYPALON	- Trade name of DuPont for chlorosulfonated polyethylene, CSPE.
IEEE	- The Institute of Electrical and Electronics Engineers.
Insulation Specimens	- Insulation samples used to monitor dimensional and weight changes as well as to measure the ultimate tensile elongation and the ultimate tensil strength.
I.R.	- Insulation resistance. During our measurements the bulk resistivity is monitored; surface currents are shunted past the ammeter using a guarding circuit.
LICA	- Low Intensity Cobalt Array. A Sandia National Laboratories' irradiation facility capable of producing a simultaneous radiation and elevated temperature exposure.

LOCA	- Loss of Coolant Accident; a hypothesized design basis event for nuclear power plants.
Sequential Test	- A sequential exposure to elevated temperature followed by irradiation followed by a steam exposure. Our sequential test did not include chemical spray during the steam exposure. Oxygen was swept from the chamber at the start of the steam exposure.
Simultaneous Test #1	- A simultaneous exposure to radiation and elevated temperature followed by a simultaneous exposure to radiation and steam. Our test did not include chemical spray. Oxygen was swept from the chamber at the start of the steam exposure.
Simultaneous Test #2	- An exposure similar to simultaneous test #1.
T	- Ultimate tensile strength.
Tap Water	- Water used for immersing cables during some insulation resistance and all voltage withstand tests. Water obtained from Sandia Area V water supply. For simultaneous test #2, post-test measurements, the water conductivity was 360 mmhos/cm.
TEFZEL	- Trade name of DuPont for a copolymer of ethylene and tetrafluoroethylene.
Tensile Specimens	- Insulation samples used to monitor dimensional and weight changes as well as to measure the ultimate tensile elongation and the ultimate tensile strength.
Voltage Withstand Test	- Part of the acceptance criteria specified by IEEE Std. 383-1974, Sections 2.3.3.4 and 2.4.4.
Ultimate Tensile Elongation	- The strain at which a tensile specimen fails.
Ultimate Tensile Strength	- The stress at which a tensile specimen fails.
XLPE	- Cross-linked polyethylene.
XLPO	- Cross-linked polyolefin.

Executive Summary

Electrical and mechanical properties of seven commercial ethylene-propylene rubber (EPR) materials, typically used as electrical cable insulation, have been monitored during three simulations of nuclear power plant aging and accident stresses. Mechanical properties for two additional EPR materials were also investigated. For one set of cables and separate tensile specimens we first performed accelerated thermal aging, then irradiated the samples to the combined aging and LOCA total dose. Finally we applied a steam exposure. For a second and third set of cables and separate tensile specimens we used simultaneous applications of elevated temperature and radiation stresses to preaccident age our specimens. We followed these aging exposures by simultaneous radiation and steam exposures to simulate a LOCA environment.

For EPR A multiconductor cables we did not observe electrical performance variations caused by differences between our simultaneous and sequential test procedures. Insulation resistance, I.R., was monitored periodically during the test exposures. A voltage withstand test was performed upon completion of the accident simulations. During this latter test the leakage current was measured. An observable electrical performance difference was noted for the EPR E multiconductor cable. For the sequentially exposed EPR E cables we were unable at the start of the LOCA simulation to make I.R. measurements at 500 Vdc. The I.R. values were less than the lowest instrument reading, namely 1 MΩ. After reducing the applied voltage to 50 Vdc we did measure normalized I.R. values of ∿ 2 MΩ-m. In contrast, the simultaneously exposed multiconductor EPR E cable had a normalized I.R. value of 37 MΩ-m at 500 Vdc. The post-test leakage current values were similar for both the simultaneous and sequentially exposed EPR E cables.

An EPR C multiconductor cable was exposed to the first simultaneous test environmental conditions only. The normalized I.R. values were greater than 3000 MΩ-m throughout the test. The post-test leakage current was less than 5 mA during a voltage withstand test of 80 Vac per mil of insulation thickness.

Electrical performance of our EPR D multiconductors depended strongly on LOCA simulation techniques. Both electrically and visually the simultaneously exposed EPR D multiconductor cables were worse than the sequentially exposed multiconductor cables. An example is provided by the post-LOCA leakage current data. At 600 Vac, the sequentially exposed multiconductor had leakage currents of ∿ 1 mA. In contrast, the simultaneously exposed multiconductors had leakage currents of several hundred milliamps.

We postulate that a jacket-insulation interaction effect contributed to the degradation of EPR D during our simultaneous tests. The EPR D insulation dimensionally swelled producing

splitting of the jacket. We hypothesize that the jacket splitting resulted in a sudden release of constrictive force on the insulators allowing cracking or breakup of the insulation. Ultimate tensile elongation measurements performed on EPR D tensile specimens suggest that by the completion of the LOCA simulation the insulation ultimate elongation was comparable to the calculated strain caused by the multiconductor geometry. Hence insulation cracking might be expected. Alternatively, sections of the insulation which adhered to the jacket during the splitting were pulled away from the conductor. Both variations of this jacket-insulation interaction hypothesis are consistent with the observed bare copper conductors evident at the completion of our second simultaneous test on EPR D multiconductors.

We present two additional hypotheses for completeness but consider them less acceptable as explanations for EPR D's behavior: (1) A jacket-insulation chemical interaction effect such as evolution of HCL from the jacket and resultant interaction with the EPR D insulation. (2) Dimensional swelling of the EPR D single conductors spirally wound around each other in a multiconductor geometry resulted in stress buildup. We note that the copper conductors would not expand sufficiently to accommodate the observed swelling of the insulation.

For insulated single conductors we do not observe large electrical performance variations caused by differences between our simultaneous and sequential test procedures. EPR A, B, D, and E are examples. EPR C, F, and G insulated single conductors were only exposed to simultaneous testing environmental conditions. For each of these single conductors the I.R. and leakage current behavior was similar to that observed for the EPR A, B, D, and E single conductors.

The simultaneously exposed EPR D single conductors performed substantially better than did their multiconductor counterparts. We hypothesize that the excellent single conductor behavior resulted from (1) the absence of jacket-insulation interaction effects and/or (2) the less severe bending of the single conductor specimens compared to the multiconductor test specimens. The single conductor specimens, unlike the multiconductor insulated conductors, did not have a "helical" bend component associated with the multiconductor geometry. Hence the insulation strain was less.

During our tests we extensively monitored mechanical properties for several of the EPR insulations. Tensile properties, moisture absorption, and dimensional changes were measured. Our results clearly indicate that EPR cannot be considered to have generic behavior with respect to these parameters.

We conclude that:

1. Future EPR cable qualification tests should not employ single conductor test specimens to establish qualification for multiconductors. Both jacket-insulation interaction effects and helicity of multiconductor geometries need to be considered in a qualification program.

2. EPR cable qualification tests should correlate test conditions to use conditions. An example is the test bend radius used for a qualification test and the minimum bend radius used during cable installation.

3. EPR qualification tests or analysis should not rely on referenced behavior of other different EPR products. We observed a large variation in EPR behavior; generic EPR response does not occur.

4. Some EPR qualification tests need not employ simultaneous thermal, radiation, and steam test conditions. EPR C provides an example of a cable product for which simultaneous testing procedures are currently not warranted. In contrast, EPR D multiconductor cable is a product for which our simultaneous testing techniques produced more cable damage than our sequential procedures.

We recommend that research tests need to establish why some EPR materials experienced more degradation than others. Without this information we can only report which aging and accident test procedures most severely degrade various EPR products but cannot begin to understand which test procedures most realistically simulate aging and accident environments. This last research goal may be impossible because proprietary issues associated with cable production and EPR formulations will make progress in this research area difficult.

1.0 INTRODUCTION

Ethylene-propylene-diene terpolymer (EPDM) and ethylene-propylene copolymer (EPM) are elastomer materials used to formulate certain cable insulations. Insulations based on EPDM and EPM are typically called either ethylene-propylene (EP) or ethylene-propylene-rubber (EPR) and are used in some electrical cabling in nuclear power plants.

When used as part of a safety-related system the EPR electrical cable must be qualified.[1-4] Type testing is the preferred qualification method.[2] NUREG-0588, Rev. 1,[2] a Nuclear Regulatory Commission (NRC) report entitled "Interim Staff Position on Environmental Qualification of Safety-Related Electrical Equipment" indicates that when "significant radiation and temperature environments may be present... the synergistic effects to these parameters should be considered during the simulated aging portion of the overall test sequence. The testing sequence used to age the equipment (or material) should be justified and the basis documented in the qualification report."[2] IEEE Standards 323-1974[3] and 383-1974[4] do not require cable qualification tests to employ simultaneous exposures to simulate accident and age stress environments. Rather, a sequential exposure to stresses is allowed.

As part of an NRC sponsored research program, we are investigating whether qualification test results are sensitive to the order of aging and accident stress application. We are also investigating the importance of simultaneous versus sequential stress exposures.

Previous research has started to address these issues. Thome[5] compares for one EPR multiconductor and one EPR single conductor electrical behavior for both simultaneous and sequential aging and accident test procedures. He reports that no significant synergisms exist. Yoshida, et al.,[6] compared for EPR tensile properties simultaneous and sequential LOCA testing methods. They concluded that the ultimate tensile elongation was sensitive to total dose, but not to the testing technique. The ultimate tensile strength was sensitive to the LOCA simulation technique with the radiation followed by steam exposure most severe. Ling and Morrison[7] exposed EPR multiconductor and single conductor cables to a simultaneous LOCA exposure. They report satisfactory cable performance during and after the exposures. Prior to performing these accident exposure, both Yoshida et al., and Ling and Morrison aged their specimens using a seven day 121°C thermal exposure followed by a 50 Mrd irradiation dose. Thome employed a 5 day 130°C, .2 Mrd/h simultaneous aging exposure.

Concurrent with this research was the development of newer EPDM compounds with reduced wall thicknesses for insulated conductors.[8] These newer compounds (commonly referred to as

/

FR-EPDM compounds) eliminated the need for a composite construction utilizing a separate jacket over each insulated conductor. Flame retardancy was achieved by incorporating fire-retardants into the insulation formulation rather than the jacket formulation. Several manufacturers currently market FR-EPDM's for nuclear use. Neither Thome nor Ling and Morrison included FR-EPDM cables in their simultaneous tests. (Yoshida, et al., does not identify whether FR-EPDM's were tested.)

In a recent publication[9] we reported EPR's cable tensile properties at the completion of accelerated aging. We concluded that defining a single test procedure for nuclear safety-related qualification of EPR elastomers is difficult and that a common worst-case sequential aging sequence could not be identified. We have recently extended this work to include electrical and tensile property behavior of EPR materials during LOCA research tests. This report documents the test results for three LOCA simulations.

The first LOCA simulation included sequential elevated temperature followed by radiation aging exposures, the accelerated aging portion of the test was followed by a sequential accident irradiation and then a 21 day LOCA steam exposure. The second and third LOCA simulations both employed simultaneous exposures for both the accelerated aging and accident simulations. Two simultaneous tests were performed so that an unexpected result of the first simultaneous test could be verified. Also, additional EPR materials not available for the first simultaneous test were included in the second test.

During all tests several commercial EPR products were exposed to aging and LOCA environments. This practice insures that test conclusions for one particular EPR cable product are not indiscriminately applied to all EPR products. By testing several products we hoped to differentiate between generic EPR conclusions and specific product conclusions. Our LOCA research test results illustrate the difficulty associated with defining a single generic qualification test procedure for all EPR cables. For several of the EPR cables we tested, the electrical properties were the same for both sequential and simultaneous LOCA research simulations. For one EPR cable product, EPR D, the electrical performance depended on whether sequential or simultaneous exposure procedures were employed. For this multiconductor cable, the simultaneous exposure technique produced worse electrical performance than did the sequential exposure technique. Surprisingly, electrical properties for the same insulation configured as a single conductor did not depend on exposure technique.

2.0 EXPERIMENTAL

2.1 Materials*

We tested seven commercial EPR products obtained from three different manufacturers:

EPR A: A three conductor control cable with an EPR insulation. Each conductor was individually jacketed with CSPE. The cable satisfied IEEE Std 383-1974.[4] The cable was purchased from the manufacturer by Sandia National Laboratories in 1977.

EPR A': The same product name and manufacturer as EPR A. The cable satisfied IEEE Std 383-1974.[4] The cable was purchased from the manufacturer by Sandia National Laboratories in 1981.

EPR B: A single conductor low voltage power cable with an EPR insulation covered with a CSPE jacket. The cable met the requirements of IEEE Std 383-1974.[3] The cable was purchased from the manufacturer by Sandia National Laboratories in 1981.

EPR C: A two conductor instrumentation cable with a flame-retardant EPR insulation. Each conductor was not individually jacketed. This cable was nuclear qualified for LOCA conditions according to suggestions of IEEE Std 323-1974[3] (qualification test report on file). The cable was purchased from the manufacturer by Sandia National Laboratories in 1981.

EPR D: A three conductor control cable with a flame-retardant EPR insulation formulation. Each conductor was not individually jacketed. The cable met the requirements of IEEE Std 383-1974.[4] This cable was purchased from the manufacturer by Sandia National Laboratories in 1981.

EPR E: A two conductor instrumentation cable with an EPR insulation. Each conductor was individually jacketed with CSPE. Recommended practices of IEEE Std 323-1974[3] were used to develop a qualification test (qualification test report on file). This cable was purchased from the manufacturer by Sandia National Laboratories in 1981.

EPR F: A single conductor 600V power and control cable with a flame-retardant EPR insulation. The cable met the requirements of IEEE Std 383-1974[4] This cable was purchased from the manufacturer by Sandia National Laboratories in 1982.

*Additional TEFZEL and cross-linked polyolefin cables were also tested. Results will be published in separate reports.

EPR G: A single conductor 600V power and control cable employing an EPR insulation covered with a CSPE jacket. The cable insulation met the requirements of IEEE Std 383.[3] This cable was purchased from the manufacturer by Sandia National Laboratories in 1982.

Our research program performed LOCA research tests on:

1. Cables as received from the factory.

2. Single conductors with primary EPR insulation and CSPE jacket (EPR A, E). These conductors were obtained by carefully removing the multiconductor outer jacket and sheaths and then separating the individual conductors from each other.

3. Single conductors with primary insulation only (EPR A, B, C, and D). These conductors were obtained by carefully removing the multiconductor outer jacket and sheaths and then separating the individual conductors from each other. For EPR A the primary jacket was then also carefully stripped from the insulators and conductor.

4. Tensile specimens (EPR A, B, C, D, E, F). For EPR A, B, D, and F prior to aging we removed jackets and sheaths from EPR insulated conductors and then carefully stripped the insulation from stranded copper conductors. For EPR C and E we obtained sheets of the EPR insulation from the cable manufacturers and cut the sheets into strips.

In addition to the commercial cable materials, we tested an EPR formulation used in Sandia National Laboratories fire-retardant aging studies[10,11] and a fire-retardant EPDM formulation used in Japanese research tests. The first formulation has been coded by Burke Industries* as 1483 EPR (Table 2.1).

*2250 South 10th Street, San Jose, CA 95112

Components	Constituents	Amount (Parts/Hundred) Rubber
Base Compound	Nordel 2722 EPDM	90
	DYNH #1 LDPE	20
	ZnO (zinc oxide)	5
	Parafin wax	5
	Zn salt of mercaptobenzimidazole (ZMB)	2
	Low-temperature reaction product of acetone and diphenzlamine (Aminox)	1
	Treated, calcined clay	60
	Vinyl-silane coagent	1
	SRF (soft reinforcing furnace) black	2
Curing Package	Litharge	5
	Dicumyl peroxide (Di-Cup R)	5
Fire-Retardant Package	Dechlorane plus 25	33
	Antimony trioxide Sb_2O_3	12

Table 2-1. Ethylene Propylene Rubber Formulation (1483 EPR)

The base compound was prepared by Burke Industries. Curing and flame-retardant ingredients were added to the base compound by the Plastics Shop at Sandia National Laboratories. A two-roll mill was used to add the curing and flame-retardant ingredients to the EPR base compound. The rubber was then molded in a flashing mold and cured for 10 minutes at 177°C (350°F). The sheets of EPR were cut into predetermined-size stripes (2.8 mm x 6.4 mm x 152 mm) using a stainless steel die.

EPR-1483 is similar to compositions A and B given by Vaidya.[8] Candidate formulations "very similar to A and B have been qualified for reduced wall nuclear control cable and instrument wire following IEEE-383 type testing, and are in commercial use."[8]

The Japanese EPDM insulation material was supplied to us by Dr. T. Seguchi of the Japan Atomic Energy Research Institute. Coded as EPR-5, it is a commercial chemically cross-linked fire-retardant EPDM insulation material. We cut the compression molded sheets into strip tensile specimens.

2.2 Facilities

We used three Sandia National Laboratories facilities to expose our samples to aging and accident environments. We used the Low Intensity Cobalt Array (LICA) facility[12,13] for EPR A and EPR-1483 tensile specimen radiation aging exposures at both ambient and elevated temperatures. During these exposures we provided fresh air to the test chambers at a rate of 60 ± 20 cc/min. The volume of each LICA chamber is approximately 1.8 liters.

We performed single stress elevated temperature exposures on EPR A and EPR-1483 tensile specimens using the thermal aging facilities developed by K. T. Gillen, R. L. Clough, and L. H. Jones.[12,13] This facility uses self-contained aging cells inside air circulating ovens. Fresh air flow to each aging cell is independently controlled and was set to 60 ± 20 cc/min for the 0.9 liter aging cell.

The High Intensity Adjustable Cobalt Array (HIACA) facility was used for aging of EPR cables and some of the EPR tensile specimens. All accident simulations for both cables and tensile specimens were performed using the HIACA facility. Figure 2.1 schematically illustrates one aspect of this facility. For our simultaneous aging and accident environmental exposures a stainless steel steam chamber was positioned inside the gamma irradiation facility. After either steam or heated air was introduced into the chamber, cobalt pencils were raised to a position around the chamber to provide the desired simultaneous radiation and steam or elevated temperature environments.

The radiation capabilities of the HIACA facility have been previously documented.[14]

Thermal aging was performed using the stainless steel steam chambers as ovens. A Chromalox Series 4231 SCR Power and Temperature Controller was used to regulate a 20 kw heater. Air circulation between the heater and chamber was maintained by four Dayton 100W Model 4C005 fans. For the second simultaneous aging exposure the Dayton fans were replaced by a single 1.5 kw (2 HP) Paxton model RM87 blower. Valves in the recirculation line provided fresh air input to insure oxygen supply throughout the thermal aging exposure. A Kurz Air Velocity Meter, Model 441 was used to monitor recirculating and fresh air flow rates to the chamber. This allowed us to calculate the amount of fresh air supplied to the chamber.

The steam system utilizes a 4.5 kw (6 HP) electric boiler which is too small to achieve the rise time requirements of LOCA testing. We store energy from the boiler in two 0.6 m^3 accumulators from which the steam is valved either to the steam chamber inside the gamma irradiation cell or to a chamber outside the irradiation cell. Alternatively, the steam can be valved to both chambers simultaneously.

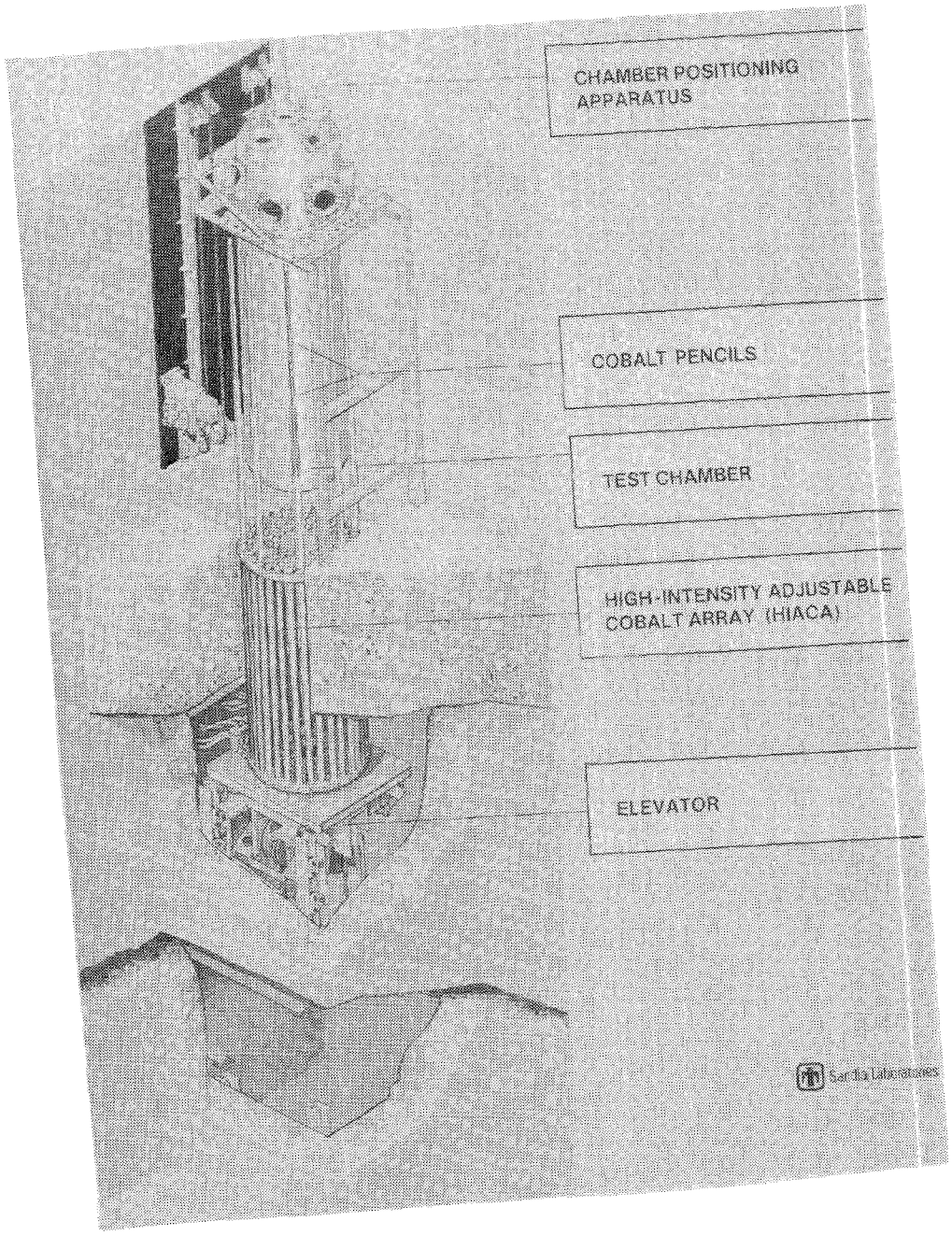

Figure 2.1. HIACA Test Facility

An Instrom^{tm} testing machine with pneumatic jaws was used to measure sample ultimate tensile strength and ultimate tensile elongation. Initial jaw separation was 50.8 mm (2 in); the samples were strained at 127 mm/min (5 in/min). An Instrom^{tm} electrical tape extensometer clamped to the sample monitored the strain.

A Hipotronics HM3A Megohmmeter was used for insulation resistance measurements. A Hipotronics HD100 Hipot Tester and a Hipotronics 715-10 Type CS14-1630 AC Dielectric Test Set were used to monitor leakage current versus applied AC voltage. The first tester was used whenever leakage currents were between 0 and 5 mA; the latter tester was used to determine leakage currents between 10 and 750 mA.

Emission spectroscopy, and chlorine and bromine content analysis were performed by Huffman Laboratories*. Details are given in Appendix B.

2.3 Procedures

2.3.1 Overview

Figure 2.2 illustrates the experimental sequence used to test EPR cables and tensile specimens. Our experimental strategy was based on the use of two steam chambers. Cables and tensile specimens in one chamber were exposed sequentially to elevated temperature, radiation aging, and accident stresses. Cables and tensile specimens in the second chamber were exposed to a simultaneous radiation and elevated temperature accelerated aging environment. The two chambers were then connected in parallel to the steam supply system and were exposed to a 21-day accident steam profile. One of the chambers was simultaneously irradiated during the steam exposure.

EPR A and EPR 1483 tensile specimens which had been aged in the LICA facility using seven different aging methods were inserted into the stainless steel chambers at appropriate test points. Hence for each of the seven aging populations, one-third of the tensile specimens were exposed to one of three accident simulations:

1. sequential accident irradiation followed by a steam exposure
2. simultaneous accident radiation and steam exposure
3. steam exposure only

*3830 High Court, P.O. Box 777, Wheat Ridge, Colorado, 80034.

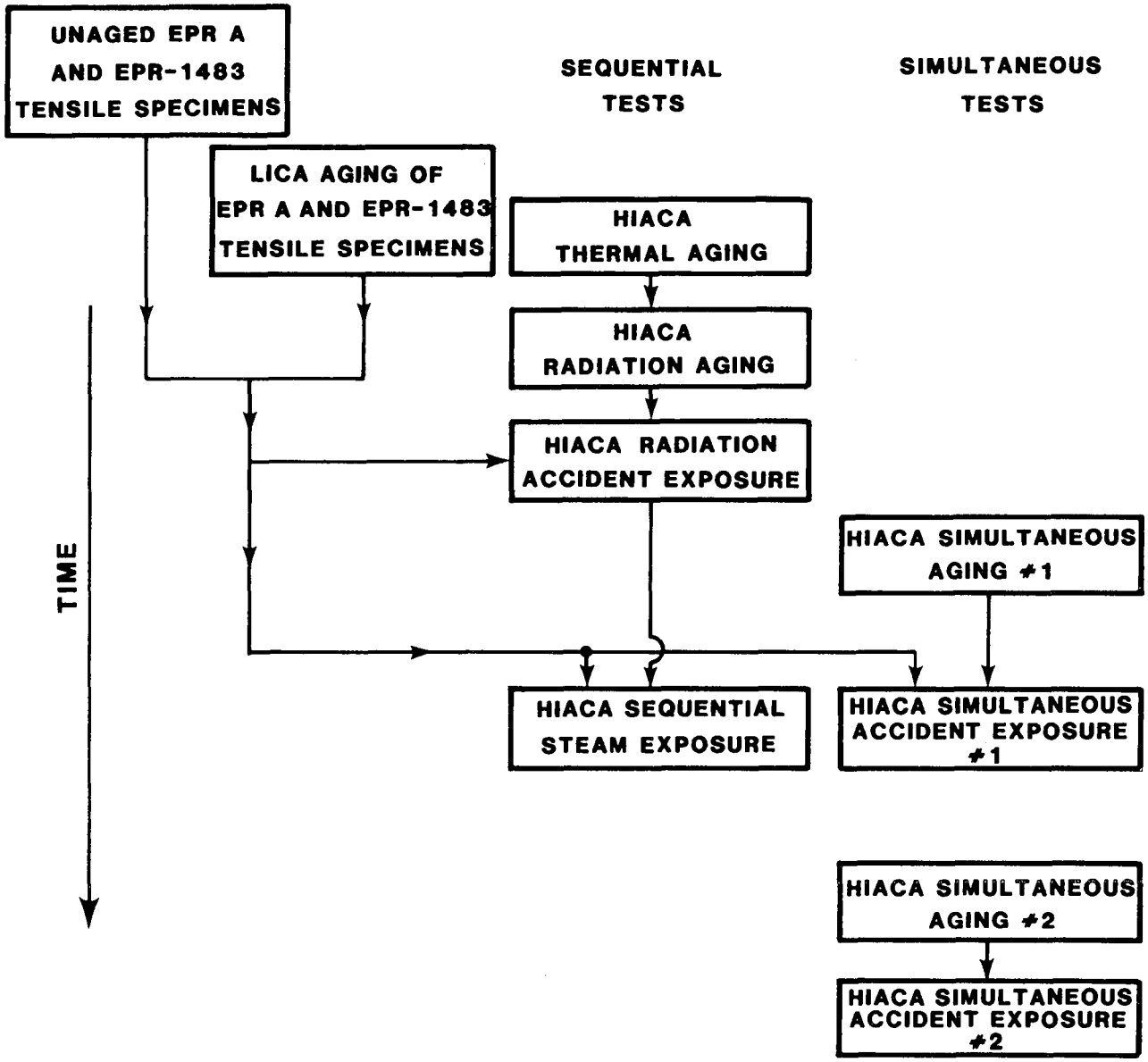

Figure 2.2. Experimental Sequence Used to Test EPR Cables and Tensile Specimens

A second simultaneous test was performed to verify some results of the first simultaneous test. This test included both simultaneous aging and accident exposures.

Each aspect of this test program will be discussed in more detail in Sections 2.3.2-2.3.5.

2.3.2 LICA Aging of Tensile Specimens

During this experiment strips of EPR-1483 and strips of EPR A were exposed to seven different aging simulations.* For each elevated temperature and radiation exposure, forty strips of EPR A and EPR-1483 were placed in the same exposure chamber. Air flow during both irradiation (chamber volume = 1.8 liters) and single stress elevated temperature exposures (chamber volume = 0.9 liters) was maintained at 60 ± 20 cc/min. Doses and dose rates are reported in rads (EPR) which is equivalent to 0.88 rads (air). The seven aging simulations were:

1. Ninety-four hour simultaneous exposure to 120 ± 1°C (248 ± 2°F) and 60 ± 4 krd/h, measured in rads (EPR) at the center of the chamber. Measured dose-rate gradients across the sample population were +30/-22 percent of the chamber center dose-rate. The chamber was rotated 180° midway through the exposure to minimize the effect of these gradients.

2. Thirty day simultaneous exposure to 120 ± 1°C (248 ± 2°F) and 60 ± 4 krd/hr, measured in rads (EPR) at the center of the chamber. Measured dose-rate gradients across the sample population were +30/-22 percent of the chamber center dose-rate. The chamber was rotated 180° midway through the exposure to minimize the effect of these gradients.

3. Twenty-eight day single stress exposure to 120 ± 1°C (248 ± 2°F) followed by a 28 day irradiation at 65 ± 5 krd/hr, measured in rads (EPR) at the center of the chamber. Ambient temperature during irradiation was 28 ± 1°C (82 ± 2°F). The chamber was rotated 180° midway through the exposure to minimize the effect of the +25/-21 percent dose-rate gradients.

---

*Note: Six of the seven aging simulations have been previously described as Experiment I in Reference 9. For completeness, this description is repeated in this report.

4. Twenty-eight day irradiation at 65 ± 5 krd/hr, measured in rads (EPR) at the center of the chamber, followed by a 28 day, 120 ± 1°C (248 ± 2°F) elevated temperature exposure. Ambient temperature during irradiation was 28 ± 1°C (82 ± 2°F). The sample chamber was rotated 180° midway through the irradiation to minimize the influence of the +25/-21 percent dose-rate gradients.

5. Fifty-five hour irradiation at 850 ± 60 krd/hr, measured in rads (EPR) at the center of the chamber, followed by a 28 day, 120 ± 1°C (248 ± 2°F) elevated temperature exposure. Ambient temperature during irradiation was 46 ± 1°C (115 ± 2°F). Measured radiation dose-rate gradients were less than +3 percent. (Lowest dose-rate was at the center of the chamber.)

6. Twenty-eight day, 120 ± 1°C (248 ± 2°F) elevated temperature exposure followed by a 55 hour irradiation at 850 ± 60 krd/hr, measured in rads (EPR) at the center of the chamber. Ambient temperature during irradiation was 46 ± 1°C (115 ± 2°F). Measured dose-rate gradients were less than +3 percent. (Lowest dose-rate was at the center of the chamber.)

7. Seven day simultaneous exposure to 139 ± 1°C (282 ± 2°F) and 290 ± 20 krd/hr, measured in rads (EPR) at the center of the chamber. Dose-rate gradients across the sample population were +65/-28 percent of the chamber center dose-rate. The chamber was rotated 180° midway through the exposure to minimize the influence of these gradients.

Arrhenius techniques were used to choose the elevated temperature exposures for thermal aging. Our thermal aging calculations are based on a postulated nuclear plant containment ambient environment of approximately 55°C (131°F), a life of approximately 5 years (for the first aging method) or 40 years (for the remaining six aging methods), and an EPR activation energy of 24 kcal/mole (1.04eV). We chose the activation energy values as a representative of single stress thermal degradation data found in the literature for EPR.[15] Our choice of thermal aging parameters to achieve a 40 year "life" is consistent with the guidance of IEEE Std 383-1974,[4] Section 1.3.5.2. It does not, however, account for possible synergisms between radiation and elevated temperature stresses.

2.3.3 HIACA Sequential Test

2.3.3.1 Test Setup

The HIACA sequential test was performed using a stainless steel steam chamber with ~ 0.4 m^3 of internal volume: the height is 200 cm and the diameter 52 cm. The top portion of the chamber (43 cm in length) contained all the penetration flanges through which cables, thermocouples, and other instrumentation entered and exited the chamber. The mandrels on which the cables were wrapped were suspended from the top portion of the chamber but were physically located inside the bottom portion of the chamber. This latter section of the chamber is 157 cm long. During radiation exposures the chamber was supported as shown in Figure 2.1. During thermal aging and the accident steam exposures, the chamber rested upright on the floor outside the Sandia Gamma Irradiation Facility; a collar around the chamber supported it.

Cables were wrapped on a 30 cm diameter around three mandrels connected together end to end. The total length of the three mandrels is 114 cm. The top of the mandrels was located 31 cm below the flange which connects the top and bottom portion of the steam chamber. After wrapping the cables on the mandrels, the cable leads were spiraled up the inside of the mandrels to the exit ports.

A rubber stopper was fed from each end of the cable and inserted into a modified Swagelok^{tm} fitting. The modified Swagelok^{tm} fitting, when tightened, compressed the rubber stopper and provided a steam seal. Figure 2.3 illustrates the sequential test setup.

We positioned the cables on the mandrels and prepared the cable flange penetrations prior to all aging and accident environmental exposures. Except for additional tightening of the modified Swagelok fittings, the cable lengths inside the chamber were not disturbed throughout the test. We used the stainless steel chamber as an oven, placed it in our radiation field, and used it as a steam pressure vessel. Insulation resistance and leakage current measurements were performed by filling the chamber bottom with water. We did visual examinations by using a crane to raise the top part of the chamber from the bottom part. Since the cables and mandrels were completely supported by the chamber top, no damage to the cables occurred during this operation.

Each cable lead outside the steam chamber was ~ 7.6 m (25 ft) long. This length was chosen to match the lengths used in the simultaneous accident environment tests. These long segments were necessary to pass during the simultaneous tests each cable from the steam chamber to the outside of the gamma irradiation cell. Insulation resistance and leakage current measurements were performed at this outside location.

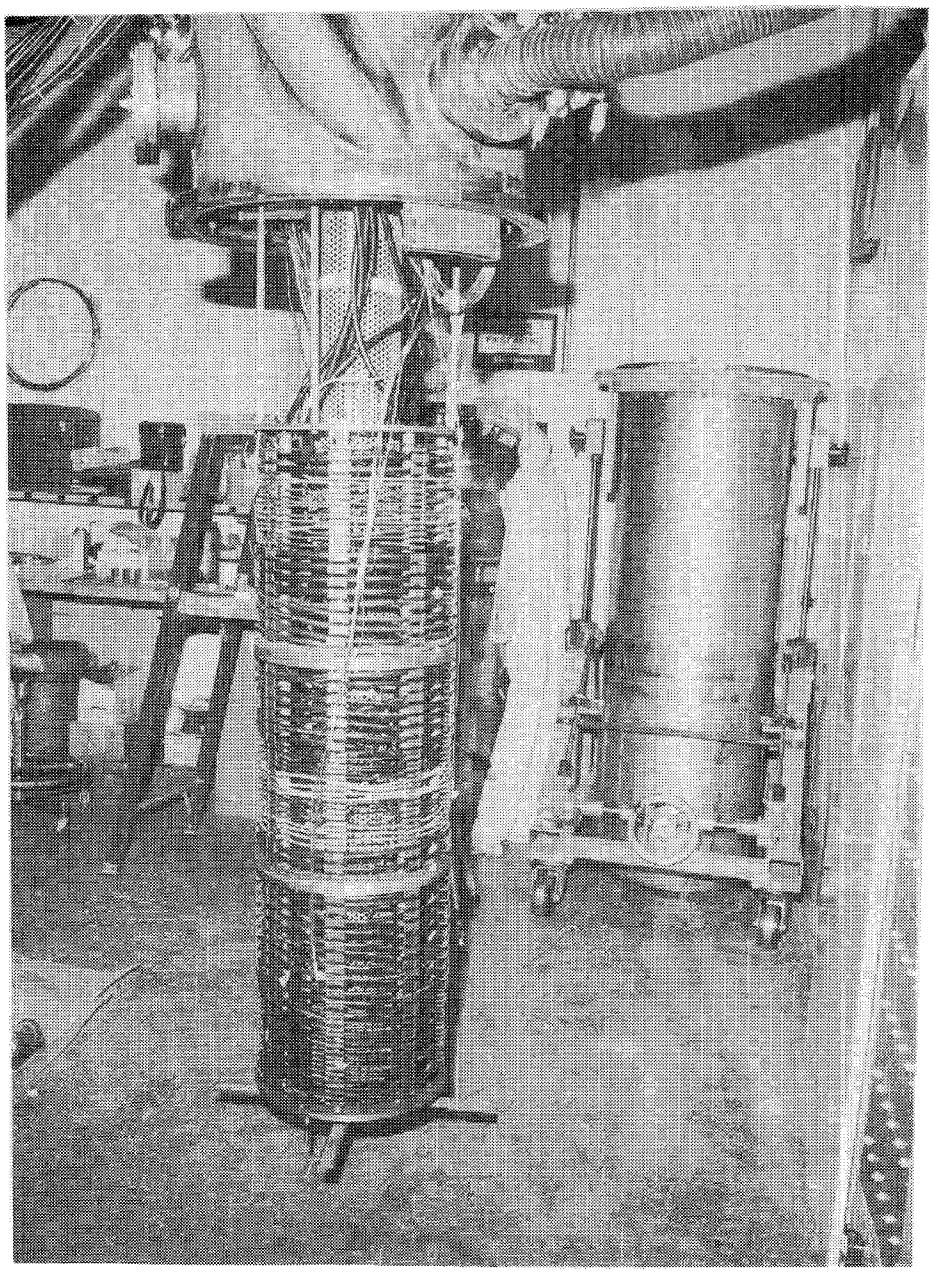

Figure 2.3. Sequential Test Setup Prior to the Start of Thermal Aging

Table 2.2 lists each cable placed in the chamber for sequential testing. The total length of each cable inside the steam chamber is given as well as each cable's location on the mandrel.

A perforated stainless steel cylinder was positioned along the centerline of the mandrels. A maximum of five 23 cm (9 in) long perforated stainless steel baskets containing insulation strips were placed inside this cylinder. During thermal aging and radiation exposures only two baskets were used. This insured that the tensile specimen insulation strips were located in relatively uniform radiation and temperature fields.

2.3.3.2 Thermal Aging

During thermal aging hot air was circulated from a heater to a port in the top of the stainless steel chamber. A rectangular aluminum duct along the inside wall of the chamber extended from the hot air entrance port to the bottom of chamber. Air flow exited the duct along its entire length and was directed parallel to the walls of the chamber (see Figure 2.4). An auxiliary duct and blower were used to remove cooler air from the top of the chamber and recirculate it to the bottom of the chamber to insure mixing. A valve on this latter recirculation line was adjusted during the first 22 hours of the 168 hour thermal exposure until the best temperature uniformity was obtained.

Cable #	Cable Description*	Total Length (m)	Length in Chamber (m)	Position below top surface of mandrel (cm)
1	EPR B: primary insulation only	20	5.8	7.1 to 8.9
2	EPR A: primary insulation only	22	7.0	8.9 to 13.2
3	EPR A: primary insulation and primary jacket	22	6.4	13.2 to 17.0
4	EPR B: intact single conductor	21	5.2	17.0 to 19.1
5	EPR A: intact multiconductor	23	7.9	19.3 to 26.4
6	EPR D: intact multiconductor	23	7.9	27.2 to 34.3
7	EPR E: intact multiconductor	21	6.4	38.6 to 41.2
8	EPR E: intact multiconductor	24	9.2	41.9 to 50.8
9	EPR B: intact single conductor	24	8.5	51.3 to 56.1
10	EPR D: primary insulation only	23	7.3	56.0 to 59.4
11	EPR E: primary composite insulation and jacket only	23	7.3	59.9 to 63.5
12	EPR B: primary insulation only	23	7.6	63.5 to 67.3
13	EPR E: intact multiconductor	33	18	67.3 to 96.5
14	EPR B: intact conductor	33	16	96.5 to 114.3

*XLPO cables were also wrapped on the mandrel during this test.

Table 2.2: Cable Positions on Mandrel During the Sequential Test

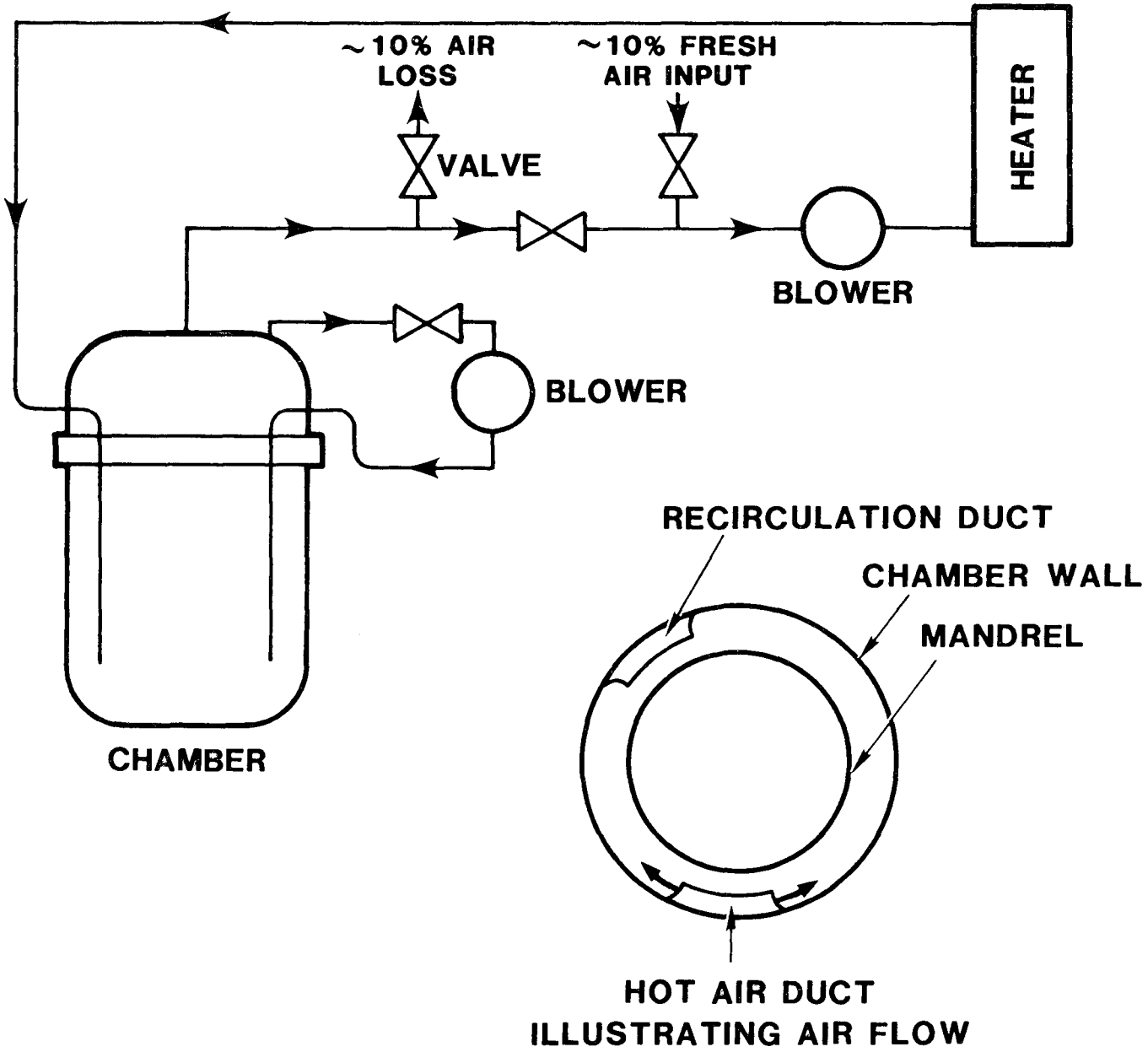

Figure 2.4. Thermal Aging Air Flow System During Sequential Aging

During recirculation of air from the chamber to the heater and back to the chamber, fresh air was added. We used air velocity measurements along the heater recirculation line to estimate the total air flow to the chamber as approximately 2 m^3/min. Of this, approximately 0.2 m^3/min. was fresh air. This insured that oxygen was not depleted during thermal aging.

Twenty-four thermocouples were positioned in the chamber to monitor temperature uniformity during thermal aging. We positioned four of the thermocouples along the outer rim of the stainless steel perforated cylinder used to support tensile specimen baskets. The remaining twenty thermocouples were positioned at various locations within 2.5 cm of the cables wrapped on the mandrels. One of the thermocouples was used for control purposes; another was used to provide a strip chart record of the thermal exposure. The remaining 22 thermocouples were connected to a datalogger; periodic temperature measurements were recorded throughout the thermal exposure. Table 2.3 presents the temperature distribution midway through the thermal exposure. Table 2.4 summarizes the temperature readings versus time for several of the thermocouple positions.

Table 2.3: Thermocouple Readings 84 Hours After Start of 168 Hour Sequential Thermal Exposure

(a) Distance below top of mandrel (cm)	Temperature (°C) 0°	90°	180°	270°
5.8	140	129(7)	137	136
20.0	142(6)	--	141	139
54.9	--	143	142(4)	144(5)
92.4	138	145(3)	138	133
109.5	135(1)	141(2)	132	131

(b) Distance below top of mandrel (cm)	Temperature (°C)
16.2	136
53.3	138
65.7	142
96.0	139

(a) Thermocouples were positioned around the circumference of the mandrel, spaced 90° apart and within 2.5 cm of the cables. The hot air duct was located at the 0° position; the recirculation duct was between the 90° and 180° position.

(b) Thermocouples were positioned along the outer rim of the perforated cylinder used to support tensile specimen baskets.

(c) (1)-(7) indicate thermocouple positions monitored by Table 2.4.

Table 2.4: Temperature Versus Time Profile During Sequential Thermal Exposure. Thermocouple positions (1)-(7) are identified in Table 2.3.

Elapsed Time	Temperature (°C) at Thermocouple Position 1	2	3	4	5	6	7
0 hrs	23	23	24	23	23	23	23
0 hrs, 10 min	51	70	78	70	84	64	65
0 hrs, 20 min	75	101	115	96	116	98	91
0 hrs, 30 min	97	123	139	116	139	123	113
0 hrs, 45 min	118	143	158	135	158	150	133
1 hr	122	142	150	138	149	151	133
1 hr, 30 min	125	141	145	140	147	149	134
2 hr	127	141	143	139	145	148	134
3 hrs	131	136	140	137	135	137	128
5 hrs	133	137	140	137	135	136	128
7 hrs	129	142	143	139	145	146	134
10 hrs	137	141	145	142	138	141	134
15 hrs	138	142	146	142	139	141	134
20 hrs	138	142	146	143	139	141	135
25 hrs	136	141	145	142	144	142	131
30 hrs	135	141	145	142	144	142	130
35 hrs	135	141	145	142	144	142	129
40 hrs	136	142	146	143	145	143	132
45 hrs	135	140	145	141	144	142	129
50 hrs	135	140	145	142	143	142	129
55 hrs	135	141	145	142	144	142	130
60 hrs	135	141	145	142	144	142	130
65 hrs	135	141	145	142	144	143	131
70 hrs	135	140	145	141	144	142	131
75 hrs	135	140	145	142	144	142	130
80 hrs	136	140	145	142	144	142	130
85 hrs	135	141	145	142	145	142	130
90 hrs	135	141	145	142	145	142	130
95 hrs	135	141	145	142	144	142	130
100 hrs	135	140	145	142	143	142	129
105 hrs	135	141	146	142	144	142	131
110 hrs	135	141	146	142	145	142	130
115 hrs	135	140	145	142	144	142	130
120 hrs	135	141	145	142	145	142	130
125 hrs	135	141	145	142	144	142	130
130 hrs	135	140	144	142	144	142	130
135 hrs	135	140	145	142	145	142	130
140 hrs	135	140	145	141	144	142	130
145 hrs	135	140	145	142	144	142	130
150 hrs	135	141	145	142	145	142	131
155 hrs	135	140	145	142	144	142	130

Table 2.4 (cont.)

Elapsed Time	Temperature (°C) at Thermocouple Position 1	2	3	4	5	6	7
160 hrs	135	141	145	142	145	142	130
165 hrs	135	140	145	142	144	142	130
168 hrs	135	141	145	142	145	142	130
169 hrs	92	89	90	91	91	91	95
171 hrs	57	58	56	58	58	56	59
173 hrs	41	42	40	41	41	41	42
175 hrs	33	33	32	33	33	32	33

Table 2.4 demonstrates the excellent temperature stability achieved once valve adjustments were completed at 22 hours. Table 2.3 illustrates that the temperature distribution within the chamber was large producing a large variation in accelerated age. The desired thermal exposure was seven days at 139°C. This elevated temperature exposure was based on Arrhenius techniques. Our thermal aging calculations were based on a postulated nuclear plant containment environment of approximately 55°C, a life of approximately 40 years and an EPR activation energy of 24 kcal/mole (1.04 eV). We chose the activation energy values as representative of single stress thermal degradation data found in the literature for EPR[15]. For these parameters a $\pm$3°C temperature gradient yields at $\pm$25% variability in the accelerated age. A $\pm$5°C gradient produces a $\pm$40% variability in the accelerated age.

Our 7 day, 139°C thermal aging exposure was generally less severe than that used by the EPR cable manufacturers during qualification tests. For example EPR A, B, D, F, and G were exposed to 150°C for at least seven days. EPR C, as a single conductor, was aged for seven days at 150°C and then used to produce a multiconductor which was aged for 7 days at 121°C, EPR E was aged at 136°C for 7 days.

2.3.3.3 Radiation Exposures

At completion of thermal aging, we removed the heater ducts from the stainless steel chamber. Accomplishment of this task was performed without disturbing the cables since the ducts were on the outside. We then performed insulation resistance measurements after filling the chamber with tap water. After draining the water and allowing the cables to dry, we performed the aging radiation exposure.

We performed this exposure using three irradiation time intervals to give a total irradiation time of 60 hrs, 15 mins:

- a five minute exposure to allow for radiation mapping of the chamber

- a 21 hour, 52 minute exposure

- a 38 hour, 18 minute exposure

A 6 hour, 34 minute interruption separated the second and third exposures. Ambient temperature during the latter two irradiations varied between 39°C and 45°C. We did not supply fresh air makeup to the chamber during the irradiations, but we did open ports of the stainless steel chamber to allow for natural air exchange between the cables and the gamma irradiation cell. The gamma irradiation cell was ventilated during the irradiation. We used a Victoreen Radicon Model 550 Integrating/Rate Electrometer with a Model 550 air ionization probe to measure the dose rate at one position along the centerline of the chamber. 106 Harshaw TLD-400's (calcium fluoride manganese activated thermoluminescent detectors) were placed at 53 positions to map the relative dose rates with respect to the single Victoreen measurement. The dose rate along the chamber centerline (40 cm below the top of the mandrel) was .65 $\pm$ .03 Mrd/h (air equivalent). The dose rate at the cable windings was 11% higher. Table 2.5 summarizes the dose rate profile with respect to distance below the top of the mandrel.

For all but a few of the cables, the average dose rate is .74 $\pm$ .06 Mrd/hr (air-equiv.). Thus the aging radiation dose was 45 $\pm$ 4 Mrd. The absorbed dose in EPR is 14% higher than the air-equivalent dose. This gives an aging dose of 51 $\pm$ 4 Mrd (in EPR).

Table 2.5: Radiation Dose Rates During Sequential Radiation Exposures

Distance below top of mandrel	Radiation dose rate (air equiv.) at cable windings
0	.59 $\pm$ .05 Mrd/h
15	.76 $\pm$ .06 Mrd/h
41	.72 $\pm$ .06 Mrd/h
69	.72 $\pm$ .06 Mrd/h
95	.76 $\pm$ .06 Mrd/h
114	.63 $\pm$ .05 Mrd/h

At completion of radiation aging we did both a visual inspection and insulation resistance measurements. We then performed the accident irradiation exposure for 171 hrs at .74 ± .04 Mrd/h (air equiv.). The total accident dose was 127 ± 10 Mrd (air equiv.) or 144 ± 12 Mrd (EPR equiv.). During the accident irradiation we monitored the air temperature at the cables. It varied between 40 and 44°C. We also placed a short section of EPR A multiconductor into the chamber. A thermocouple was inserted inside this multiconductor five centimeters from the end. This temperature during the accident irradiation was 47-50°C.

After the accident irradiation we once again did a visual examination and performed insulation resistance measurements. The entire chamber with cables was then stored at ambient conditions until the start of the LOCA steam simulation (51 days after the completion of the accident irradiation).

2.3.3.4 Steam Exposure

Figure 2.5 summarizes our intended steam temperature test profile. It is similar to the IEEE 323-1974, Appendix B profile[3], but also different in several respects, most notably:

1. After four days of steam exposure we interrupted the steam exposure to remove baskets containing tensile specimens.

2. We used a 104°C saturated steam exposure after four days until the end of the test.

3. We did not apply chemical spray during the exposure.

4. We did not start our transient ramps at 60°C.

Two nonconformances kept us from achieving this steam profile.

1. During the initial ramp a penetration fitting for one of three EPR E cables leaked excessively. It was immediately retorqued and the steam ramp restarted. The elapsed time to achieve the first ramp was thirteen minutes. We added 15 minutes to the duration of the first 171°C peak of the profile.

2. On day 9 of the steam exposure our steam supply system failed and the steam chamber cooled down to ambient temperatures and pressures. On day 11 we opened the chamber and performed ambient insulation resistance measurements. We resumed the steam exposure on day 12 and continued the steam exposure until day 24. Our total steam exposure lasted 21 days.

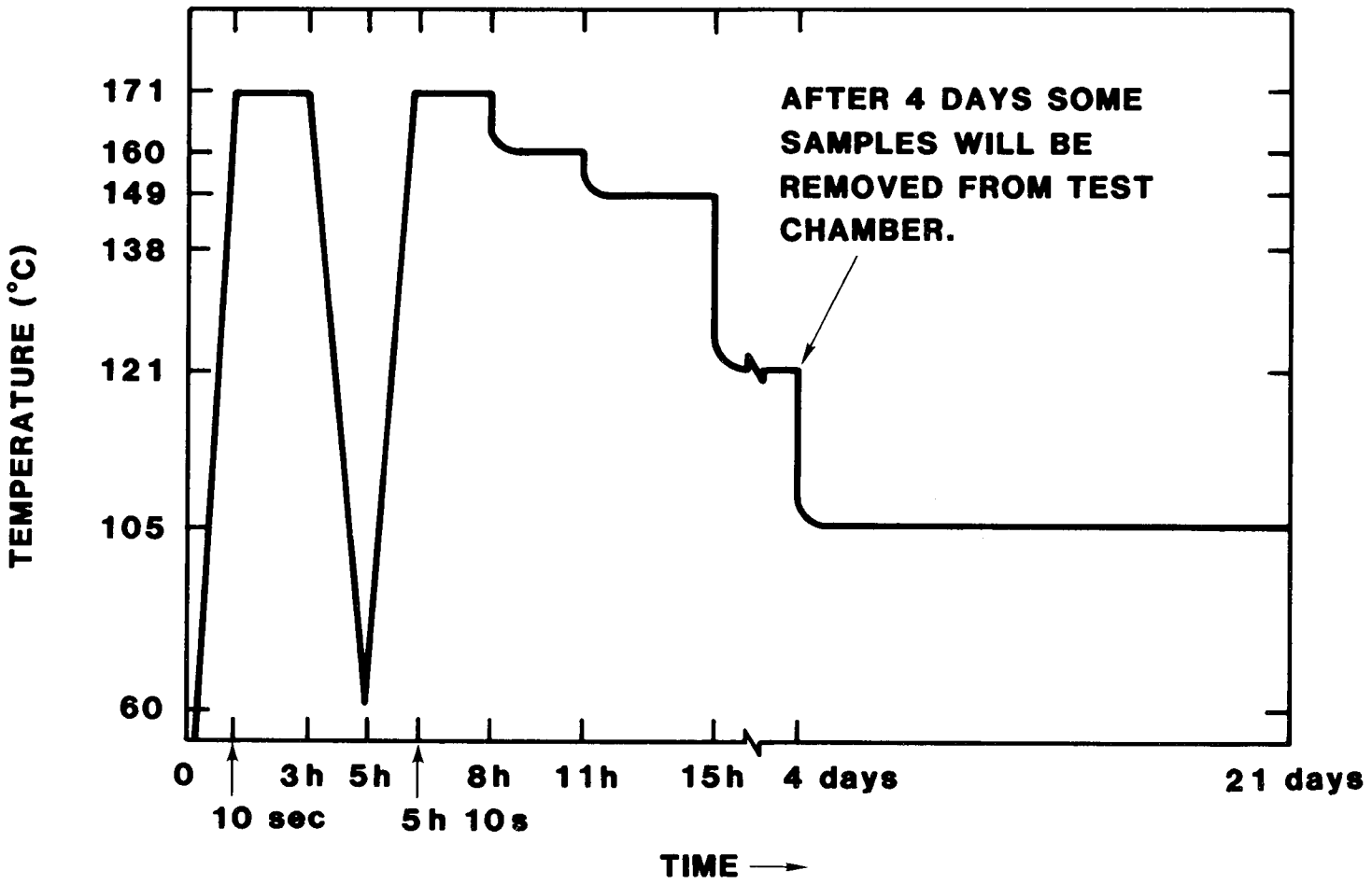

Figure 2.5. Sequential Steam Accident Exposure Profile (as proposed by test plan); pressures correspond to saturated steam conditions in Albuquerque, NM (171°C corresponds to 106 psig).

Table 2.6 summarizes our test conditions during the steam exposure. The steam conditions for simultaneous test #1 are also summarized to illustrate the similarities between the sequential and simultaneous #1 test. Note: both steam chambers were connected in parallel to the steam supply system.

Throughout the steam exposure the cables were loaded at 480 Vac and 0.6 A. This exposure was interrupted to allow for insulation resistance measurements.

At the completion of the steam exposure we immediately removed the tensile insulation specimens and then weighed them and measured their dimensions within six hours. After the chamber had cooled we performed a visual examination and then filled the chamber with tap water. Insulation resistance and leakage current measurements were then performed. These measurements were made without disturbing the cables that were wrapped on the mandrels. We did not follow the procedures of IEEE Std 383-1974,[4] Section 2.4.4 which states that the cables "should be straightened and recoiled around a mandrel with a diameter of approximately 40 times the overall cable diameter" prior to performing the voltage withstand tests.

Table 2.6

Steam Profiles Achieved During the Sequential and Simultaneous #1 Steam Exposures. Except during transient ramps and where noted,*, the temperatures correspond to saturated steam conditions in Albuquerque, New Mexico. An * indicates the chamber was opened to remove samples or the steam system had failed and saturated steam conditions were not maintained.

Elapsed Time	Sequential Chamber Temperature (°C)	Simultaneous #1 Chamber Temperature (°C)
0.0	Introduced steam to both chambers	
2 s	129	134
27 s	94	174
52 s	82	167
1 m, 42 s	74	150
3 m, 47 s	70	151
6 m, 42 s	68	150
10 m, 02 s	67	151
11 m, 42 s	66	150
12 m, 07 s	173	150
12 m, 57 s	173	175
15 m	171	173
30 m	171	173
1 h, 0 m	172	173
2 h, 0 m	171	173

Table 2.6 (cont.)

Elapsed Time	Sequential Chamber Temperature (°C)	Simultaneous #1 Chamber Temperature (°C)
3 h, 0 m	171	172
3 h, 15 m	171	173
3 h, 30 m	165	167
3 h, 45 m	159	161
4 h, 0 m	152	153
4 h, 30 m	133	134
	Pressure Transducer Connected to Simultaneous Chamber Changed	
5 h, 0 m	105*	108*
5 h, 15 m	93*	112*
5 h ,15 m, 22 s	171	163
5 h, 15 m, 47 s	172	174
5 h, 18 m	171	172
6 h	171	172
7 h	172	172
8 h, 12 m	171	172
8 h, 18 m	170	171
8 h, 23 m	168	169
8 h, 38 m	163	164
8 h, 48 m	160	161
9 h	160	162
10 h	160	161
11 h	160	161
11 h, 20 m	160	161
11 h, 30 m	154	155
11 h, 40 m	149	150
12 h	150	151
13 h	150	151
14 h	150	151
15 h	150	151
15 h, 10 m	150	151
15 h, 20 m	147	147
15 h, 30 m	140	140
15 h, 40 m	133	134
15 h, 50 m	123	123
16 h	122	122
17 h	122	122
19 h	121	122
21 h	122	122
1 d, 1 h	122	122
1 d, 11 h	122	123
1 d, 21 h	122	123
2 d, 2 h	122	123
2 d, 12 h	122	123
2 d, 22 h	122	123
3 d, 8 h	121	123
3 d, 18 h	121	123

Table 2.6 (cont.)

Elapsed Time	Sequential Chamber Temperature (°C)	Simultaneous #1 Chamber Temperature (°C)
3 d, 23 h	121	122
4 d, 0 h, 42 m	121	123
4 d, 1 h, 11 m	111	115
4 d, 1 h, 20 m		Opened chamber
4 d, 1 h	105	87*
4 d, 1 h, 51 m	Opened chamber	
4 d, 2 h, 12 m	78*	75*
4 d, 2 h, 30 m		Reintroduced steam
4 d, 2 h 42 m	75*	106
4 d, 3 h	Reintroduced steam	
4 d, 3 h, 11 m	105	105
4 d, 8 h	104	105
4 d, 13 h	105	105
4 d, 22 h	105	105
5 d, 8 h	104	105
5 d, 18 h	105	105
6 d, 4 h	104	105
6 d, 14 h	104	105
7 d, 0 h	105	105
7 d, 10 h	105	105
7 d, 20 h	105	106
8 d, 6 h	105	106
8 d, 16 h	105	106
9 d, 2 h	105	106
9 d, 2 h, 42 m	103	104
	Steam supply failure	Steam supply failure
9 d, 3 h, 11 m	95*	96*
9 d, 4 h, 11 m	64*	75*
9 d, 5 h, 11 m	48*	56*
9 d, 6 h, 11 m	37*	45*
9 d, 8 h, 11 m	27*	33*
9 d, 10 h, 11 m	23*	28*
12d, 4 h, 25 m	20*	20*
12 d, 4 h, 27 m	22*	21*
		Reintroduced steam
12 d, 4 h, 29 m	22*	102
12 d, 4 h, 30 m	22*	103
	Reintroduced steam	
12 d, 4 h, 31 m	105	106
12 d, 4 h, 32 m	105	106
12 d, 4 h, 45 m	104	105
12 d, 5 h	105	105
12 d, 10 h	104	105
12 d, 18 h	104	105
13 d	104	105
13 d, 10 h	104	105
13 d, 20 h	105	105
14 d, 6 h	104	105

Table 2.6 (cont.)

Elapsed Time	Sequential Chamber Temperature (°C)	Simultaneous #1 Chamber Temperature (°C)
14 d, 16 h	105	105
15 d, 2 h	104	105
15 d, 12 h	104	105
15 d, 22 h	105	105
16 d, 8 h	104	105
16 d, 18 h	105	105
17 d, 4 h	105	105
17 d, 14 h	104	105
18 d	104	105
18 d, 10 h	104	105
18 d, 20 h	104	105
19 d, 6 h	104	105
19 d, 16 h	104	105
20 d, 1 h	104	104
20 d, 11 h	105	105
20 d, 22 h	105	105
21 d, 7 h	105	106
21 d, 17 h	105	105
22 d, 3 h	105	105
22 d, 13 h	104	105
22 d, 23 h	105	106
23 d, 9 h	105	106
23 d, 19 h	105	106
24 d, 5 h	105	105
24 d, 15 h	105	106
25 d, 1 h	105	106
25 d, 1 h, 55 m		Steam shut off Chamber opened
25 d, 2 h, 15 m	105	86*
25 d, 2 h, 40 m	Steam shut off	
25 d, 2 h, 45 m	94*	70*
25 d, 3 h, 15 m	72*	61*

2.3.4 HIACA Simultaneous Test #1

2.3.4.1 Test Setup

The HIACA simultaneous test #1 was performed using a stainless steel steam chamber with $\sim$ .3 m^3 of internal volume. The height is 125 cm and the diameter 52 cm. The top portion of the chamber (43 cm in length) contained all the penetration flanges through which cables, thermocouples, and other instrumentation entered and exited the chamber. The mandrels on which the cables were wrapped were suspended from the top portion of the chamber but were physically located inside the bottom portion of the chamber. This latter section of the chamber is 81 cm long. During both the aging and the accident exposures the chamber was supported as shown in Figure 2.1. This allowed for a simultaneous radiation exposure with the thermal aging and the accident steam exposures.

Cables were wrapped on two mandrels connected together end to end. The top of the mandrels was located 13 cm below the flange which connects the top and bottom portion of the steam chamber. Because of nonuniformities in the radiation field for most of the top mandrel, most of the cables were wrapped on the bottom mandrel. We wrapped the single conductors on the inside of the mandrel using a 25 cm diameter. The multiconductors were wrapped on the outside of the mandrel on a 30 cm diameter. After wrapping the cables on the mandrels, the cable leads were spiraled up the inside of the mandrels to the exit ports.

A rubber stopper was fed from each end of the cable and inserted into a modified Swagelok^{tm} fitting. The modified Swagelok^{tm} fitting, when tightened, compressed the rubber stopper and provided a steam seal. Figure 2.6 illustrates the simultaneous test #1 setup.

We positioned the cables on the mandrels and prepared the cable flange penetrations prior to all aging and accident environmental exposures. Except for additional tightening of the modified Swagelok fittings, the cable lengths inside the chamber were not disturbed throughout the test. We used the stainless steel chamber as an oven, placed it in our radiation field, and used it as a steam pressure vessel. Insulation resistance and leakage current measurements were performed by filling the chamber bottom with tap water. We did visual examinations by using a crane to raise the top part of the chamber from the bottom part. Since the cables and mandrels were completely supported by the chamber top, no damage to the cables occurred during this operation.

Each cable lead outside the steam chamber was $\sim$ 7.6 m (25 ft) long. These long segments were necessary to pass each cable from the steam chamber to the outside of the gamma irradiation cell. Insulation resistance and leakage current measurements were performed at this outside location.

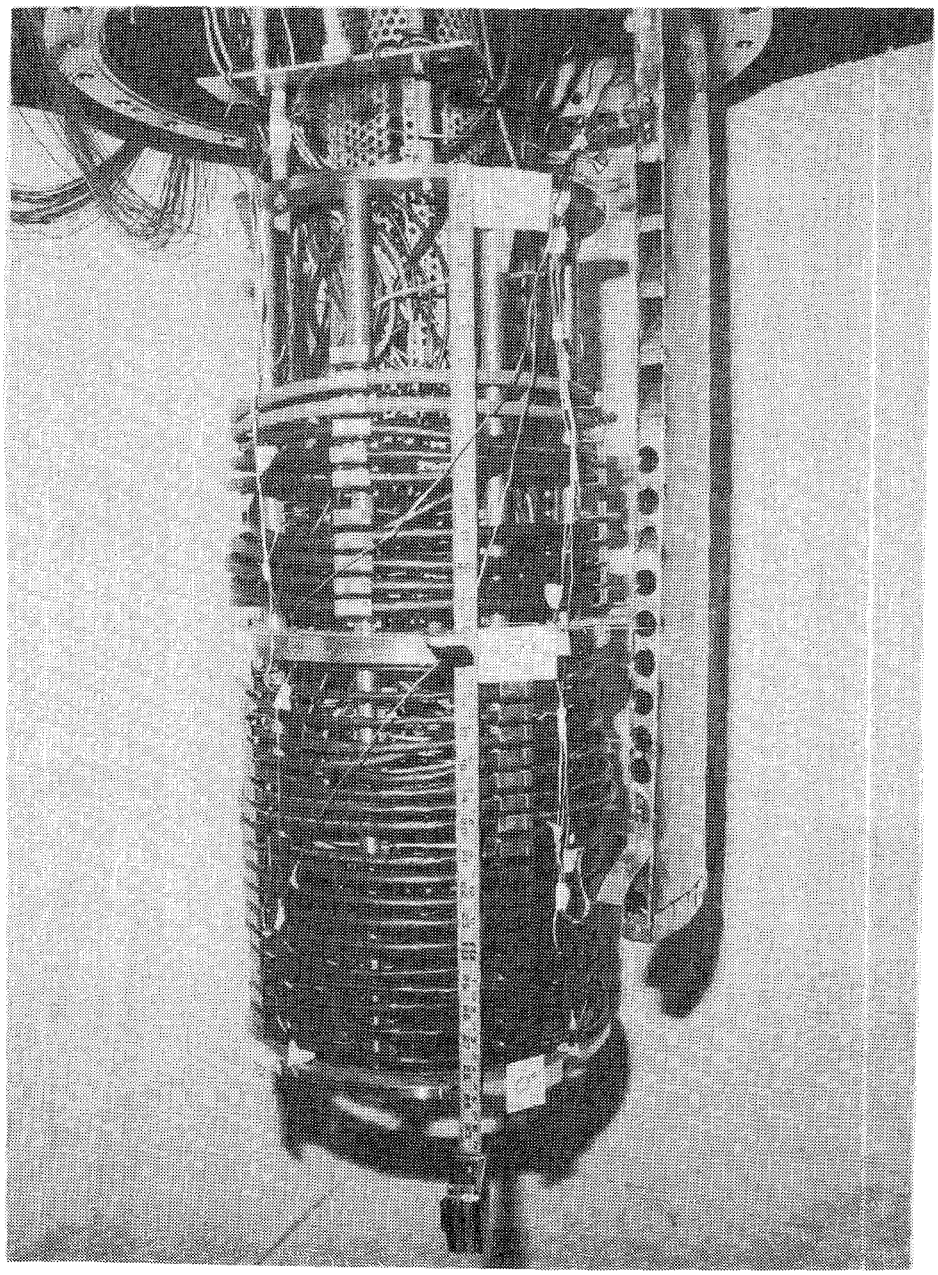

Figure 2.6. Simultaneous Test #1 Setup Prior to the Start of Thermal Aging

Table 2.7 lists each cable placed in the chamber for simultaneous #1 testing. The total length of each cable inside the steam chamber is given as well as each cable's location on the mandrel.

A perforated stainless steel cylinder was positioned along the centerline of the mandrels. Two 23 cm (9 in) long perforated stainless steel baskets containing insulation specimens were placed inside this cylinder during the aging and accident exposures.

2.3.4.2 Simultaneous Thermal and Radiation Aging

We positioned the stainless steel chamber in the gamma irradiation facility and connected it to the heater via a port in the top of the chamber. A rectangular aluminum duct along the inside wall of the chamber extended from the hot air entrance port to the bottom of the chamber. Air flow exited the duct along its entire length and was directed parallel to the walls of the chamber (see Figure 2.6). Unlike for the sequential test, an auxiliary duct and blower was not used to remove cooler air from the top of the chamber to insure proper mixing and better temperature uniformities. Rather, during the first four and a half hours of thermal aging the heater was turned off three times and the test chamber opened to allow for adjustment of the air flow distribution from the hot air duct. (Previous measurements using a dummy load illustrated that the air flow pattern was sensitive to the cable wrapping configuration; therefore adjustments were necessary for each cable setup.) After restarting the heater the third time, the chamber overheated for approximately an hour. (Maximum temperature during the transient was 175°C.)

We thermally aged the cables for 171-1/2 hours and then allowed the chamber to naturally cool to ambient conditions. Since the heater was off three times for the first four and a half hours, the actual aging time was ~ 169 hours, similar to the 168 hour exposure used during the sequential test.

During recirculation of air from the chamber to the heater and back to the chamber, fresh air was added. We used air velocity measurements along the heater recirculation line to estimate the total air flow to the chamber as approximately $2m^3$/min. Of this, approximately $0.2m^3$/min was fresh air. This insured that oxygen was not depleted from the chamber during aging.

Cable Description*	Cable Length Inside Chamber (m)	Distance Below Top of Mandrel (cm)
25 cm diameter wrappings		
EPR A: insulated single conductor	5.5	26-30
EPR A: insulated and jacketed single conductor	5.6	30-34
EPR C: insulated single conductor	5.1	41-45
EPR A': insulated single conductor	6.1	45-48
EPR A': insulated and jacketed single conductor	5.7	49-53
EPR D: insulated single conductor	6.8	53-57
EPR E: insulated and jacketed single conductor	5.6	57-60
EPR B: insulated single conductor	5.9	62-66
EPR B: insulated and jacketed single conductor	6.9	66-71
30 cm diameter wrappings		
EPR A': multiconductor	6.2	28-35
EPR C: multiconductor	7.1	38-47
EPR D: multiconductor	6.2	46-55
EPR A: multiconductor	7.3	53-62
EPR E: multiconductor	8.4	64-71

*XLPO Cables were also wrapped on the mandrel during this test.

Table 2.7: Cable Positions on Mandrel During Simultaneous Test #1

Twenty thermocouples were positioned in the chamber to monitor temperature uniformity during thermal aging. We positioned three of the thermocouples along the outer rim of the stainless steel perforated cylinder used to support tensile specimen baskets. The remaining seventeen thermocouples were positioned at various locations within 2.5 cm of the cables wrapped on the mandrels. One of the thermocouples was used for control purposes; another was used to provide a strip chart record of the thermal exposure. The remaining 18 thermocouples were connected to a datalogger; periodic temperature measurements were recorded throughout the thermal exposure. Table 2.8 presents the temperature distribution midway through the thermal exposure. Table 2.9 summarizes the temperature readings versus time for several of the thermocouple positions.

Table 2.8: Thermocouple Readings 85 Hours After the Start of the 171-1/2 Hour Thermal Aging Exposure (Part of simultaneous #1 radiation and thermal exposure)

(a)

Distance below top of mandrel (cm)	Temperature (°C) 0°	90°	180°	270°
14	137	136	137	137 (7)
27	139 (5)	138	139 (6)	139
52	143	140 (3)	---	140 (4)
67	136 (1)	139 (2)	142	139

(b)

Distance below top of mandrel (cm)	Temperature (°C)
13	135
38	142
61	139

(a) Thermocouples were positioned around the circumference of the mandrel, spaced 90° apart and within 2.5 cm of the cables. The hot air duct is close to the 0° position.

(b) Thermocouples were positioned along the outer rim of the perforated cylinder used to support tensile specimen baskets.

(c) (1)-(7) indicate thermocouple positions monitored by Table 2.4.

Table 2.9: Temperature Versus Time Profile During Simultaneous #1 Thermal and Radiation Aging Exposure. Thermocouple positions (1)-(7) are identified in Table 2.8.

Elapsed Time	Temperature (°C) at Thermocouple Position 1	2	3	4	5	6	7
0	19	19	19	19	19	18	19
20 min	128	153	165	154	102	143	116
1 hr	141	143	142	145	139	137	137
1 hr, 20 min	140	141	141	143	139	135	136
Heater off at 1 hr, 20 min							
2 hrs, 10 min	57	54	53	58	57	55	58
Heater on at 2 hr, 10 min							
2 hrs, 20 min	131	150	140	123	128	150	124
3 hrs	140	144	143	137	142	146	141
Heater off at 3 hrs							
3 hrs, 25 min	84	81	81	84	85	80	84
Heater on at 3 hrs, 25 min							
3 hrs, 40 min	138	148	143	135	137	150	140
4 hrs	141	146	145	140	143	148	144
Heater off at 4 hrs							
4 hrs, 30 min	77	75	72	74	75	77	79
Heater on at 4 hrs, 30 min							
4 hrs, 45 min	132	147	161	151	149	143	127
5 hrs	134	140	143	142	139	139	134
5 hrs, 15 min	140	145	152	150	147	144	137
5 hrs, 30 min	158	166	175	172	168	164	154
5 hrs, 45 min	155	160	163	163	160	160	155
6 hrs	151	154	158	157	155	154	150
6 hrs, 15 min	139	141	141	141	141	143	142
6 hrs, 30 min	135	137	138	138	137	138	137
7 hrs	135	137	139	139	137	138	135
10 hrs	134	137	138	139	137	138	135
15 hrs	135	137	138	138	137	137	135
20 hrs	134	137	139	138	137	138	135
25 hrs	136	138	140	140	138	138	136

Table 2.9 (cont.)

Elapsed Time	Temperature (°C) at Thermocouple Position 1	2	3	4	5	6	7
30 hrs	136	138	140	140	139	139	137
35 hrs	136	138	141	140	139	139	137
40 hrs	136	138	140	140	139	139	137
45 hrs	136	138	140	140	139	139	137
50 hrs	136	138	140	140	138	139	137
55 hrs	136	138	140	140	138	139	137
60 hrs	136	138	140	140	139	139	136
65 hrs	136	139	141	140	139	139	137
70 hrs	136	138	140	140	139	139	137
75 hrs	136	138	141	140	139	139	137
80 hrs	136	138	141	140	139	139	137
85 hrs	136	139	140	140	139	139	137
90 hrs	136	138	140	140	139	139	137
95 hrs	136	139	140	140	139	139	137
100 hrs	136	138	140	140	139	139	137
105 hrs	136	138	140	140	139	139	137
110 hrs	136	138	141	140	139	139	137
115 hrs	136	138	140	140	138	139	137
120 hrs	136	138	140	140	138	138	137
125 hrs	134	137	139	140	137	137	134
130 hrs	134	137	140	139	137	137	134
135 hrs	134	137	139	139	138	137	134
140 hrs	134	137	140	139	138	137	134
145 hrs	134	137	139	139	138	137	134
150 hrs	136	138	140	139	138	138	136
155 hrs	136	138	140	140	138	138	137
160 hrs	134	137	140	139	138	137	135
165 hrs	135	137	139	139	138	137	135
170 hrs	134	137	140	139	137	137	134
171-1/2 hrs	135	137	140	139	138	137	135
172 hrs	93	90	91	93	91	89	--
173 hrs	36	27	25	27	39	25	28

For 122.5 hours of the 171.5 hour thermal exposure we simultaneously irradiated the cables and tensile specimens. We performed this radiation exposure using three irradiation time intervals:

- 114 hr exposure starting 6 hrs, 40 min after the start of the thermal aging exposure
- 1 hr, 10 min exposure starting 146 hours after the start of the thermal aging exposure
- 6 hrs, 20 min exposure starting 148 hours after the start of the thermal aging exposure

After completion of the simultaneous radiation and thermal exposures, we performed room temperature dosimetry to establish the aging dose rate. A Victoreen Radicon Model 550 Integrating/Rate Electrometer with a Model 550 air ionization probe was used to measure the dose rate at one position along the centerline of the chamber. Fifty-two Harshaw TLD-400's (calcium fluoride manganese activated thermoluminescent detectors) were placed at 25 positions to map the relative dose rates with respect to the Victoreen measurement. The dose rate along the chamber centerline (50 cm below the top of the mandrel) was .32 Mrd/h (air-equiv). For all but three of the cables (see Table 2.7 for cable positions during aging), the average dose rate where the cables were wrapped on the mandrels was .33 $\pm$ .03 Mrd/h (air-equiv.). Thus the aging radiation dose was 40 $\pm$ 3 Mrd. The absorbed dose in EPR is 14% higher than the air-equivalent dose. This gives an aging dose of 46 $\pm$ 3 Mrd (in EPR)

In addition to mapping the aging dose rate profile, we also mapped the dose rate profiles for each of the three Co-60 source arrangements that were used during the simultaneous radiation and steam exposures. This data is presented in Table 2.10.

At completion of the simultaneous aging program we did both a visual inspection and insulation resistance measurements. The entire chamber with cables was then stored at ambient conditions until the start of the LOCA steam and radiation simulation (8 days after completion of the aging exposure).

Table 2.10: Radiation Dose Rates (air-equiv) Used During Simultaneous Test #1. Measurements were performed at ambient air conditions upon completion of the aging exposure.

Measurement location below top of mandrel	Aging Dose Rate (Mrd/h)	Accident Dose Rates* Mrd/h 1	2	3
50 cm (along centerline)	.32 ± .01	.62 ± .03	.16 ± .01	.062 ± .002
Within 2.5 cm of the cables		Average of several measurement locations around circumference of the mandrel.		
14 cm	.28 ± .03	.59 ± .05	.13 ± .01	.06 +.04** -.03
37 cm	.34 ± .03	.67 ± .05	.17 ± .02	.08 +.06** -.05
55 cm		.77 ± .06		
72 cm	.32 ± .03	.68 ± .05	.17 ± .02	.07 ± .01

* The three different dose rates columns refer to the three Co-60 configurations used during simultaneous test #1.

**Large uncertainties reflect gradients in radiation field.

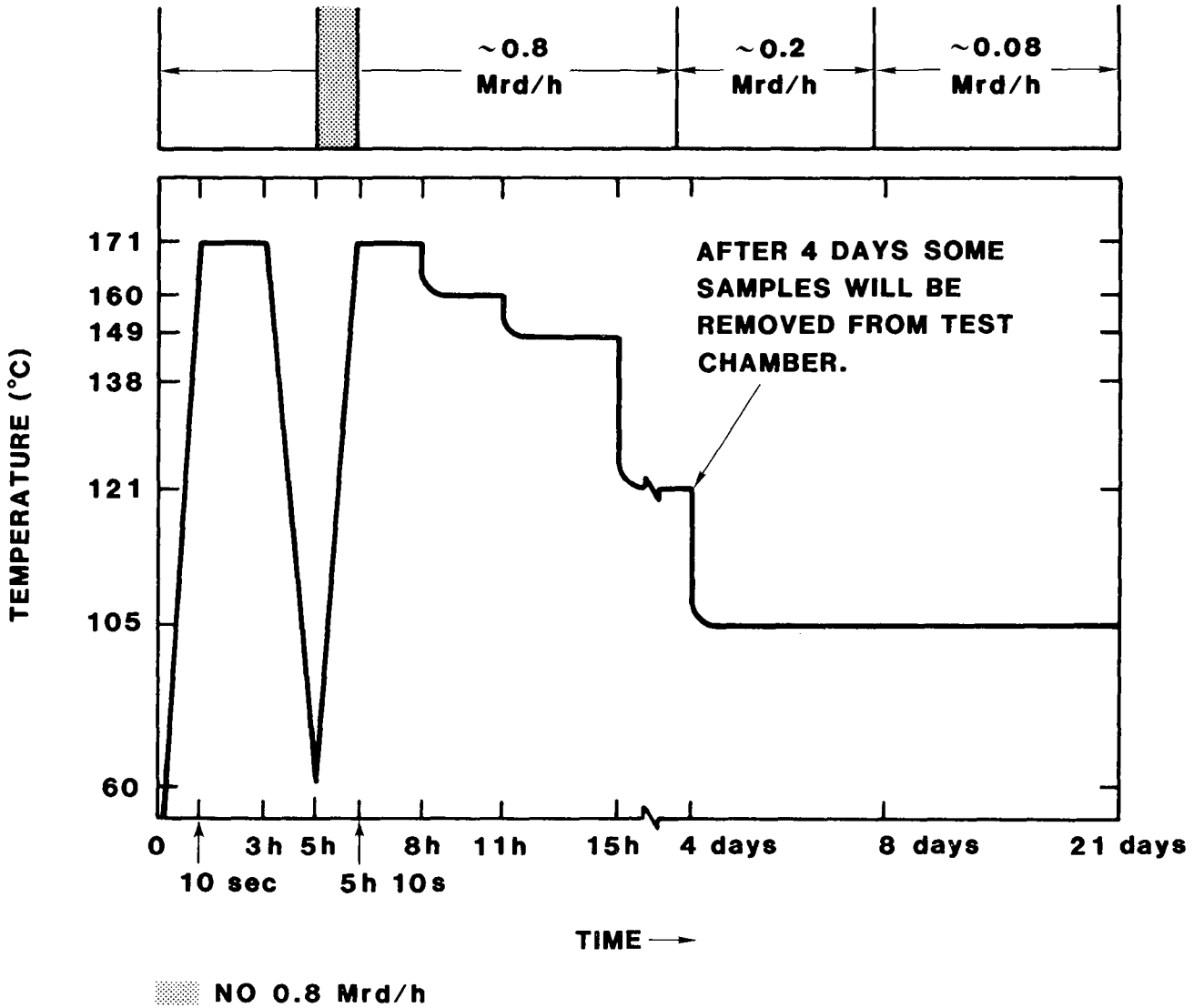

Figure 2.7. Simultaneous Test #1 Accident Exposure Profile (as proposed by test plan). Pressures correspond to saturated steam conditions in Albuquerque, NM, (171°C corresponds to 106 psig).

2.3.4.3 Simultaneous Steam and Radiation Exposure

Figure 2.7 summarizes our intended steam and radiation profile. The steam profile is similar to the IEEE 323-1974, Appendix B profile,[3] but also different in several respects, most notably:

1. After four days of steam exposure we interrupted the steam exposure to remove baskets containing tensile specimens.

2. We used a 104°C saturated steam exposure after four days until the end of the test.

3. We did not apply chemical spray during the exposure.

4. We did not start our transient ramps at 60°C.

Two nonconformances kept us from achieving this steam and radiation profile.

1. The initial ramp was achieved in less than 30 seconds (see Table 2.6). However, a steam leak in the sequential chamber resulted in the simultaneous chamber cooling to 150°C during the first 13 minutes of the profile. We added 15 minutes to the duration of the first peak of the profile.

2. On day 9 of the steam exposure our steam supply system failed and the steam chamber cooled to ambient temperatures and pressures. Twenty-one hours later we stopped the irradiation of the samples. On day 11 we opened the chamber and performed ambient insulation resistance measurements as well as a visual inspection. We resumed the steam and radiation exposures on day 12 and continued these exposures until day 25. Our total steam exposure lasted 21 days.

Table 2.6 summarizes our steam temperatures during the simultaneous test #1. The steam conditions for the sequential test are also provided to illustrate the similarities between the sequential and simultaneous #1 test. Note: both steam chambers were connected in parallel to the steam supply system.

Table 2.11 presents the accident irradiation history for simultaneous test #1. The total accident dose was 113 $\pm$ 30 Mrd (air-equiv.). This gives a total accident and aging dose of 153 $\pm$ 33 Mrd (air-equiv.) or 174 $\pm$ 38 Mrd (in EPR). For comparison, the sequential test total dose was 172 $\pm$ 14 Mrd (air-equiv.) or 195 $\pm$ 16 Mrd (in EPR).

Table 2.11: Simultaneous Test #1 Accident Irradiation History. Reported dose rates are air equivalent values obtained from Table 2.10 (average values for the 37, 55, and 72 cm measurement locations). Absorbed doses in EPR will be 14% higher.

Time	Total Accident Dose (air equiv)	Event
0 hrs	0	Start 1st steam ramp
0 hrs, 30 min	0	Start irradiation at .71 Mrd/h
5 hrs	3.2 ± .3	Stop irradiation and prepare for 2nd steam ramp
5 hrs, 15 min	3.2 ± .3	Start 2nd steam ramp
5 hrs, 23 min	3.2 ± .3	Start irradiation at .71 Mrd/h
4 d, 1 hr, 5 min	68 ± 6	Stop irradiation and prepare to remove tensile specimens
4 d, 1 hr, 20 min	68 ± 6	Open steam chamber to remove tensile specimens
4 d, 2 hr, 30 min	68 ± 6	Restart steam exposure
4 d, 3 hr, 15 min	68 ± 6	Restart irradiation at .17 Mrd/h
8 d, 2 hr	84 ± 8	Reduce irradiation to .08 Mrd/h
9 d, 3 hr	86 ± 10	Unanticipated cooldown of steam chamber begins
9 d, 23 hr	88 ± 11	Stopped irradiation
11 d, 4 hr, 30 min	88 ± 11	Restarted steam exposure
11 d, 4 hr, 45 min	88 ± 11	Restarted irradiation (.08 Mrd/h)
24 d, 1 hr, 50 min	113 ± 30	Stopped radiation and steam exposures, opened chamber to removed tensile specimens

Throughout the steam exposure the cables were loaded at 480 Vac and 0.6 A. This exposure was interrupted to allow for insulation resistance measurements and during the unanticipated cooldown.

At the completion of the steam exposure we removed the tensile insulation specimens and then weighed them and measured their dimensions within six hours. After the chamber had cooled we performed a visual examination and then filled the chamber with tap water. Insulation resistance and leakage current measurements were then performed. These measurements were made without disturbing the cables that were wrapped on the mandrels. We did not follow the procedures of IEEE Std 383-1974,[4] Section 2.4.4 which states that the cables "should be straightened and

recoiled around a mandrel with a diameter of approximately 40 times the overall cable diameter" prior to performing the voltage withstand tests.

2.3.5 HIACA Simultaneous Test #2

2.3.5.1 Test Setup

The HIACA simultaneous test #2 was performed using a stainless steel steam chamber with ~ 0.4 m^3 of internal volume. The height is 200 cm and the diameter 52 cm. The top portion of the chamber (43 cm in length) contained all the penetration flanges through which cables, thermocouples, and other instrumentation entered and exited the chamber. The mandrels on which the cables were wrapped were suspended from the top portion of the chamber but were physically located inside the bottom portion of the chamber. This latter section of the chamber is 81 cm long. During both the aging and the accident exposures the chamber was supported as shown in Figure 2.1. This allowed for a simultaneous radiation exposure with the thermal aging and the accident steam exposures.

Cables were wrapped on three mandrels connected together end to end. The top of the mandrels was located 13 cm below the flange which connects the top and bottom portion of the steam chamber. Because of nonuniformities in the radiation field for most of the top mandrel, all of the cables were wrapped on the bottom two mandrels. We wrapped the single conductors on the inside of the mandrels using a 25 cm diameter. The multiconductors were wrapped on the outside of the mandrel on a 30 cm diameter. After wrapping the cables on the mandrels, the cable leads were spiraled up the inside of the mandrels to the exit ports.

A rubber stopper was fed from each end of the cable and inserted into a modified Swagelok^{tm} fitting. The modified Swagelok^{tm} fitting, when tightened, compressed the rubber stopper and provided a steam seal. Figure 2.8 illustrates the simultaneous test #2 setup.

We positioned the cables on the mandrels and prepared the cable flange penetrations prior to all aging and accident environmental exposures. Except for additional tightening of the modified Swagelok fittings, the cable lengths inside the chamber were not disturbed throughout the test. We used the stainless steel chamber as an oven, placed it in our radiation field, and used it as a steam pressure vessel. Insulation resistance and leakage current measurements were performed by filling the chamber bottom with water. We did visual examinations by using a crane to raise the top part of the chamber from the bottom part. Since the cables and mandrels were completely supported by the chamber top, no damage to the cables occurred during this operation.

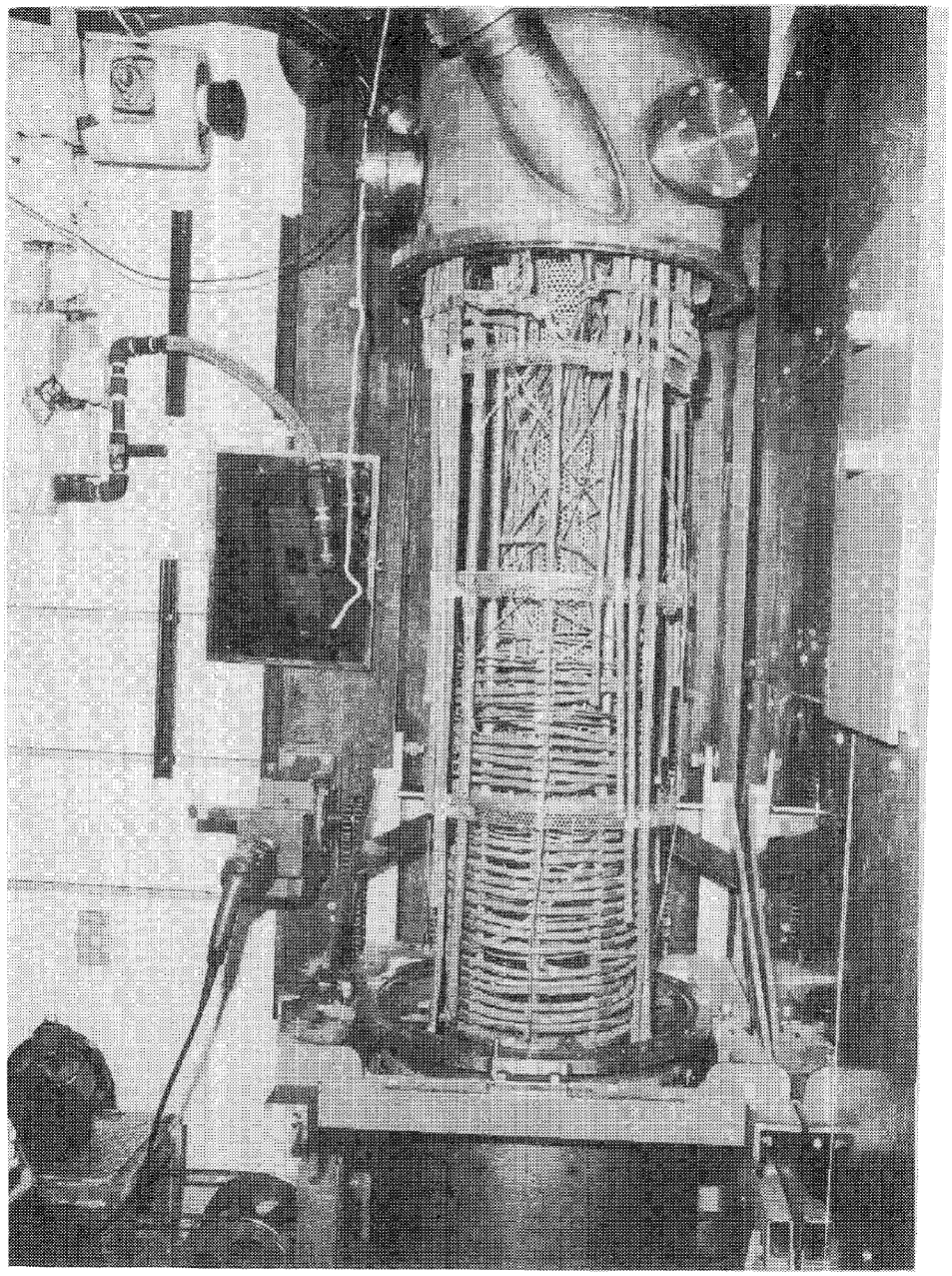

Figure 2.8. Simultaneous Test #2 Setup at the Completion of Aging

Each cable lead outside the steam chamber was ∿ 7.6 m (25 ft) long. These long segments were necessary to pass each cable from the steam chamber to the outside of the gamma irradiation cell. Insulation resistance and leakage current measurements were performed at this outside location.

Table 2.12 lists each EPR cable placed in the chamber for simultaneous #2 testing. (Note: Several XLPO and TEFZEL cables were also tested and are not listed.) The total length of each cable inside the steam chamber is given as well as each cable's location on the mandrel.

A perforated stainless steel cylinder was positioned along the centerline of the mandrels. Two 23 cm (9 in) long perforated stainless steel baskets containing insulation specimens were placed inside this cylinder during the aging and accident exposures.

2.3.5.2 Simultaneous Thermal and Radiation Aging

We positioned the stainless steel chamber in the gamma irradiation cell and connected it to a heater and blower. Airflow from the heater passed through a manifold containing twenty valves. Each valve was connected to a copper tube which entered a port to the interior of the chamber. The copper tubes were bundled into groups of 5 tubes and positioned vertically 90° apart around the circumference of the mandrel. Holes in the tubes directed airflow away from the cables towards the wall of the chamber. (Figure 2.8 illustrates the thermal aging setup.) Airflow to different positions in the chamber was controllable by valve adjustments external to the chamber. Hence we were able to adjust the temperature uniformity inside the chamber after the start of thermal aging without opening the chamber (as was done for simultaneous test #1).

We thermally aged the cables for 169 hours and then allowed the chamber to cool to ambient conditions. During thermal aging, airflow from the heater to the chamber included fresh air. We used air velocity measurements along the heater recirculation line to estimate the total airflow to the chamber as approximately 1.4 m^3/min. Of this, approximately 0.2 m^3/min was fresh air. This insured that oxygen was not depleted from the chamber during aging.

Table 2.12: Cable Positions on Mandrel During Simultaneous Test #2*

Cable Description		Cable Length Inside Chamber (m)	Distance Below Top of Mandrel (cm)
25 cm diameter wrappings			
EPR F:	insulated single conductor #1	5.5	49-52
EPR G:	insulated and jacketed single conductor #1	5.6	53-56
EPR D:	insulated single conductor #1	5.5	67-70
EPR F:	insulated single conductor #2	5.5	77-80
EPR G:	insulated and jacketed single conductor #2	5.5	82-85
EPR D:	insulated single conductor #2	6.1	95-99
30 cm diameter wrappings			
EPR D:	multiconductor #1	7.0	86-91
EPR D:	multiconductor #2	7.2	106-111

*TEFZEL and XLPO cables were also wrapped on the mandrel during this test.

Twenty-four thermocouples were positioned in the chamber to monitor temperature uniformity during thermal aging. We positioned five of the thermocouples at three positions along the outer rim of the stainless steel perforated cylinder used to support tensile specimen baskets. Seventeen thermocouples were positioned at 16 different locations within 2.5 cm of the cables wrapped on the mandrels. Two thermocouples were positioned near the top of the chamber at the exit ports. Twenty-two of these thermocouples were connected to a datalogger, one was connected to a strip chart recorder, another was used for control purposes. Table 2.13 presents the temperature distribution midway through the thermal exposure. Table 2.14 summarizes the temperature values versus time for several of the thermocouple positions.

Table 2.13: Thermocouple Readings 85 Hours After the Start of a 169 Hour Thermal Aging Exposure (Part of simultaneous #2 radiation and thermal exposure).

(a) Distance below top of mandrel (cm)	Temperature (°C) 0°	90°	180°	270°
44 cm	140	139	140	142 (7)
67 cm	142	140 (5)	140	141 (6)
91 cm	140 (3)	139	141 (4)	140
111 cm	133	132	140 (1)	130 (2)

(b) Distance below top of mandrel (cm)	Temperature (°C)
40	138
58	137
99	133

(a) Thermocouples were positioned around the circumference of the mandrel, spaced 90° apart and within 2.5 cm of the cables. The copper heating tubes were also positioned around the circumference of the mandrel, spaced 90° apart, and displaced 45° from the thermocouples.

(b) Thermocouples were positioned along the outer rim of the perforated cylinder used to support tensile specimen baskets.

(c) (1)-(7) indicate thermocouple positions monitored by Table 2.14.

Elapsed Time	Temperature (°C) at Thermocouple Position 1	2	3	4	5	6	7
0 hrs	34	35	34	35	35	35	35
0 hrs, 18 min	81	78	74	83	79	85	77
0 hrs, 28 min	103	97	96	106	102	107	102
0 hrs, 48 min	133	124	128	136	134	139	137
0 hrs, 58 min	144	135	138	147	145	150	149
1 hr, 8 min	147	136	142	147	148	150	151
1 hr, 18 min	139	129	136	138	140	141	143
1 hr, 28 min	133	125	130	133	133	137	139
2 hrs	133	131	136	138	140	141	142
3 hrs	136	129	140	137	138	141	142
4 hrs	140	133	139	140	137	140	141
5 hrs	142	132	141	143	138	141	142
10 hrs	140	131	140	141	137	139	140
15 hrs	141	132	140	141	138	140	141
20 hrs	140	131	140	141	138	138	141
25 hrs	140	130	139	141	139	140	141
30 hrs	139	129	139	140	138	140	141
35 hrs	139	129	139	140	138	139	141
40 hrs	140	130	140	141	140	140	142
45 hrs	140	130	140	142	140	141	142
50 hrs	140	130	140	141	139	140	142
55 hrs	140	130	140	141	140	140	142
60 hrs	140	130	140	141	139	140	142
65 hrs	paper feed failure						
70 hrs	140	130	140	141	140	141	142
75 hrs	140	129	140	141	139	141	142
80 hrs	140	130	140	142	140	141	142
85 hrs	140	130	140	141	140	141	142
90 hrs	140	130	140	142	140	141	143
95 hrs	139	129	140	141	140	140	142
100 hrs	140	129	140	142	140	141	142
105 hrs	139	129	140	142	140	141	142
110 hrs	140	130	141	142	140	142	143
115 hrs	139	128	140	142	140	141	142
120 hrs	139	129	140	142	140	141	142
125 hrs	139	129	140	142	140	141	142
130 hrs	139	128	140	142	140	141	142
135 hrs	139	128	140	142	140	141	143
140 hrs	138	128	139	141	139	140	142
145 hrs	139	128	140	142	140	141	143
150 hrs	138	128	140	142	140	141	143
155 hrs	138	128	148	141	140	141	142
160 hrs	138	128	140	142	140	141	143
165 hrs	139	130	141	142	139	141	142
169 hrs	139	131	141	142	139	140	141
170.5 hrs	64	68	64	64	65	65	69
172.5 hrs	41	41	41	41	40	41	41

Table 2.14: Temperature Versus Time Profile During Simultaneous Test #2 Thermal and Radiation Aging Exposure. Thermocouple positions (1)-(7) are identified in Table 2.13.

For 143 hours of the 169 hour thermal exposure we simultaneously irradiated the cables and tensile specimens. This radiation exposure was continuous. We used our simultaneous test #1 dosimetry corrected for Co-60 decay to estimate the gamma dose rates during aging (see Table 2.15). The average dose rate was .30 ± .03 Mrd/h (air-equiv). Thus the aging radiation dose was 43 ± 4 Mrd. The absorbed dose in EPR is 14% higher than the air-equivalent dose. This gives an aging dose of 49 ± 5 Mrd (in EPR)

At completion of the simultaneous aging program we performed a visual inspection, insulation resistance and AC leakage current measurements. The entire chamber with cables was then stored at ambient conditions until the start of the LOCA steam and radiation simulation (8 days after completion of the aging exposure.)

Table 2.15: Radiation Dose Rates (air-equiv) Used During Simultaneous Test #2. Dose rates were calculated from Table 2.10 data allowing for 8 months Co-60 decay between exposures.

Measurement location below top of mandrel	Aging Dose Rate (Mrd/h)	Accident Dose Rates* Mrd/h 1	2	3
50 cm (along centerline)	.29 ± .01	.57 ± .03	.15 ± .01	.057 ± .002
Within 2.5 cm of the cables				
14 cm	.26 ± .03	.54 ± .05	.12 ± .01	.06 ± .04** .03
37 cm	.31 ± .03	.61 ± .05	.16 ± .02	.07 ± .05
55 cm		.71 ± .06		
72 cm	.29 ± .03	.62 ± .05	.16 ± .02	.06 ± .01

* The three different dose rate columns refer to the three Co-60 configurations used during simultaneous test #2.

**Large uncertainties reflect gradients in radiation field.

Note: Co-60 pencils extend from 10 cm to 130 cm below the top of the mandrel. Hence the 72 cm dosimetry data is applicable to those cables and tensile specimens positioned between 72 and 111 cm below the mandrel.

2.3.5.3 Simultaneous Steam and Radiation Exposure

Figure 2.9 summarizes our intended steam and radiation profile. The steam profile is similar to the IEEE 323-1974, Appendix B profile[3], but also different in several respects, most notably:

1. After four days of steam exposure we interrupted the steam exposure to remove baskets containing tensile specimens.

2. We used a 104°C saturated steam exposure after four days until the end of the test.

3. We did not apply chemical spray during the exposure.

4. We did not start our transient ramps at 60°C.

Three nonconformances kept us from achieving the steam and radiation profile.

1. Prior to the first ramp we momentarily passed steam through the chamber (which was open to ambient conditions)

2. During the first 171°C saturated steam peak water accumulated in the bottom of the steam chamber and submerged some cables. We estimate the maximum water level as between 67 and 91 cm below the top of the mandrel. (See Table 2.12 for cable positions.) We drained the water from the chamber 1-1/2 hours after the start of the first steam peak. This problem did not recur.

3. On day 16 of the steam exposure our steam supply system failed and the steam chamber cooled to ambient temperatures and pressures. Eight hours later we stopped the irradiation of the samples. On day 18 we opened the chamber and performed ambient insulation resistance and leakage resistance measurements. We also performed a visual inspection. We then removed one EPR D single conductor and one EPR D multiconductor cable as well as all the tensile specimens. On day 21 we resumed the steam and radiation exposures for the cables. We ended these exposures on day 25 for a total steam exposure of 21 days.

Table 2.16 summarizes our steam temperatures during simultaneous test #2. Table 2.17 presents the accident irradiation history. The total accident dose was 106 $\pm$ 20 Mrd (air-equiv). This gives a total accident and aging dose of 146 $\pm$ 23 Mrd (air-equiv) or 166 $\pm$ 26 Mrd (in EPR).

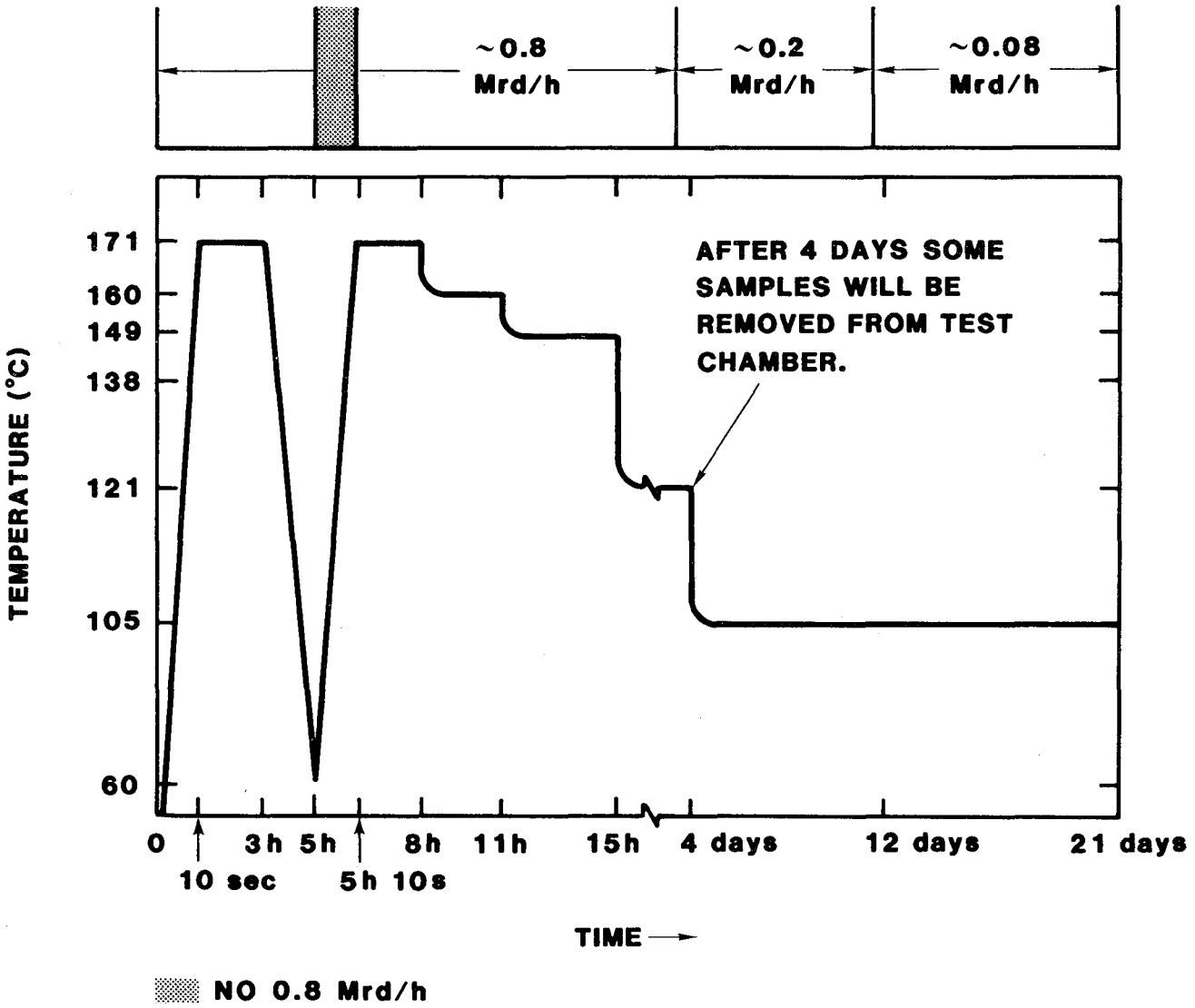

Figure 2.9. Simultaneous Test #2 Profile (as proposed by test plan). Pressures correspond to saturated steam conditions in Albuquerque, NM (171°C corresponds to 106 psig).

Table 2.16

Steam Profile Achieved During Simultaneous Test #2. Except during transient ramps and where noted,*, the temperatures correspond to saturated steam conditions in Albuquerque, New Mexico. An * indicates the chamber was opened to remove samples or that saturated steam conditions were not maintained.

Elapsed	Chamber temperature (°C) at distance below top of mandrel			
	111 cm	91 cm	67 cm	44 cm
0 hrs	26*	22*	30*	27*
momentarily passed steam through the chamber				
10 sec	75*	88*	85*	86*
20 sec	65*	79*	78*	79*
30 sec	60*	72*	71*	74*
40 sec	56*	65*	66*	70*
1 min	52*	57*	60*	67*
2 min	49*	51*	55*	61*
2 min, 30 sec	49*	50*	54*	60*
First ramp started; water accumulation				
2 min, 40 sec	142*	162*	157*	165*
2 min, 50 sec	143*	165*	169*	171*
3 min	---	169*	170*	171*
4 min	135*	167*	171*	171*
5 min	137*	165*	171*	171*
17 min	141*	160*	169*	171*
27 min	141*	159*	169*	171*
1 hr	140*	157*	168*	171*
1 hr, 17 min	144*	159*	166*	168*
1 hr, 27 min	146*	159*	166*	168*
Start drawing water from chamber				
1 hr, 37 min	168*	169*	170*	170*
1 hr, 47 min	171	172	172	171
2 hrs	171	172	172	172
3 hrs	171	172	171	171
3 hrs, 17 min	171	172	172	172
3 hrs, 37 min	165	165	165	165
4 hrs	156	156	156	156
4 hrs, 27 min	138	138	138	138
5 hrs	116	117	116	116
5 hrs, 20 min	100	104	103	105
5 hrs, 20 min, 10 sec	130	136	127	143
5 hrs, 20 min, 20 sec	162	162	162	164
5 hrs, 20 min, 30 sec	171	171	171	171
6 hrs	171	171	171	171
7 hrs	171	171	171	171
8 hrs	171	171	171	171

Table 2.16 (cont.)

Elapsed	Chamber temperature (°C) at distance below top of mandrel 111 cm	91 cm	67 cm	44 cm
8 hrs, 20 min	171	172	171	171
8 hrs, 30 min	169	170	170	170
9 hrs	160	161	161	161
10 hrs	160	161	160	160
11 hrs	161	161	161	161
11 hrs, 40 min	160	160	160	161
11 hrs, 50 min	158	158	158	158
12 hrs	152	153	152	153
12 hrs, 10 min	149	149	149	149
13 hrs	149	150	149	149
15 hrs	149	149	149	149
15 hrs, 20 min	140	140	140	140
15 hrs, 30 min	133	133	133	133
15 hrs, 40 min	123	123	124	123
15 hrs, 50 min	121	122	121	121
16 hrs	121	121	121	122
20 hrs	121	122	121	122
1 d, 6 hrs	122	122	122	122
1 d, 16 hrs	122	122	122	122
2 d, 2 hrs	122	122	122	122
2 d, 12 hrs	122	122	122	122
2 d, 22 hrs	122	122	122	122
3 d, 8 hrs	122	122	122	122
3 d, 18 hrs	122	122	122	122
4 d, 20 min	121	121	121	121
Opened chamber				
4 d, 50 min	90*	90*	90*	89*
4 d, 1 hr, 20 min	88*	88*	88*	88*
Reintroduced steam				
4 d, 1 hr, 50 min	105	106	106	106
4 d, 4 hrs	105	105	105	105
4 d, 14 hrs	105	106	106	106
5 d	105	106	106	106
5 d, 10 hrs	105	105	105	105
5 d, 20 hrs	106	106	106	106
6 d, 6 hrs	105	105	105	105
6 d, 16 hrs	105	106	106	106
7 d, 2 hrs	105	105	105	105
7 d, 12 hrs	106	106	106	106
7 d, 22 hrs	106	106	106	106
8 d, 8 hrs	106	106	106	106
8 d, 18 hrs	106	107	107	106
9 d, 4 hrs	106	106	106	106
9 d, 14 hrs	106	106	106	106
10 d	106	106	106	106
10 d, 10 hrs	106	106	106	106

Table 2.16 (cont.)

Elapsed	Chamber temperature (°C) at distance below top of mandrel 111 cm	91 cm	67 cm	44 cm
10 d, 20 hrs	105	106	106	106
11 d, 6 hrs	105	105	105	105
11 d, 16 hrs	106	106	106	106
12 d, 2 hrs	106	106	106	106
12 d, 12 hrs	106	106	106	106
12 d, 22 hrs	106	106	106	106
13 d, 8 hrs	106	106	106	106
13 d, 18 hrs	105	106	106	105
14 d, 4 hrs	105	106	106	106
14 d, 14 hrs	106	106	106	106
15 d	107	107	107	107
15 d, 10 hrs	106	106	106	106
15 d, 20 hrs	106	106	106	106
16 d, 6 hrs	106	106	106	106
16 d, 14 hrs	105	105	105	105
Steam supply failure				
16 d, 15 hrs	92*	93*	92*	93*
16 d, 17 hrs	60*	61*	62*	61*
16 d, 19 hrs	47*	47*	47*	48*
16 d, 21 hrs	40*	40*	40*	40*
16 d, 23 hrs	36*	36*	36*	36*
17 d	35*	35*	35*	35*
17 d, 5 hrs	32*	32*	32*	32*
17 d, 10 hrs	31*	31*	31*	31*
17 d, 20 hrs	30*	29*	30*	30*
21 d, 1 hr, 42 min	27*	28*	28*	29*
21 d, 1 hr, 43 min	27*	28*	29*	32*
21 d, 1 hr, 44 min	28*	30*	102*	102*
Reintroduced steam				
21 d, 1 hr, 45 min	103	103	103	103
21 d, 1 hr, 46 min	105	105	105	105
21 d, 2 hrs	105	105	105	105
21 d, 5 hrs	106	105	106	106
21 d, 10 hrs	105	106	105	106
21 d, 20 hrs	105	105	106	106
22 d, 6 hrs	105	105	105	105
22 d, 16 hrs	105	106	106	106
23 d, 2 hrs	105	105	106	105
23 d, 12 hrs	105	106	106	106
23 d, 22 hrs	106	107	107	106
24 d, 8 hrs	105	105	105	105
24 d, 18 hrs	105	105	105	105
25 d, 4 hrs	105	106	106	106
Steam turned off				

Table 2.17: Simultaneous Test #2 accident Irradiation History. Reported dose rates are air equivalent values obtained from Table 2.15 (average values for the 37, 55, and 72 cm measurement locations.) Absorbed doses in EPR will be 14% higher.

Time	Total Accident Dose (air equiv)	Event
0 hrs	0	Start steam exposure
0 hrs, 14 min	0	Start irradiation at .65 Mrd/h
5 hrs, 8 min	3.3 ± .3 Mrd	Stop irradiation and prepare for 2nd steam ramp
5 hrs, 20 min	3.3 ± .3 Mrd	Start 2nd steam ramp
5 hrs, 34 min	3.3 ± .3 Mrd	Start irradiation at .65 Mrd/h
4 d, 20 min	63 ± 5 Mrd	Stop irradiation and prepare to remove tensile specimens
4 d, 1 hr, 25 min	63 ± 5 Mrd	Restart steam exposure
4 d, 1 hr, 43 min	63 ± 5 Mrd	Start irradiation at .16 Mrd/h
5 d, 2 hr	67 ± 5 Mrd	Interrupt irradiation for 12 minutes
11 d, 23 hr, 20 min	93 ± 9 Mrd	Reduce irradiation to .06 Mrd/hr
12 d, 22 hr	94 ± 10 Mrd	Interrupted irradiation for 14 minutes
12 d, 21 hr, 50 min	97 ± 13	Switched Co-60 configuration, dose rate = .06 Mrd/h
16 d, 14 hr	99 ± 14 Mrd	Start of unanticipated cooldown
16 d, 23 hr, 35 min	100 ± 15 Mrd	Stop irradiation
21 d, 1 hr, 45 min	100 ± 15 Mrd	Restart steam exposure
21 d, 4 hrs, 14 min	100 ± 15 Mrd	Restart irradiation at .06 Mrd/h
25 d, 4 hrs	106 ± 20 Mrd	End steam and radiation exposure

Throughout most of the steam exposure the cables were loaded at 480 Vac and 0.6 A. Exceptions were during the first transient peak (severe water leakage from the Tefzel cables also in the chamber required us to reconfigure the loading circuit), during insulation resistance measurements, and during the unanticipated cooldown period.

During the unanticipated cooldown we removed the tensile insulation specimens and then weighed them and measured their dimensions. These samples were not reinserted into the chamber prior to restarting the steam exposure.

At the completion of the steam and radiation exposures we performed a visual examination and then filled the chamber with water. Insulation resistance and leakage current measurements were then performed. These measurements were made without disturbing the cables that were wrapped on the mandrels. We did not follow the procedures of IEEE Std 383-1974, Section 2.4.4 which states that the cables "should be straightened and recoiled around a mandrel with a diameter of approximately 40 times the overall cable diameter" prior to performing the voltage withstand tests.

3.0 Results

3.1 EPR A and EPR A'

EPR A multiconductor cables, single conductor cables, and insulation specimens were exposed during the sequential and simultaneous #1 tests. These materials were purchased in 1977. A 1981 purchase of the "same or improved" cable product was obtained prior to simultaneous test #1. Multiconductor and single conductor "1981 cables" were exposed during this latter test; results are identified as for EPR A'. We generated the single conductor cables by carefully disassembling multiconductor cables.

3.1.1 Electrical results

Insulation resistance (I.R.) measurements were performed periodically throughout the aging and accident exposures. Figures 3.1-3.3 illustrate the I.R. behavior for the single conductor, single conductor with primary jacket, and multiconductor, respectfully. Figure 3.4 gives I.R. results for EPR A'. For the single conductor, I.R. measurements were performed between the conductor and the grounded steam chamber (which contained either steam or water). For the multiconductors, I.R. measurements were performed between the conductor and the grounded steam chamber with the other conductors of the multiconductor guarded. Insulation Resistance measurements recorded for day 11 were during the unanticipated room temperature cooldown and are several orders of magnitude larger than those recorded during the steam exposure.

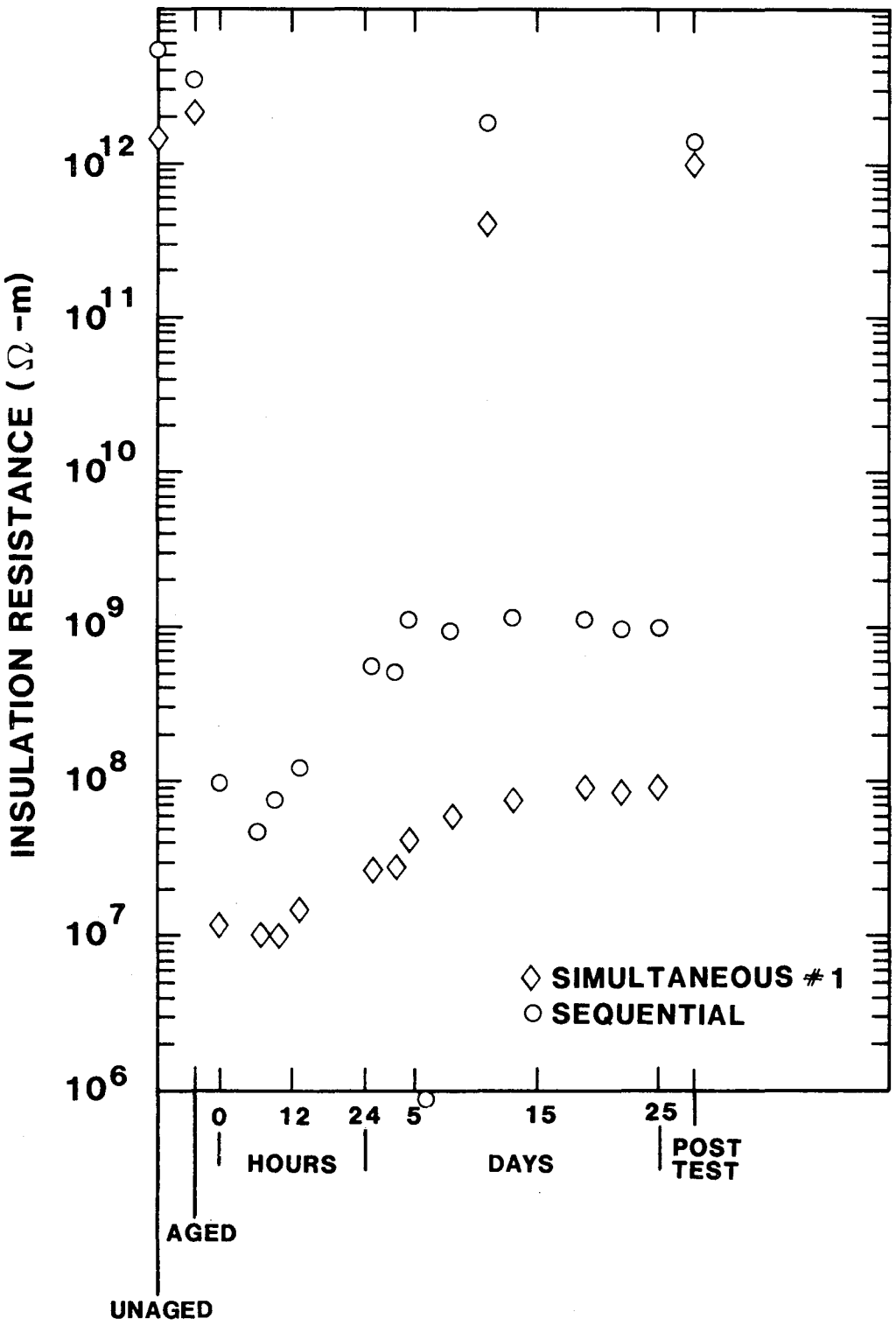

Figure 3.1. Insulation Resistance for EPR A: Single Conductor with Primary Insulation

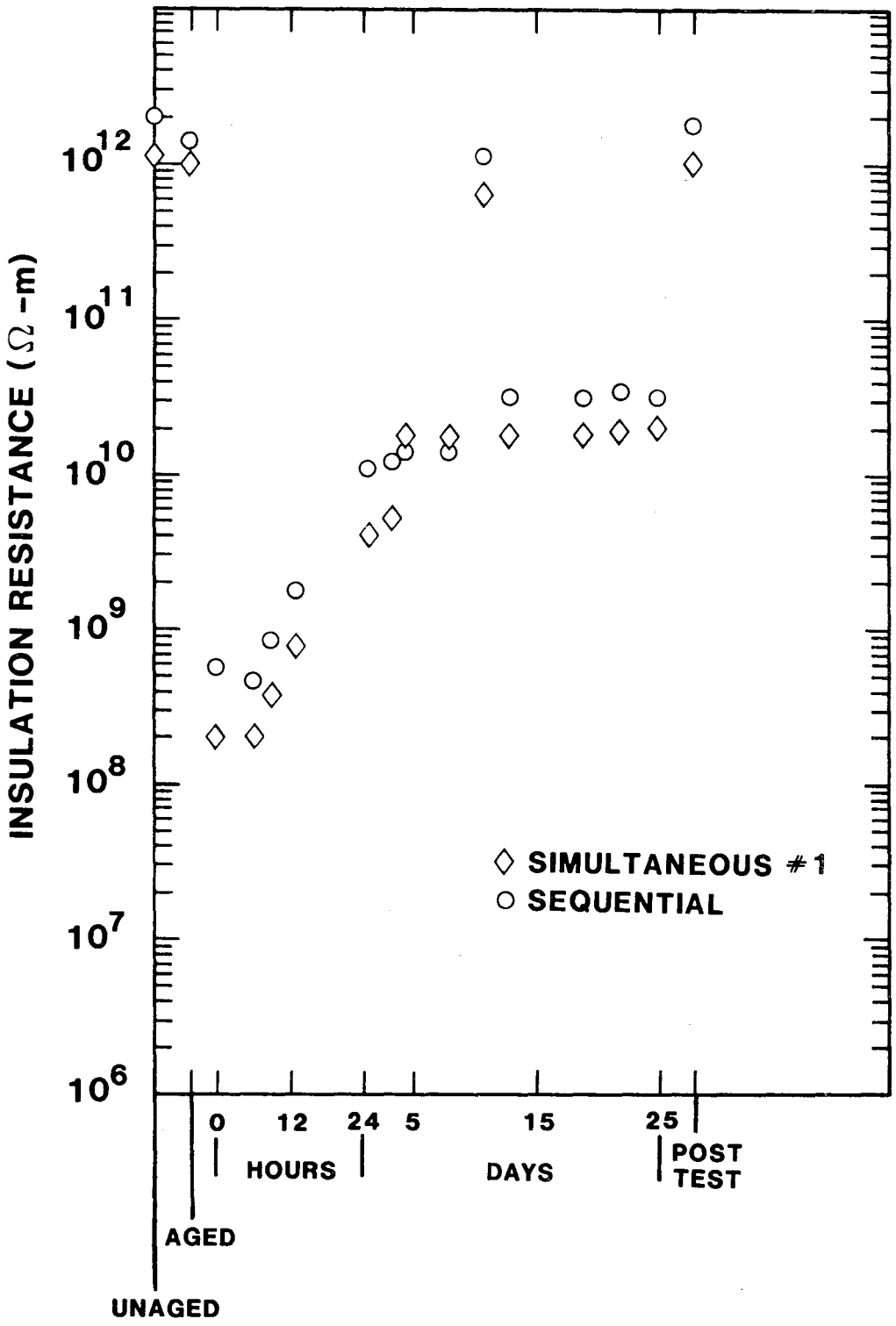

Figure 3.2. Insulation Resistance for EPR A: Single Conductor with Primary Insulation and Jacket

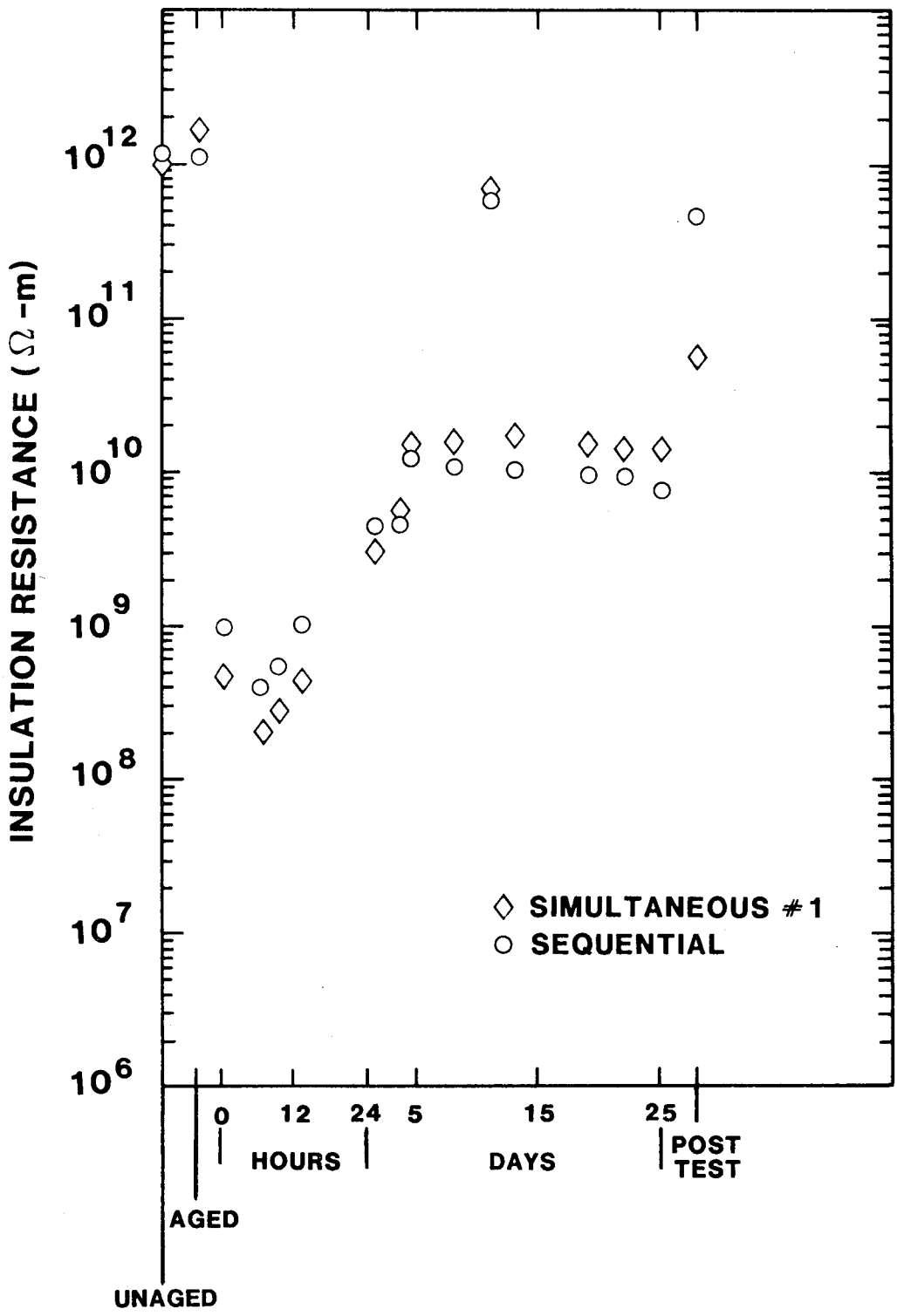

Figure 3.3. Insulation Resistance for EPR A Multiconductor

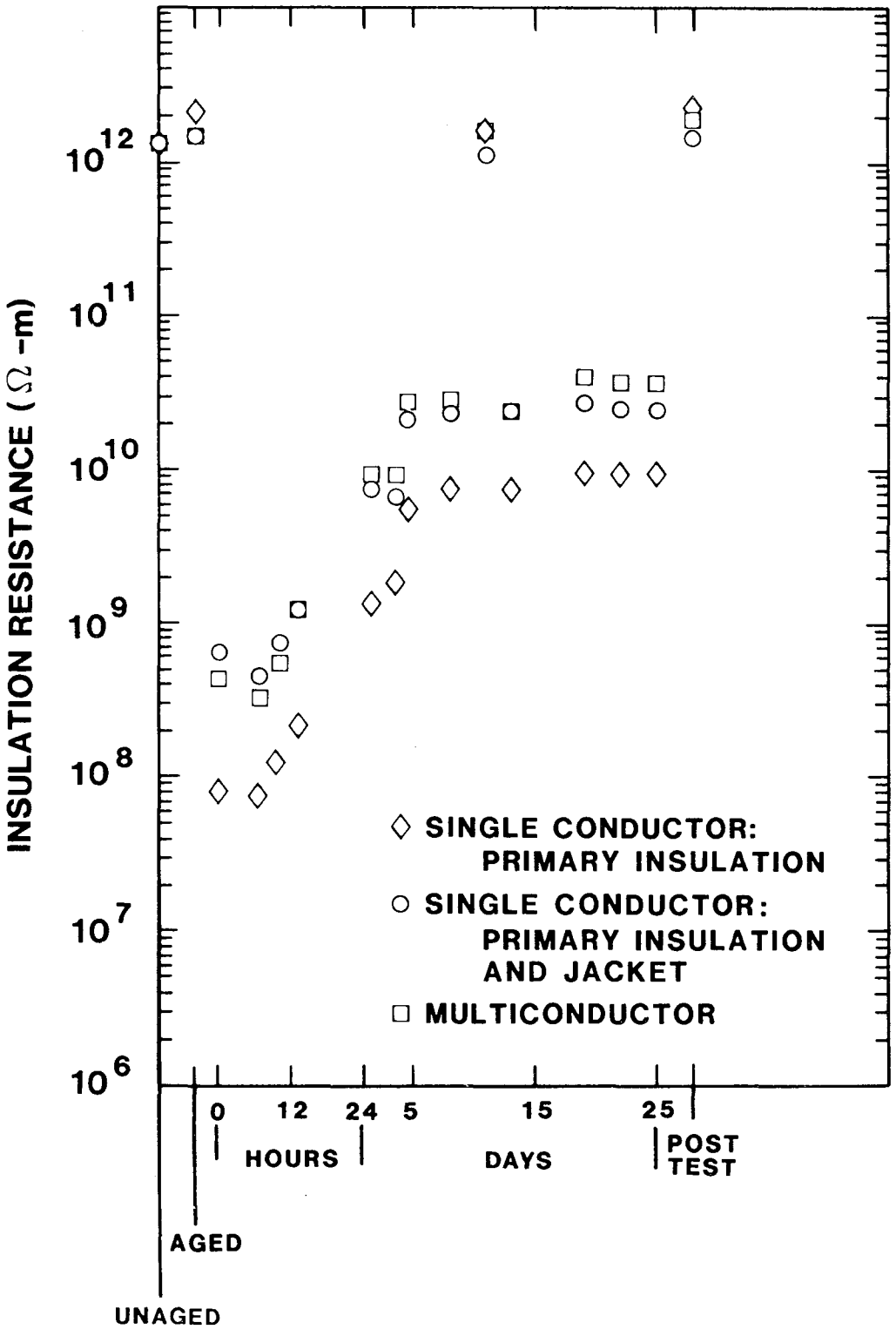

Figure 3.4. Insulation Resistance for EPR A' Cables During Simultaneous Test #1

Leakage current data obtained during post-test measurements is summarized in Table 3.1 During these tests, the cables were immersed into a grounded water bath. The single conductor measurements were between the conductor and a grounded tap water bath. For multiconductors, one conductor of the multiconductor was electrified, the others were grounded as was the water bath.

3.1.2 Insulation Specimens

We obtained tensile specimens by carefully disassembling a multiconductor, stripping the single conductor primary jacket from the insulation (they were not bonded together) and then removing the stranded conductor from the center of the insulation. Some of these EPR A tensile specimens were exposed with the cables during the HIACA sequential and simultaneous #1 tests. In addition, other tensile specimens were aged by seven different simulations (see Section 2.3.2) using Sandia's LICA facility. At completion of aging, we inserted these latter samples into the HIACA steam chambers at appropriate test points so that for each of the seven aging populations, one-third of the tensile specimens were exposed to one of three accident simulations:

1. Sequential accident irradiation then steam exposure (the sequential accident test)

2. Simultaneous accident irradiation and steam exposure (simultaneous accident test #1)

3. Steam exposure only (the steam exposure of the sequential test).

Unaged tensile specimens were also exposed to these accident simulations.

After four days of the LOCA simulations all samples were removed from the steam chamber. This was necessitated by EPR A's unexpected response to the accident environments. Many samples experienced complete reversion and lost their original form. For many sample groups, monitoring weight, dimensional, and tensile property changes was impossible. Table 3.2 summarizes the visual appearance of the sample groups at the completion of the four day LOCA exposures. We define:

Blooming: Migration of components (waxes, oils, activators) to the surface due to induced stresses. Surface is not broken.

Measling: Migration of components (waxes, oils, activators) to the surface. Surface is broken.

Reversion: Change to a linear polymer that allows flow

and use these terms to describe the visual appearance of EPR A.

Leakage Current (mA)

Applied Voltage	Sequential Test	Simultaneous Test #1
EPR A: primary insulation		
600 Vac	0.7	0.7
1200 Vac	1.3	1.3
1800 Vac	2.0	1.9
2400 Vac	2.6	3.0
EPR A': primary insulation with jacket		
600 Vac	0.7	0.7
1200 Vac	1.3	1.4
1800 Vac	1.9	2.1
2400 Vac	2.5	2.7
EPR A: multiconductor		
600 Vac	1.1	1.2
1200 Vac	2.0	2.3
1800 Vac	3.0	3.4
2400 Vac	4.0	4.5
EPR A': primary insulation		
600 Vac		0.6
1200 Vac		1.2
1800 Vac		1.8
2400 Vac		3.1
EPR A': primary insulation with jacket		
600 Vac		0.5
1200 Vac		1.0
1800 Vac		1.5
2400 Vac		2.0
EPR A': multiconductor		
600 Vac		1.0
1200 Vac		1.9
1800 Vac		2.9
2400 Vac		3.8

Table 3.1: Post-Test Leakage Current Values for EPR A and A' Cables. Measurements were made at the completion of a one minute electrification for the 600, 1200, and 1800 Vac exposures and at the completion of a five minute electrification at 2400 Vac.

Table 3.2: EPR A Visual appearance after 4 day LOCA steam exposures.

Aging Method*	Simultaneous Radiation & Steam	Sequential Radiation Then Steam	Steam Only
Unaged	Silverish regions	Relaxation of stresses induced by stripping of wire	--
4 d T + R**	Silverish regions; dried out	Blooming and permanent set	Slight drying out
30 d T + R	Slight reversion	Surface cracking Considerable blooming Silverish regions	Complete reversion
28 d T → 28 d R	Blooming Small permanent set	Severe blooming Mild permanent set	Relaxation of stresses induced by stripping of wire
28 d R → 28 D T	Complete reversion	Surface cracking Some reversion near ends Loss of ingredients	Complete reversion
28 d T → 55 h R	Dried out Small amount of permanent set	Blooming Slight reversion	Some permanent set Some stress relaxation
55 h R → 28 d T	Considerable permanent set Partial reversion but rentention of form	Severe blooming Some reversion but retention of form	Almost total reversion
7 d T + R	Range of reversion from minor to severe	Surface cracking Dry surface Silverish regions	Severe surface cracking Substantial reversion but some retention of form
HIACA aging (with cables)	Some reversion but retention of form	Mild blooming	

*See Section 2.3.2 for aging details.
**$\sim$5 year life. All other aging procedures represent $\sim$40 year life.

We did note a range of visual appearance among the five to ten samples of each aging group. Our tensile specimens were a randomized selection of samples obtained from each of the three conductors of the EPR A multiconductor. Since each conductor's insulation may have been processed slightly differently, we expect behavioral differences within a single aging and accident group of samples.

Table 3.3.a presents tensile property data for those samples aged in the HIACA test chambers while Table 3.3.b illustrates similar data for the samples aged using the LICA facility.

3.2 EPR B

EPR B single conductor cables (with and without a jacket) and insulation tensile specimens were exposed during the sequential test and simultaneous test #1.

3.2.2 Electrical Results

Insulation resistance (I.R.) measurements were performed periodically throughout the aging and accident exposures. Figure 3.5 illustrates the I.R. behavior of an EPR B single conductor with only primary insulation while Figure 3.6 shows I.R. measurement results for an EPR B single conductor with both a primary insulation and a chlorosulfonated polyethylene jacket. Insulation resistance measurements recorded for day 11 were during the unanticipated room temperature cooldown and are several orders of magnitude larger than those recorded during the steam exposure. For both constructions I.R. behavior was not sensitive to the differences between our simultaneous and sequential testing procedures.

In Table 3.4 we summarize our leakage current data obtained during post test measurements. We observed no significant leakage current differences caused by the differences between our simultaneous and sequential test procedures.

3.2.2 Insulation Specimens

Insulation specimens were used to monitor weight changes, dimensional changes, and tensile properties. We removed specimens after the first four days and also at the completion of the steam exposure.

Table 3.5 summarizes the percentage increase in insulation specimen weight, length, and outer diameter during the LOCA simulations. Except for some shrinkage in the EPR B during sequential testing, weight and size changes are comparable for the two LOCA simulations.

	Sequential HIACA Exposures		Simultaneous HIACA Exposures	
	Ultimate Tensile Elongation e/e_o	Ultimate Tensile Strength T/T_o	Ultimate Tensile Elongation e/e_o	Ultimate Tensile Strength T/T_o
Unaged	1.00 ± .02 (360 ± 30%)	1.00 ± .07 (8.7 ± 0.3 MPa)	1.00 ± .02 (360 ± 30%)	1.00 ± .07 (8.7 ± 0.3 MPa)
Aged	.29 ± .03	.96 ± .09	.05 ± .03	.23 ± .02
After Sequential Accident Irradiation	.16 ± .01	.86 ± .13		

Table 3.3.a: Tensile Properties for EPR A Samples Aged Using the HIACA Facility (the Sequential and Simultaneous #1 Tests).

Aging Method***	After Aging		After Sequential Accident Irradiation	
	Ultimate Tensile Elongation e/e_o	Ultimate Tensile Strength T/T_o	Ultimate Tensile Elongation e/e_o	Ultimate Tensile Strength T/T_o
Unaged	1.00 ± .08 (360 ± 30%)	1.00 ± .03 8.7 ± 0.3 MPa)	.32 ± .04	.65 ± .03
4 d T + R	0.88 ± .08	0.98 ± .06	.26 ± .03	.61 ± .05
30 T + R	< .03*	∿ 0.2*	**	**
28 d T → 28 d R	0.33 ± .04	0.85 ± .03	.18 ± .03	.59 ± .14
28 d R → 28 d T **	< .03*	0.26 ± .07*		**
28 d T → 55 h R	0.31 ± .04	0.99 ± .21	.19 ± .04	.64 ± .06
55 h R → 28 d T	0.06 ± .03	0.21 ± .02	∿ .03	.18 ± .01
7 d T + R	0.03 ± .03	0.26 ± .02	∿ .03*	< .36*

NOTES: (1) Errors reflect one standard deviation of three measurements.
(2) Insulation thickness is nominally 0.8 mm.
* Samples were extremely brittle and sometimes cracked in the pneumatic jaws used for the tensile measurements.
** Samples were too brittle to measure.
*** See Section 2.3.2 for aging details.

Table 3.3.b: Relative Tensile Properties of EPR A After LICA Aging + HIACA Sequential Accident Irradiation.

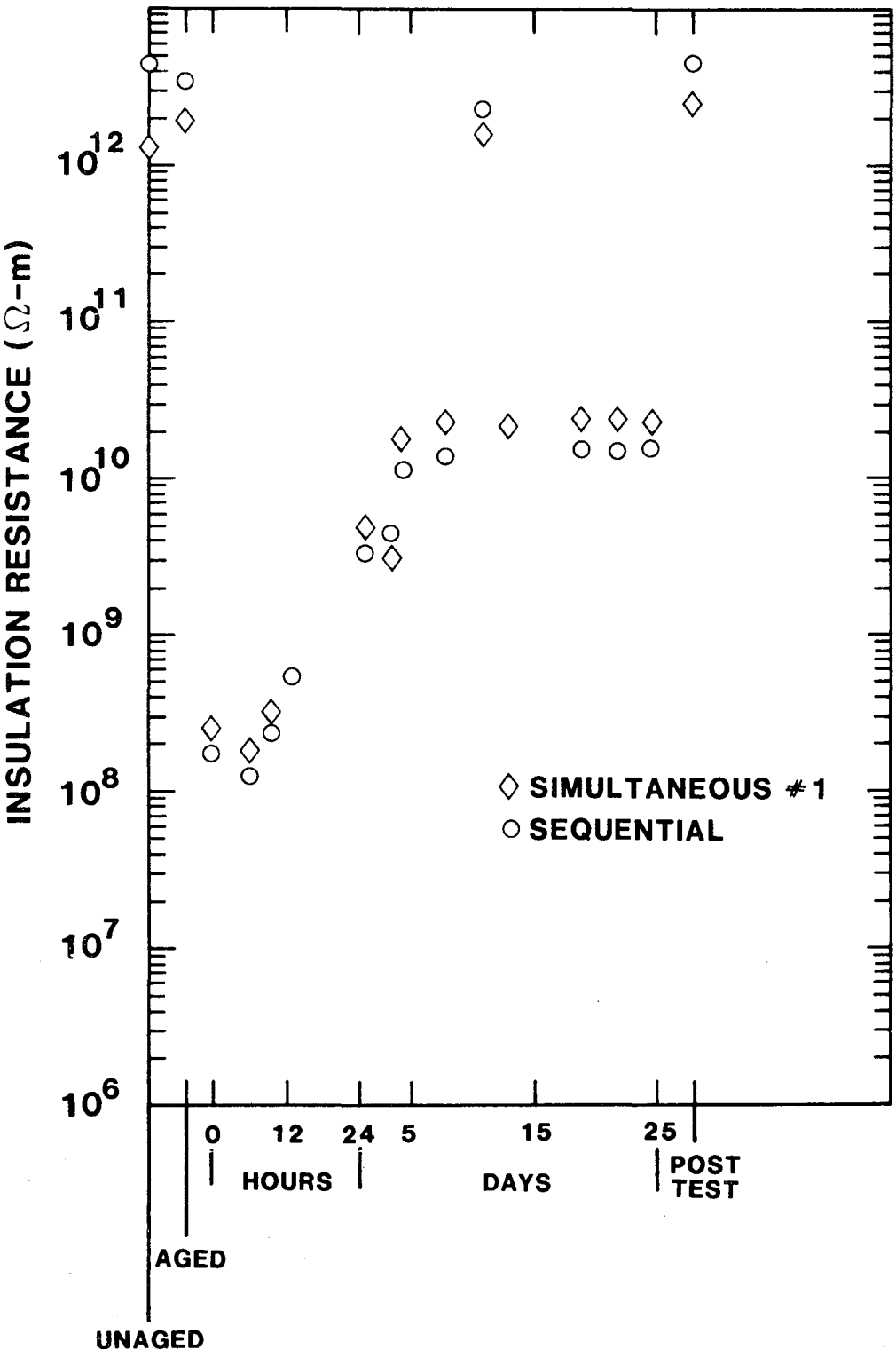

Figure 3.5. Insulation Resistance for EPR B Single Conductors with Primary Insultation

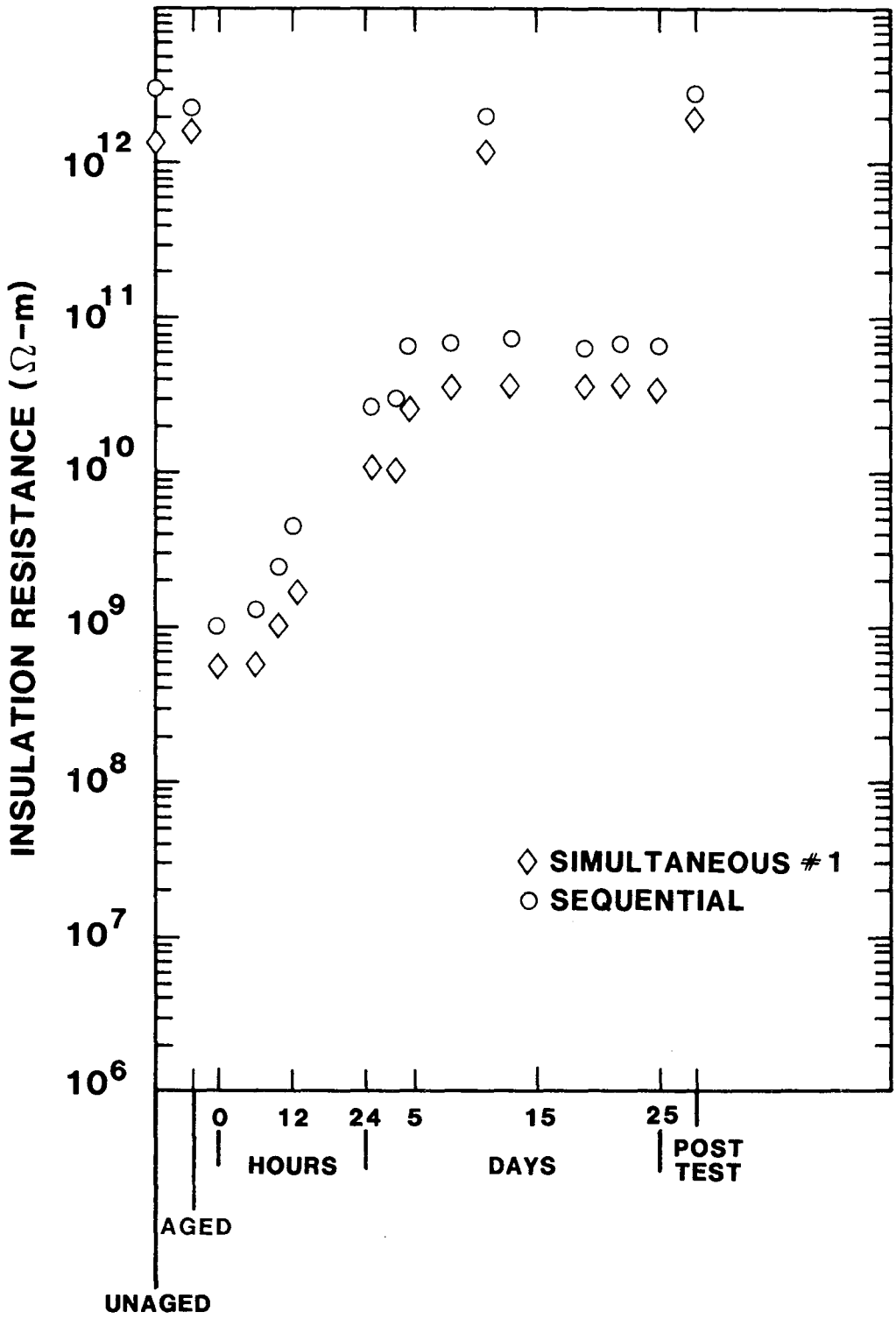

Figure 3.6. Insulation Resistance for EPR B Single Conductors with Primary Insulation and Jacket

Applied Voltage	Leakage Current (mA) Sequential Test	Simultaneous Test #1
Primary insulation only		
600 Vac	0.8	0.6
1200 Vac	1.5	1.2
1800 Vac	2.2	1.7
2400 Vac	2.9	2.3
Primary insulation and jacket		
600 Vac	0.8	0.7
1200 Vac	1.5	1.3
1800 Vac	2.2	1.9
2400 Vac	2.9	2.5

Table 3.4: Leakage Current Values for EPR B Single Conductor Cables at the Completion of Test Exposures. Measurements were made at the completion of one minute electrification for the 600, 1200, and 1800 Vac exposures and at the completion of a five minute electrification at 2400 Vac. Measurements were between the copper conductor and a grounded water bath.

	Sequential Test	Simultaneous Test #1
Weight Increase		
4 d LOCA	2 ± 1	0 ± 1
End of LOCA	4 ± 1	-1 ± 1
Length Increase		
4 d LOCA	0 ± 3	-2 ± 3
End of LOCA	-2 ± 3	0 ± 3
Outer Diameter Increase		
4 d LOCA	-5 ± 3	-5 ± 3
End of LOCA	-18 ± 3	-5 ± 3

Table 3.5: Percentage Increase for EPR B Insulation Specimen Properties

Ultimate tensile elongation and ultimate tensile strength were measured prior to aging, after aging, after 4 days of LOCA exposure, and at the completion of the LOCA exposure. Tensile measurements were made within 24 hours of removing the tensile specimens from the steam environment and also several months after removing the specimens from the steam chamber. We monitored the weight of the samples to ensure that it had stabilized prior to performing these latter measurements. Results are given in Table 3.6.

3.3 EPR C

An EPR C multiconductor and an EPR C single conductor cable were exposed to simultaneous test #1. (This product was not received from the manufacturer until after the start of the sequential test.) We generated the single conductor cable by carefully disassembling a multiconductor cable. We obtained compression molded sheets of EPR C material from the manufacturer and produced tensile specimens which were exposed during both the sequential and simultaneous #1 tests.

3.3.1 Electrical Results

Insulation resistance (I.R.) measurements were performed periodically throughout the aging and accident exposures. Figures 3.7 and 3.8 illustrate the I.R. behavior for the single conductor and multiconductor, respectively. For the single conductor, I.R. measurements were performed between the conductor and the grounded steam chamber (which contained either steam or water). For the multiconductor, I.R. measurements were performed between the conductor and the ground wire and shield of the multiconductor construction with the second conductor of the multiconductor guarded. Insulation resistance measurements recorded for day 11 were during the unanticipated room temperature cooldown and are several orders of magnitude larger then those recorded during the steam exposure.

In Table 3.7 we summarize our leakage current data obtained during post-test measurements. During these tests, one conductor of the multiconductor was connected to the high voltage terminal of the testing unit. The other conductors and the shield and ground wire were grounded. The cable was immersed into a grounded water bath. The single conductor measurements were between the conductor and a grounded water bath.

Condition	Sequential Test		Simultaneous Test #1	
	e/e_o	T/T_o*	e/e_o	T/T_o*
Unaged	1.00±.10 (330 ± 30%)	1.00±.03 (7.1 ± 0.4 MPa)	1.00±.10 (330 ± 30%)	1.00±.03 (7.1 ± 0.4 MPa)
Aged	.37±.06	1.21±.04	.28±.08	.58±.10
After Sequential $R_{Accident}$	.20±.05	1.00±.10		
4 d LOCA	.20±.04 .23±.04**	.71±.05 .62±.04**	.17±.03 .21±.04**	.70±.08 .74±.08**
End of LOCA	.20±.04 .24±.04**	.78±.06 .67±.05**	.14±.03 .14±.03**	.74±.05 .60±.13**

*We normalized T/T_o using the unaged cross-sectional areas.

**These measurements were made within 24 hours after removing samples from the steam chamber.

Table 3.6: Ultimate Tensile Properties for EPR B. The LOCA tensile measurements (except those marked by **) were performed after the sample weight had stabilized.

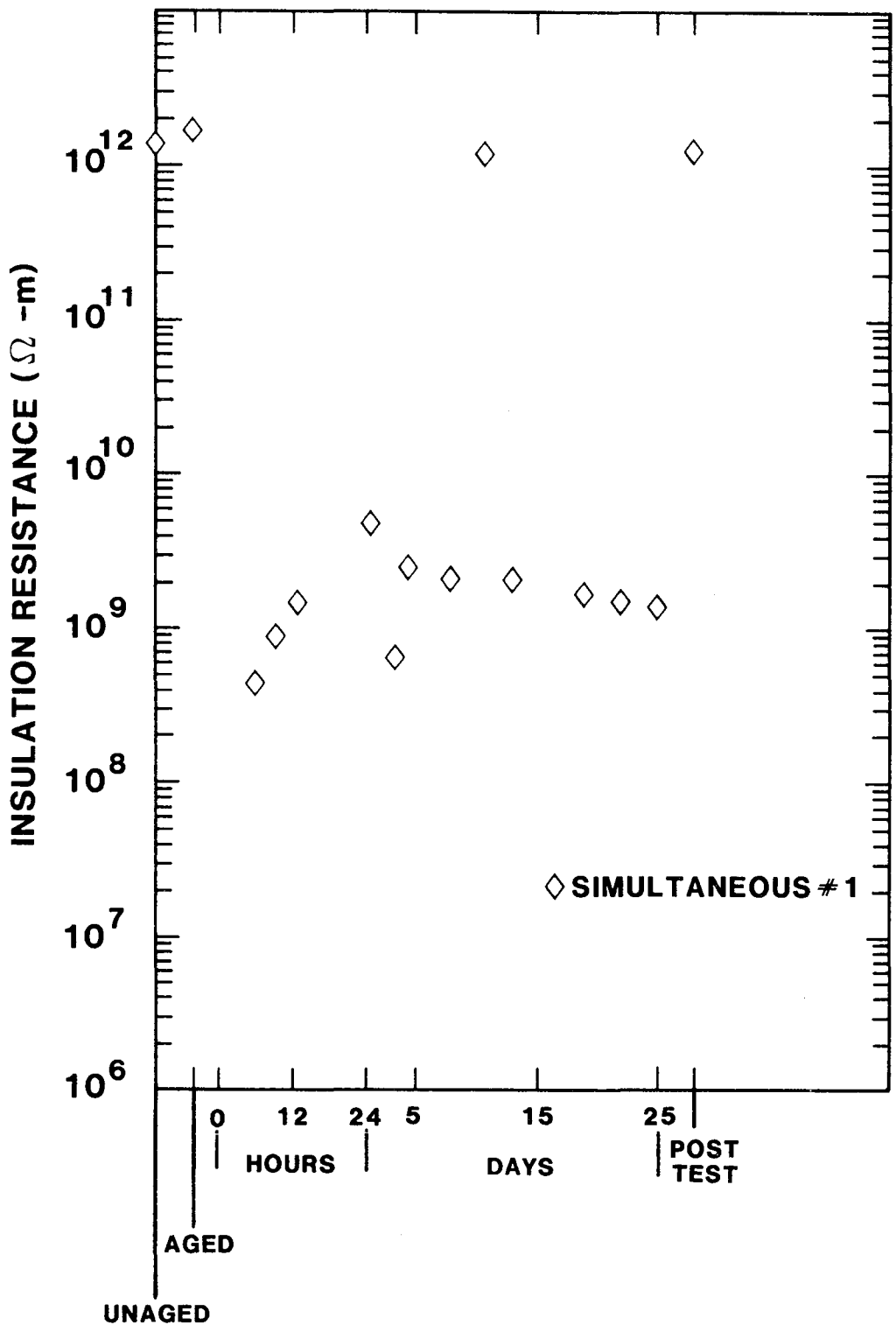

Figure 3.7. Insulation Resistance for EPR C Single Conductor with Primary Insulation

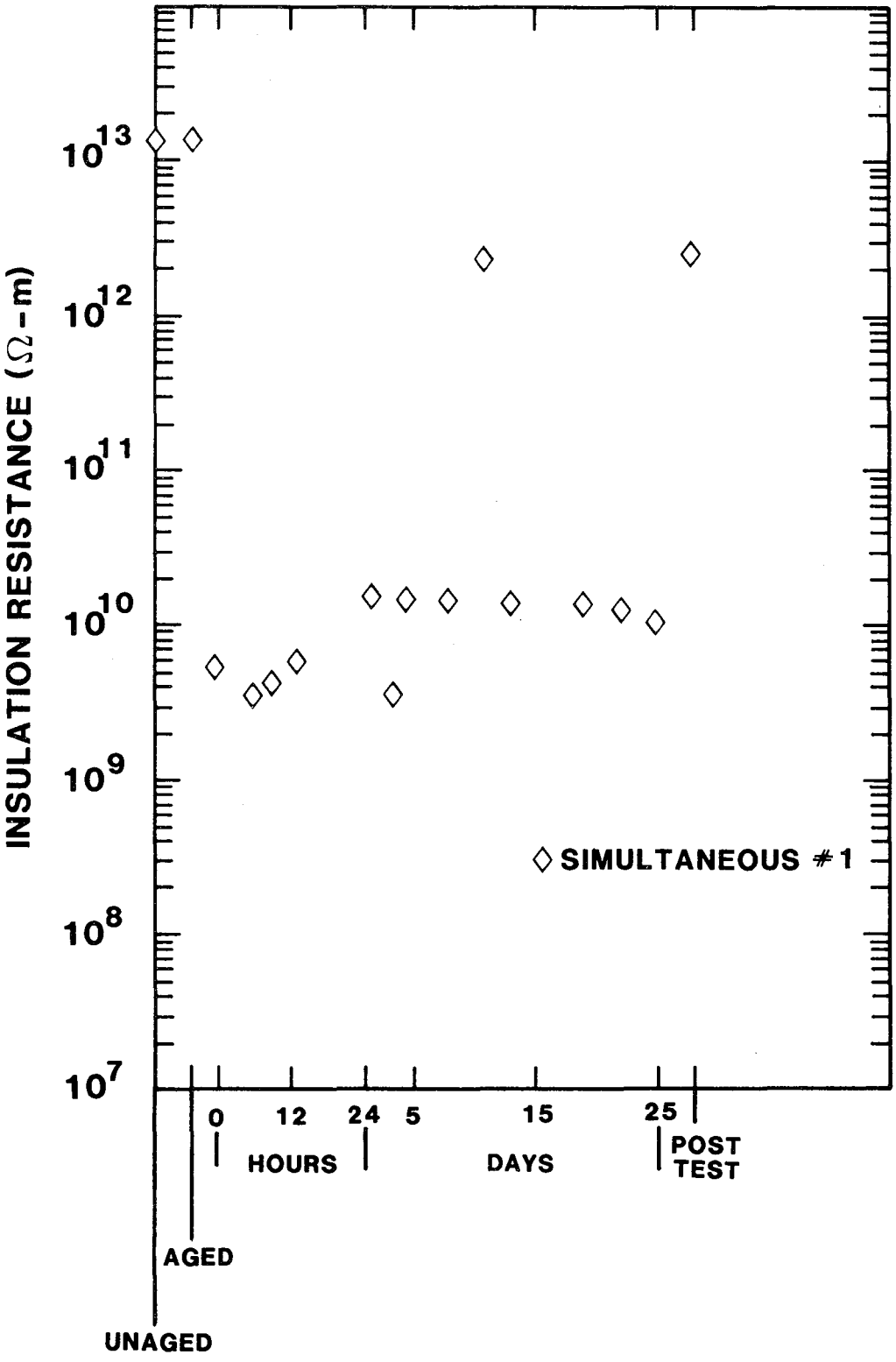

Figure 3.8. Insulation Resistance for EPR C Multiconductor

Applied Voltage	Leakage Current (mA) Simultaneous Test #1
Single Conductor	
600 Vac	0.7
1200 Vac	1.4
2000 Vac	2.5
Multiconductor	
600 Vac	1.3
1200 Vac	2.5
2000 Vac	4.1

Table 3.7: Leakage Current for EPR C Single Conductor and Multiconductor Cables After Simultaneous Test #1. Measurements were made at the completion of a one minute electrification for the 600, 1200 Vac exposures and at the completion of a five minute electrification at 2000 Vac.

3.3.2 Insulation Specimens

Insulation specimens were used to monitor weight changes, dimensional changes, and tensile properties. We removed specimens after the first four days and at the completion of the steam exposure. Table 3.8 summarizes the percentage increase in specimen weight, length, width, and thickness during the LOCA simulations. Ultimate tensile elongation and ultimate tensile strength were measured prior to aging, after aging, after 4 days of LOCA exposure and at the completion of the LOCA exposure. Tensile measurements were made within 24 hours of removing the tensile specimens from the steam environment and also several months after removing the specimens from the chamber. We monitored the weight of the samples to ensure that it had stabilized prior to performing these latter measurements. Results are given in Table 3.9.

3.4 EPR D

EPR D multiconductor cables, single conductor cables, and insulation specimens were exposed to all three tests: the sequential test and both simultaneous tests.

3.4.1 Multiconductor Results

The EPR D multiconductor cable visually had the same general appearance at the completion of both simultaneous tests. After both exposures, the jacket was longitudinally split (see Figures 3.9a and 3.9b) and the bundle of inner conductors had bulged partly out of the jacket. The circumference of the jacket was not large enough to contain the bundle of conductors originally enclosed by the jacket. The exposed gap in the jacket was approximately 0.6 cm wide.

Measurements made at the completion of simultaneous test #2 on an EPR D multiconductor clearly revealed that the bundle of conductors had swelled. The circumference of the bundle was approximately 3.3 cm. Measurements performed on an unexposed "new" cable yielded a circumference (with jacket removed) of approximately 2.8 cm. The diameters of each of the exposed multiconductor single conductors was between .47 and .51 cm. As received from the factory, single conductors have a diameter of approximately .41 cm. Weight measurements performed on insulation removed from the stranded conductors indicated a weight increase of 50% compared to "as received from the factory" insulation. (Measurements were made within a week of the end of the steam exposure to first allow for electrical measurements, hence 50% represents a lower bound for the weight increase since moisture desorption started after removing the samples from the steam environment.)

The multiconductor jacket had also swelled, but not sufficiently to contain the swelled bundle of conductors. The circumference of the jacket (measured circumferentially from one side of the gap to the other side) was approximately 3.7 cm. For unexposed cable, the circumference was 3.6 cm.

	Sequential Test	Simultaneous Test #1
Weight Inrease		
4 d LOCA	8 ± 2	9 ± 2
End of LOCA	9 ± 2	23 ± 2
Length Increase		
4 d LOCA	0 ± 3	2 ± 3
End of LOCA	0 ± 3	5 ± 3
Width Increase		
4 d LOCA	0 ± 1	2 ± 2
End of LOCA	5 ± 6	7 ± 2
Thickness Increase		
4 d LOCA	12 ± 10	8 ± 9
End of LOCA	20 ± 7	20 ± 6

Table 3.8: Percentage Increase for EPR C Insulation Specimen Properties

Condition	Sequential Test e/e_o	Sequential Test T/T_o*	Simultaneous Test #1 e/e_o	Simultaneous Test #1 T/T_o*
Unaged	1.00±.08 (513 ± 10%)	1.00±.02 (12.2 ± 0.8 MPa)	1.00±.08 (513 ± 10%)	1.00±.02 (12.2 ± 0.8 MPa)
Aged	.38±.05	.82±.06	.58±.16	.73±.11
After Sequential $R_{Accident}$	.11±.01	.83±.05		
4 d LOCA	.11±.02 .14±.02**	.63±.06 .65±.06**	.21±.03 .29±.03**	.69±.06 .68±.03**
End of LOCA	.13±.03 .14±.03**	.66±.07 .58±.05**	.15±.03 .22±.02**	.62±.07 .59±.03**

*We normalized T/T_o using the unaged cross-sectional areas.

**These measurements were made within 24 hours after removing samples from the steam chamber.

Table 3.9: Ultimate Tensile Properties for EPR C. The LOCA tensile measurements (except those marked by **) were performed after the sample weight had stabilized.

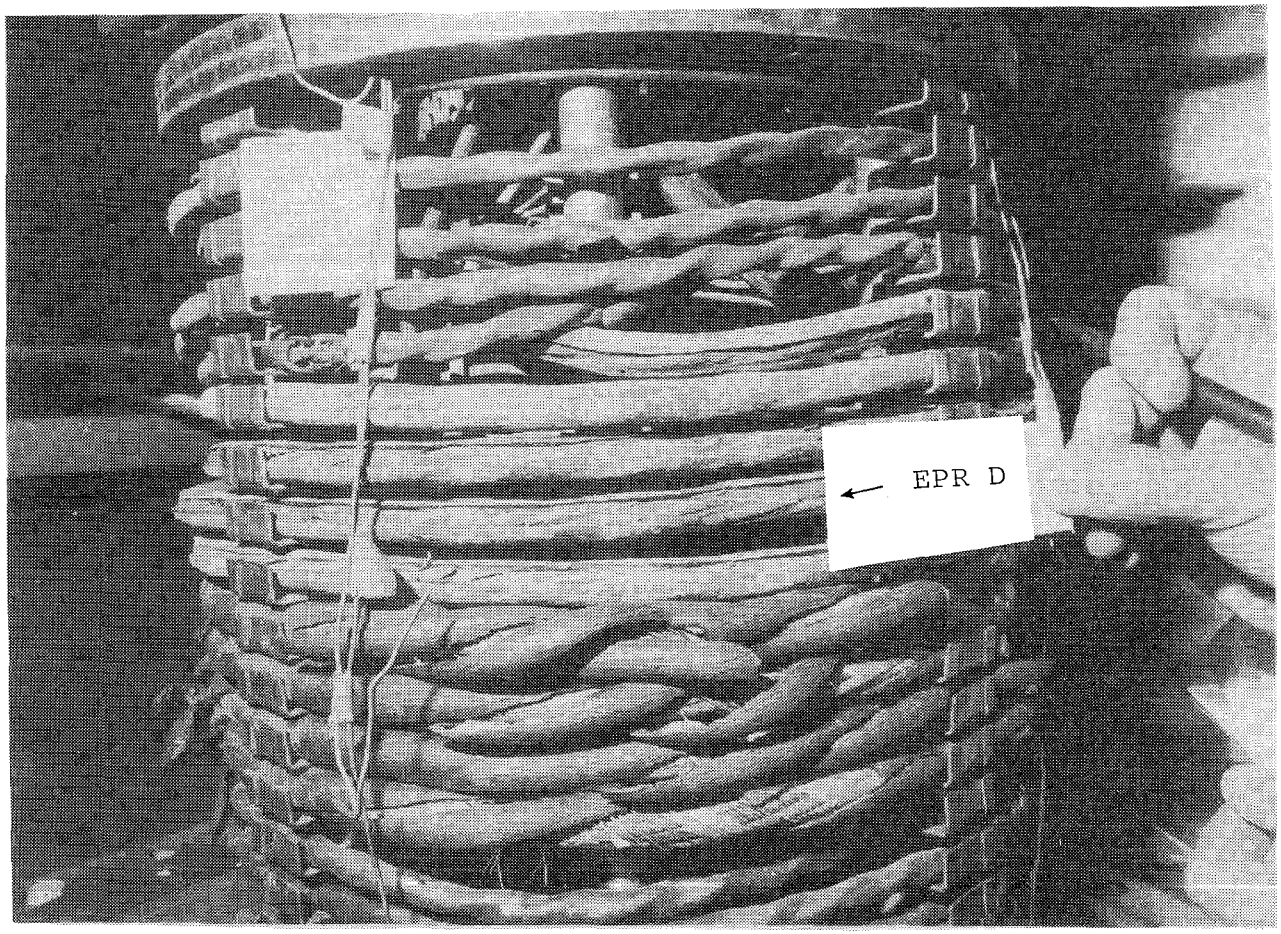

Figure 3.9a. Cables at Completion of Simultaneous Test #1

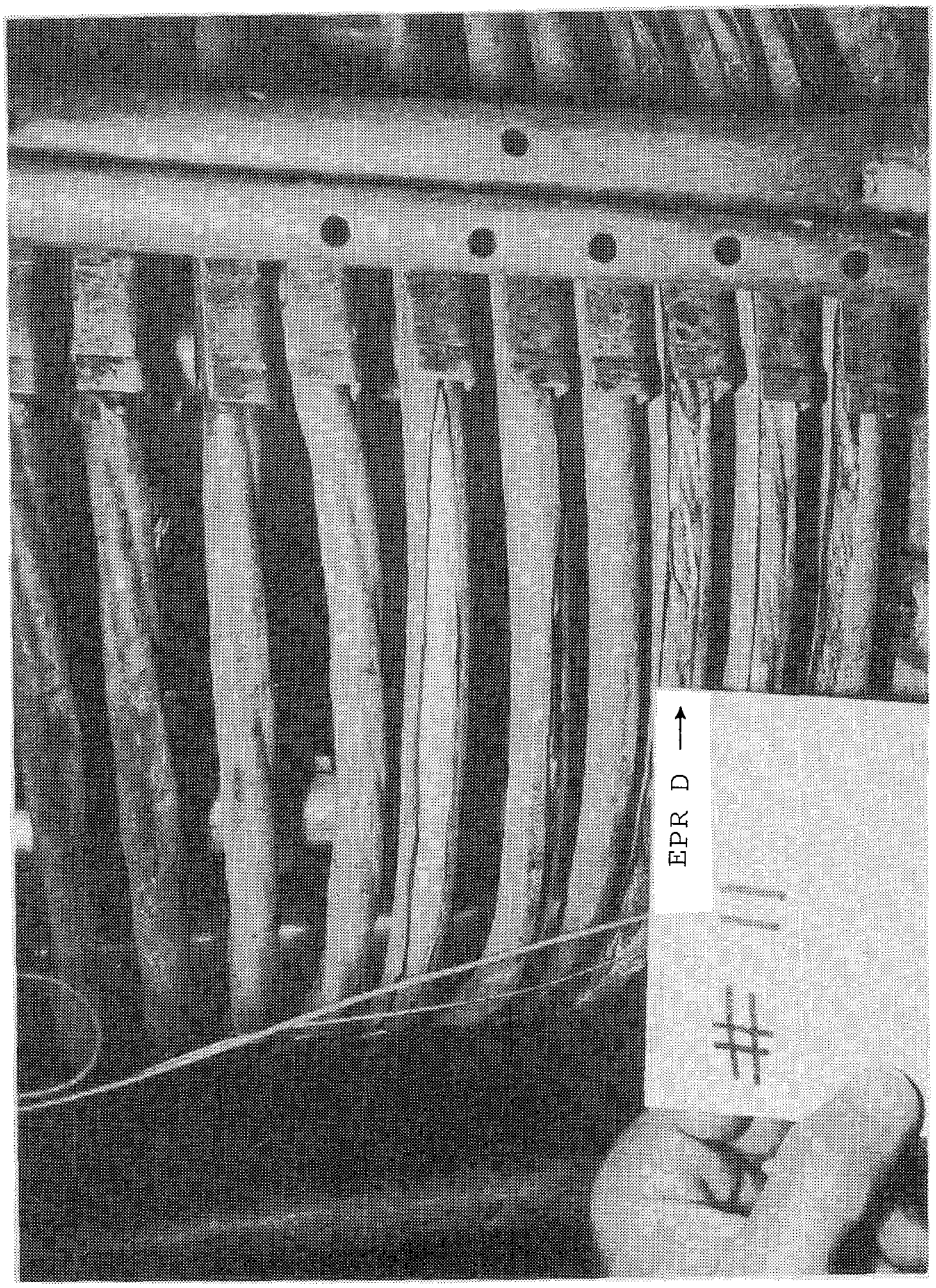

Figure 3.9b. Cables on Day 18 of Simultaneous Test #2

Bare oxidized copper conductors (∿ 1.9 cm in length) were visible for each of the EPR D cables exposed during the second simultaneous test. (This observation was made on day 18 during the unexpected steam cooldown (see Figure 3.9b.). Segments of the insulation had fallen off the conductor on the side where the jacket had split allowing the bare conductors to be observed. This was noted without handling of the multiconductors. For the multiconductor exposed during simultaneous test #1, similar behavior was observed during post test examinations but after handling. After careful removal of the jacket from the multiconductor, pin holes were discovered in the insulation where the cable had rested on stainless steel clips (part of the mandrel support system, see Figure 3.9b). A greenish-blue residue (possibly copper sulfide) was noted at the pin hole locations. A few centimeters away from this location a ∿ 1 cm chunk of insulation fell off the white conductor during post-test removal of the split jacket. Both the copper conductor and the cracked surface of the insulation were bluish-green, suggesting that the insulation crack had developed prior to handling. Several centimeters from this location we purposely split the same conductor's insulation to insure that the greenish-blue residue had not diffused through the insulation rather than along a crack. We conclude that the insulation integrity had been breached prior to handling.

For both simultaneous tests, the EPR D multiconductor cables exhibited large leakage currents during post-test measurements (Table 3.10). Insulation resistance measurements performed during the LOCA simulations illustrate electrical degradation beginning several days after the start of the accident test (Figures 3.10-3.12).

In contrast to the simultaneous testing results, the EPR D multiconductor cable which we exposed to the sequential test had an intact jacket (see Figure 3.13). The multiconductor diameter was approximately 1.1 cm; the same as for an unexposed "new" multiconductor cable. This EPR D multiconductor cable exhibited small leakage currents during post-test measurements (see Table 3.11). Periodically insulation resistance measurements were performed throughout the sequential test. Results are shown in Figure 3.14. Insulation resistance measurements recorded for day 11 were during the unanticipated room temperature cooldown and are several orders of magnitude larger than those recorded during the steam exposure. The insulation resistance values at the end of the sequential test are several orders of magnitude higher than those measured after the simultaneous tests.

3.4.2 Single Conductor Results

The EPR D single conductor cables were obtained by carefully removing the multiconductor outer jacket and sheaths and then separating the individual insulated conductors. Thus our EPR D single conductors were obtained from the same cable reel as our EPR D multiconductor cables.

	Leakage Current (mA)								
	Simultaneous Test #1			Simultaneous Test #2					
				Multiconductor #1			Multiconductor #2		
Applied Voltage	black	red	white	black	red	white	black	red	white
Unaged									
600 Vac				0.5	0.5	0.5	0.5	0.5	0.5
Aged									
600 Vac				0.5	0.5	0.5	0.7	0.6	0.6
Post Test									
600 Vac	180	>750	>750	200	150	540	Measurements not performed		
1200 Vac	>750								

Table 3.10: Leakage Current Values for EPR D Multiconductors. Measurements were performed at the completion of simultaneous test #1 and on day 20 (during the unanticipated cooldown) for simultaneous test #2. Post test leakage current measurements were not performed on multiconductor #2. This cable was removed from the steam chamber prior to the restart of steam and radiation exposures on day 21 and kept for future analysis. Figure 3.9b illustrates the bare copper conductor evident for this cable. All measurements were made at the completion of one minute electrification. Measurements were between the copper conductor and a grounded water bath. For simultaneous test #2 the water bath had a conductivity of 360 μmhos/cm.

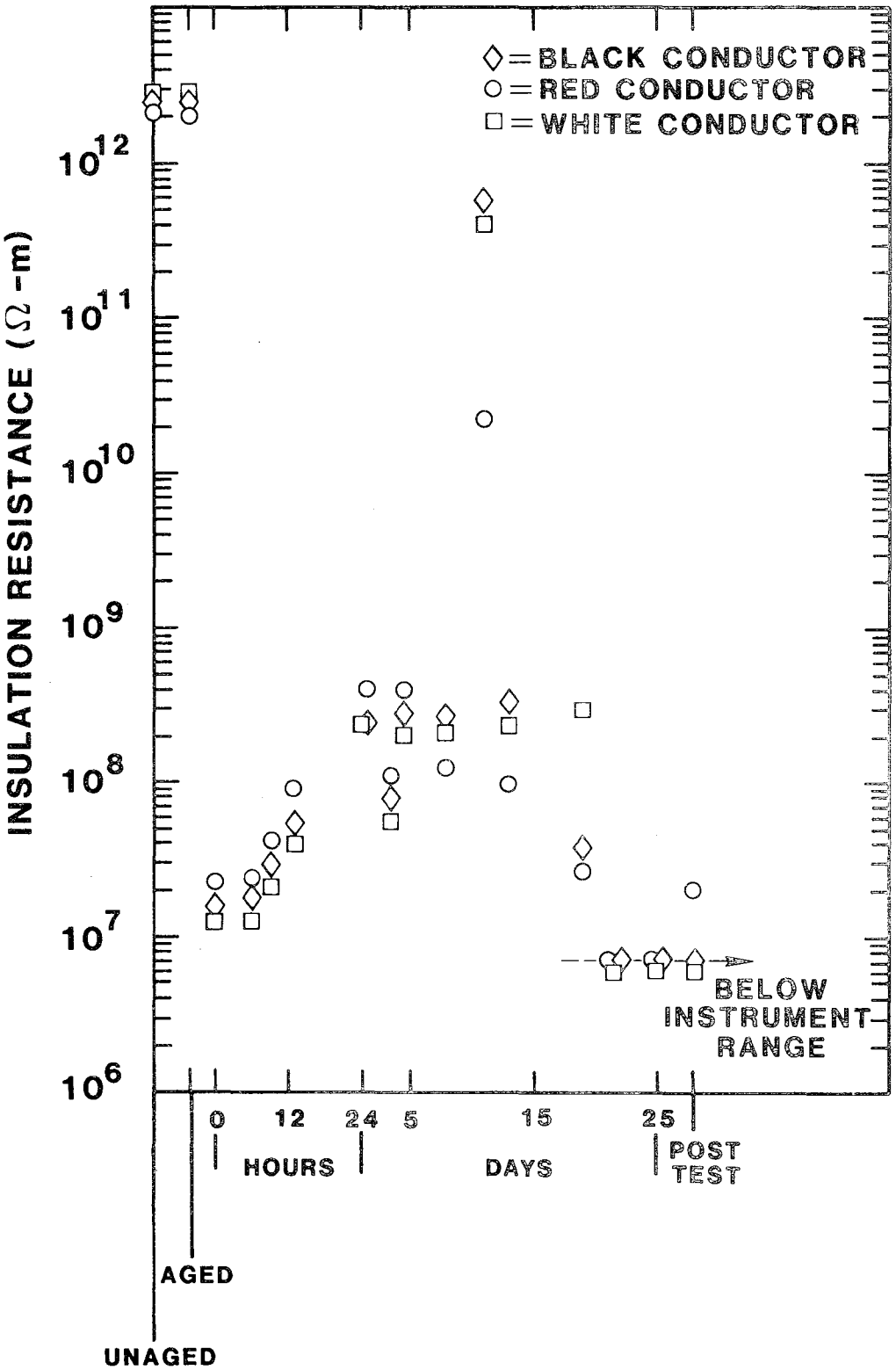

Figure 3.10. Insulation Resistance Measurements for an EPR D Multiconductor During Simultaneous Test #1. Measurements for day 11 were at room temperature during an unanticipated cooldown.

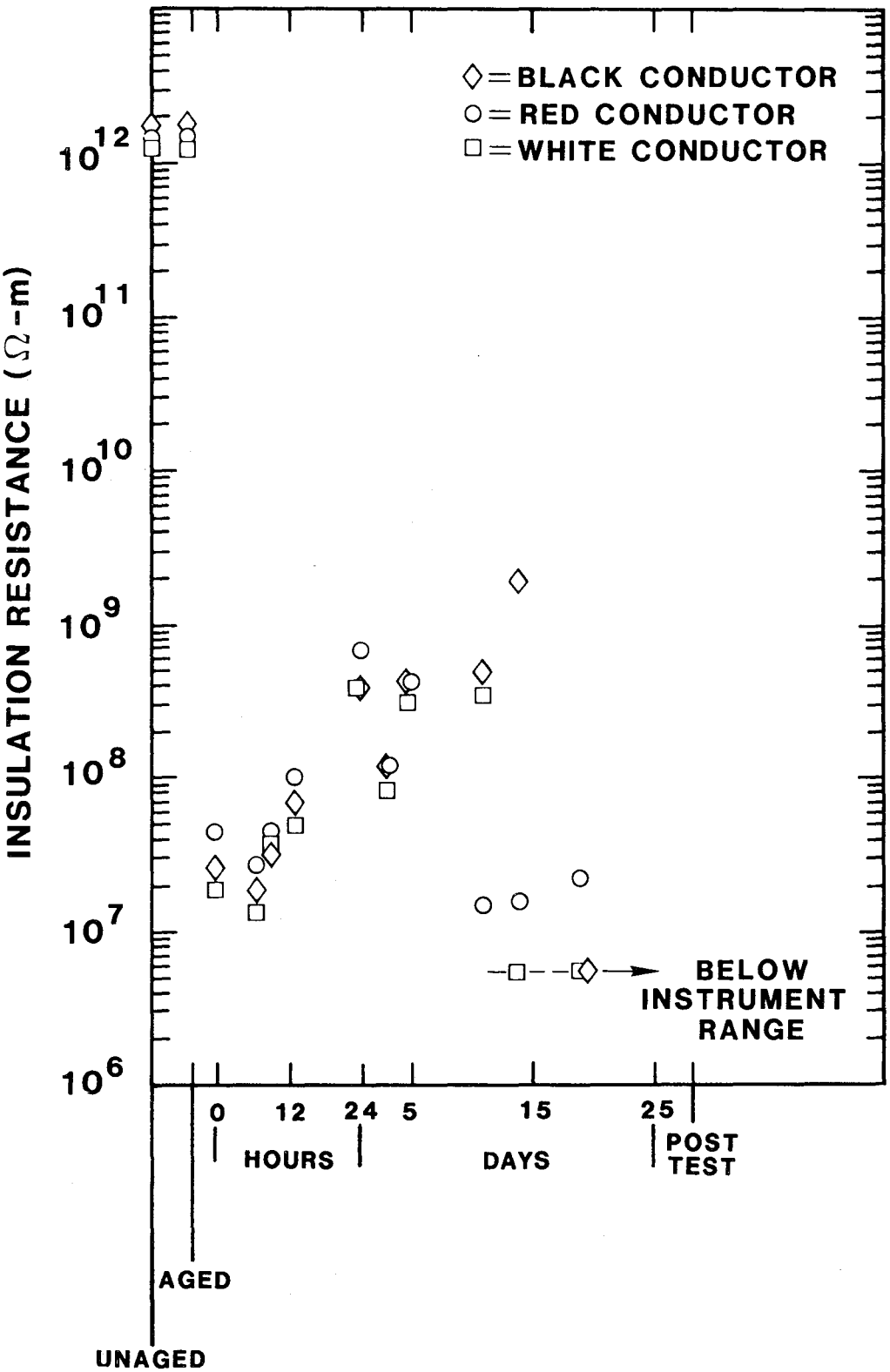

Figure 3.11. Insulation Resistance Measurements for EPR D Multiconductor #1 During Simultaneous Test #2. After ambient measurements on day 18 during unanticipated cooldown, I.R. testing for this cable was terminated.

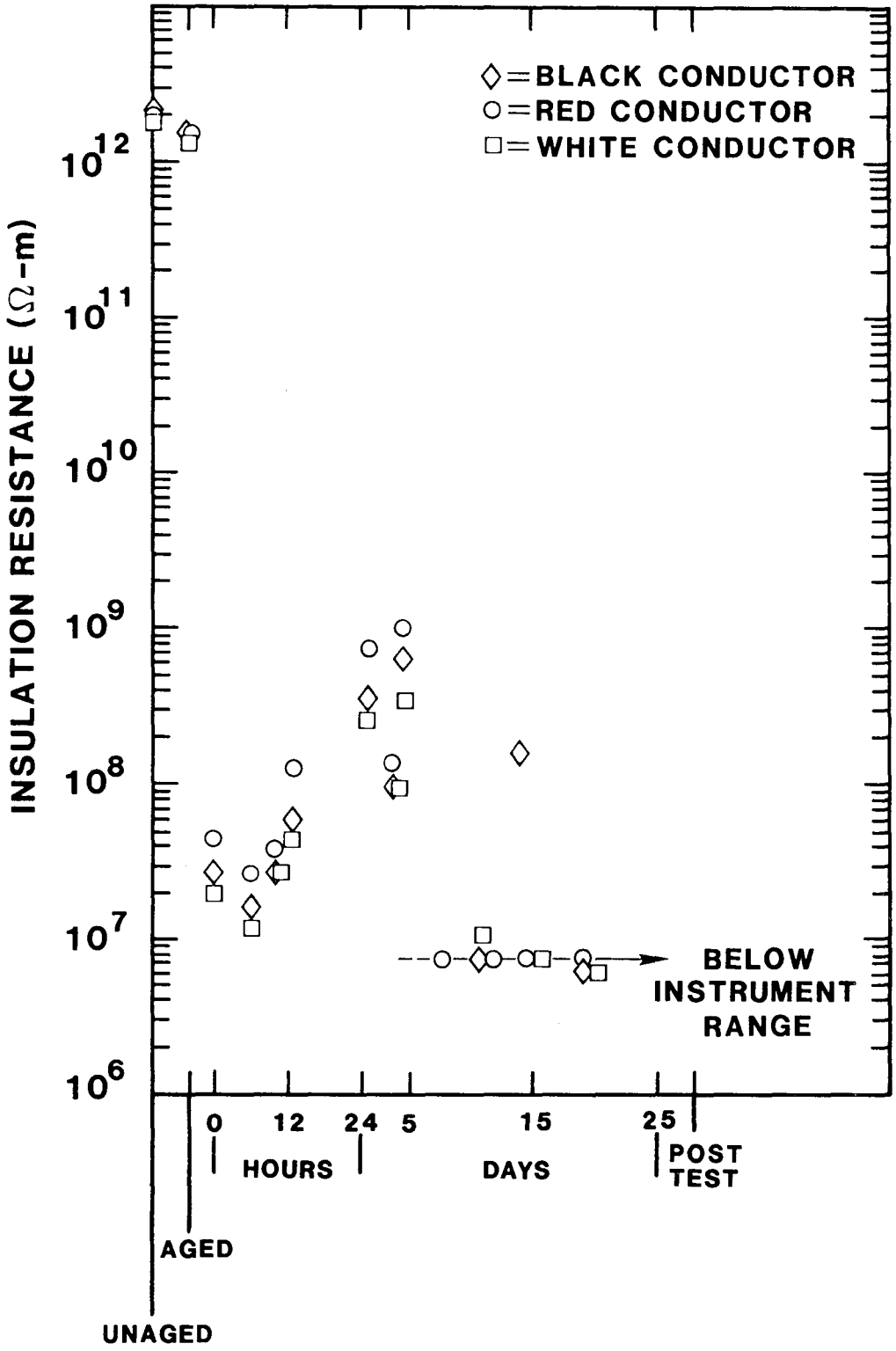

Figure 3.12. Insulation Resistance Measurements for EPR D Multi-conductor #2 During Simultaneous Test #2. After ambient measurements on day 18 during unanticipated cooldown, I.R. testing for this cable was terminated.

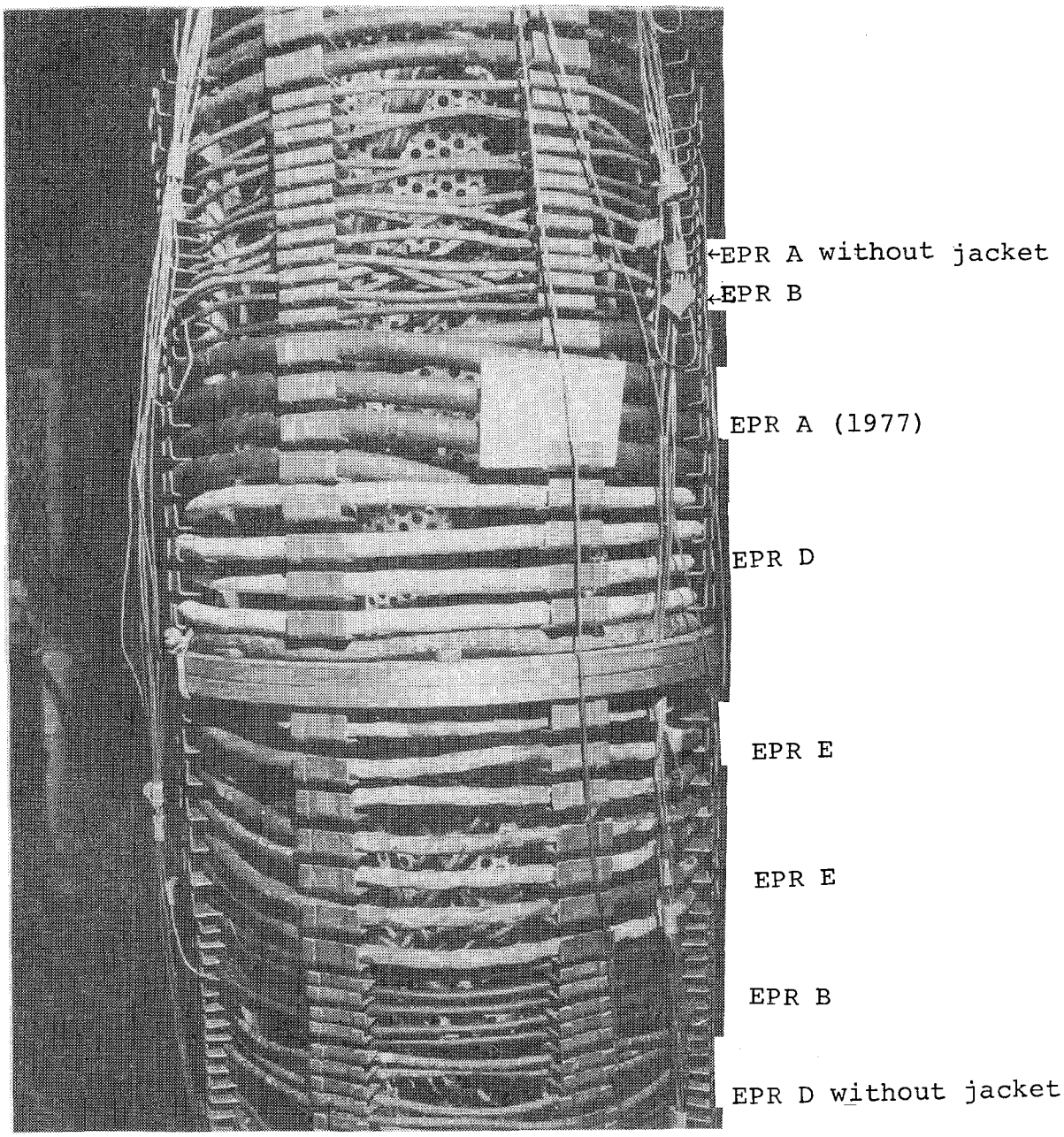

Figure 3.13. Cables at Completion of the Sequential Test

Applied Voltage	Leakage Current (mA) black conductor	red conductor	white conductor
600 Vac	1.2	1.3	1.2
1200 Vac	2.5	2.6	2.5
1800 Vac	3.7	4.0	3.8
2400 Vac	4.9	5 > x > 10	5.0

Table 3.11: Leakage Current Values for EPR D Multiconductor at the Completion of the Sequential Test Exposure. Measurements were made at the completion of one minute electrification for the 600, 1200, and 1800 Vac exposures and at the completion of a five minute electrification at 2400 Vac. Measurements were between the copper conductor and a grounded water bath. Leakage current instrumentation was not available to measure leakage currents of 5 to 10 mA.

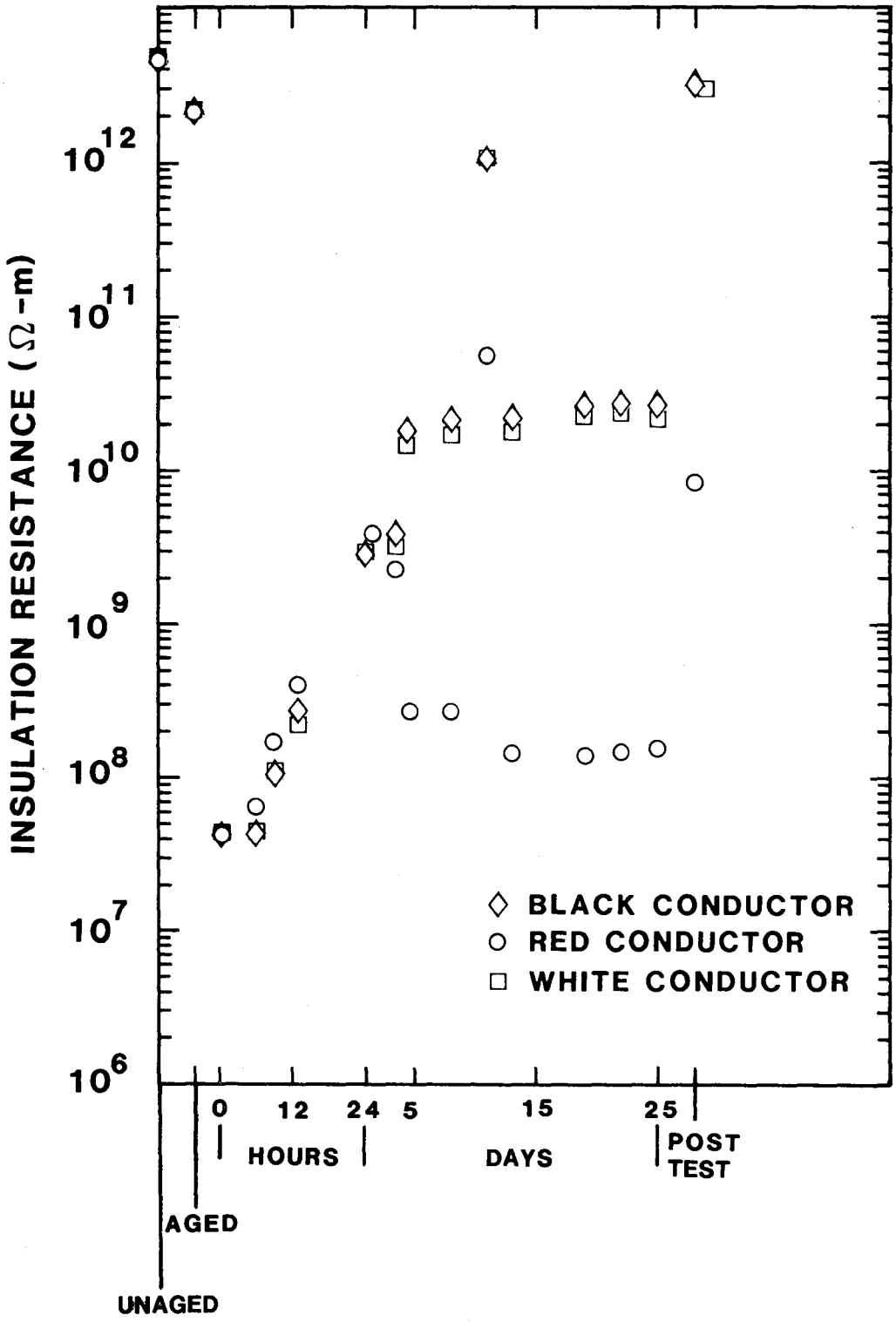

Figure 3.14. Insulation Resistance for EPR D Multiconductor During the Sequential Test

In contrast to the poor electrical properties exhibited by the multiconductors during simultaneous testing, the single conductors had low leakage currents and high insulation resistance values at the completion of the simultaneous tests (Table 3.12 and Figure 3.15). Visually, the insulation was intact with no bare conductor evident. Measurements performed at the completion of the second simultaneous test indicate that the single conductor insulation had swelled. (The outer diameter was ∿ .46 cm compared to ∿ .41 cm for unexposed "new" single conductors). Weight measurements demonstrated that the single conductor insulation increased in weight during the steam exposure by at least 30%. (This measurement was taken within one week of the completion of the steam exposure and represents a lower bound for the weight gain.)

For the sequential test the EPR D single conductors also had low leakage currents and high insulation resistance values at the completion of the steam exposure (Table 3.13 and Figure 3.16). Visually the insulation was intact with no bare conductor evident. The insulation had swelled (the outer diameter was ∿ .46 cm compared to ∿ .41 cm for unexposed "new" single conductors). Weight measurements were not performed.

3.4.3 Insulation Specimens

Insulation specimens were used to monitor both weight changes and tensile properties. We removed specimens after the first four days of the steam exposure and also at the completion of the steam exposure. (For simultaneous test #2 the specimens were removed during the unanticipated cooldown on day 18.)

Table 3.14 summarizes the percentage increases in insulation specimen weight, length, and outer diameter for the LOCA simulations. Simultaneous LOCA test #2 contained both unaged and simultaneously aged specimens. For both simultaneous LOCA exposures, the simultaneously aged specimens had substantial weight and dimensional increases. The sequentially exposed specimens had smaller weight and dimensional changes during the LOCA simulation (especially after 4 days LOCA exposure). The unaged specimens exposed to a simultaneous LOCA had relatively (when compared to the other EPR D results) small weight and dimensional changes.

After removal from the steam exposure, the EPR D insulation specimens desorbed the moisture collected during the steam exposure. Figure 3.17 illustrates this behavior.

Applied Voltage	Leakage Current (mA)		
	Simultaneous Test #1	Simultaneous Test #2	
		Single Conductor #1	Single Conductor #2
Unaged			
600 Vac		0.5	0.5
Aged			
600 Vac		0.5	0.6
Post Test			
600 Vac	1.0	0.8	0.8*
1200 Vac	2.2	1.7	
1800 Vac	3.6	2.7	
2400 Vac	10 > x > 5	5.0	

*Measurement made during unanticipated cooldown and cable removed from chamber prior to restarting the steam exposure

Table 3.12: Leakage Current for EPR D Single Conductors During Simultaneous Tests. Measurements were made at the completion of a one minute electrification for the 600, 1200, and 1800 Vac exposures and at the completion of a five minute electrification at 2400 Vac. Measurements were between the copper conductor and a grounded water bath.

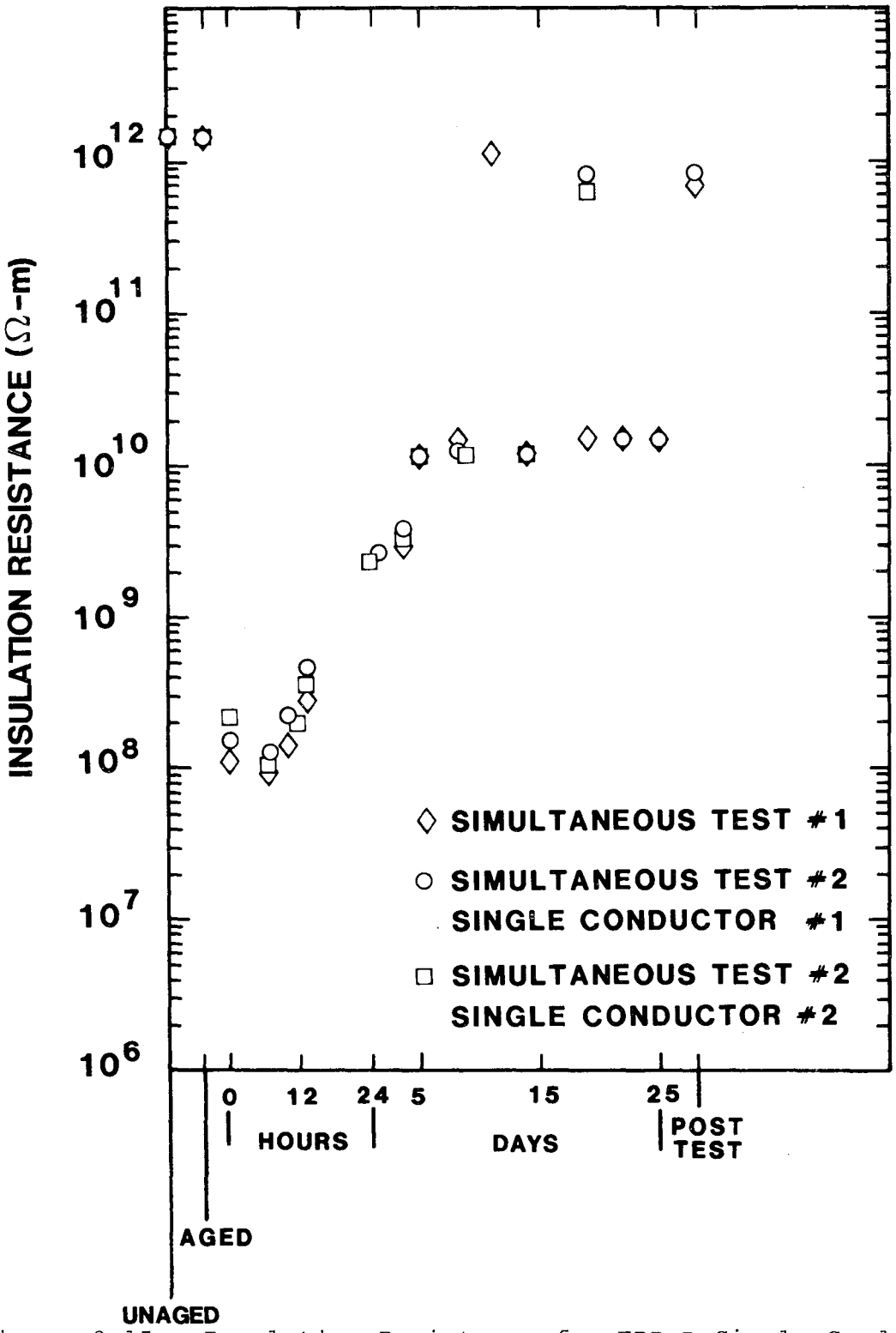

Figure 3.15. Insulation Resistance for EPR D Single Conductors During Simultaneous Tests. Simultaneous test #1 data for day 11 is at room temperature; simultaneous test #2 data for day 18 is at room temperature. This data was obtained during unanticipated cooldowns during the steam exposures.

Applied Voltage	Leakage Current (mA)
600 Vac	1.0
1200 Vac	2.0
1800 Vac	3.1
2400 Vac	4.5

Table 3.13: Leakage Current for EPR D Single Conductor at Completion of Sequential Steam Exposure. Measurements were made at the completion of one minute electrification for the 600, 1200, and 1800 Vac exposures and at the completion of a five minute electrification at 2400 Vac. Measurements were between the copper conductor and a grounded water bath.

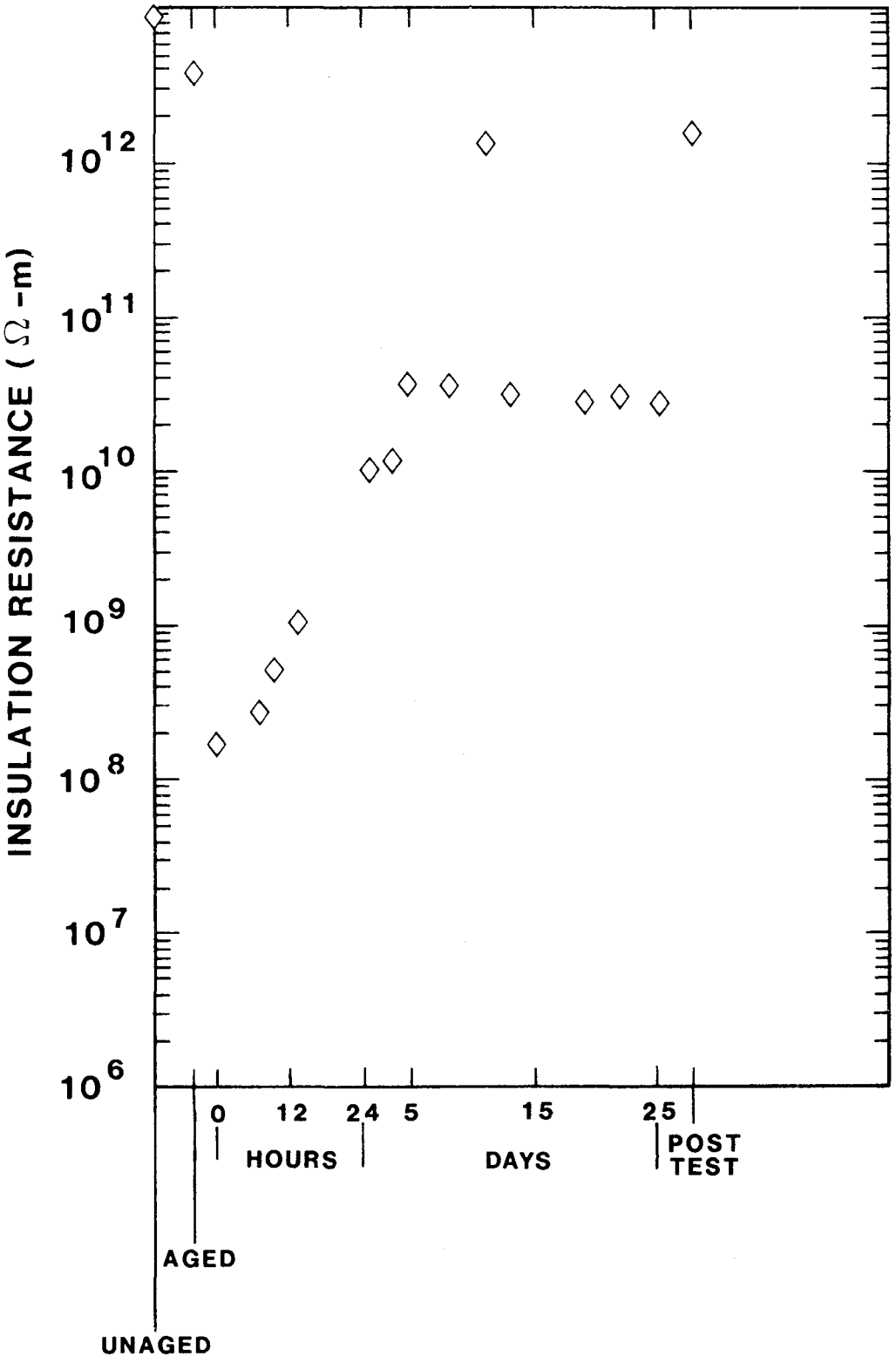

Figure 3.16. Insulation Resistance for EPR D Single Conductor During the Sequential Test

	Sequential Test	Simultaneous Test #1	Simultaneous Test #2 Aged at Start of LOCA	Simultaneous Test #2 Unaged at Start of LOCA
Weight Increase				
4 d LOCA	52 ± 3	120 ± 4	144 ± 5	16 ± 2
Unanticipated Cooldown			172 ± 5	23 ± 2
End of LOCA	121 ± 4	173 ± 5		
Length Increase				
4 d LOCA	2 ± 3	28 ± 3	33 ± 4	2 ± 3
Unanticipated Cooldown			42 ± 4	7 ± 3
End of LOCA	5 ± 3	35 ± 3		
Outer Diameter Increase				
4 d LOCA	14 ± 5	38 ± 4	41 ± 3	5 ± 3
Unanticipated Cooldown			47 ± 3	10 ± 3
End of LOCA	38 ± 5	53 ± 3		

Table 3.14: Percentage Increase for EPR D Insulation Specimen Properties

The insulation specimens were also used as tensile specimens. Ultimate tensile elongation and ultimate tensile strength were measured prior to aging, after aging, after 4 days of LOCA exposure and at the completion of the LOCA exposure. Since moisture absorption may act as a plasticizer and substantially influence tensile properties, we performed tensile measurements (1) within 24 hours of removing the tensile specimens from the steam environment (simultaneous test #1 and sequential test) and (2) several months after removing the tensile specimens from the steam environment (all three tests). We monitored the weight of the samples to insure that it had stabilized prior to performing these latter measurements. Results are given in Table 3.15.

For both sets of measurements, the dimensions of the samples (both inner and outer diameters) were different than for unaged specimens. Our reported tensile strength values were calculated using the unaged cross-sectional areas. This was necessitated by the difficulty of measuring the inner diameters for the swollen insulation. (Qualitatively, the sequentially exposed specimens had smaller inner diameters than unaged specimens while the simultaneously exposed specimens had larger inner diameters.)

3.4.4 Jacket and Insulation Chemical Analysis

A white powder migrated to the surface of the chlorinated polyethylene jacket of EPR D multiconductors during both the sequential and simultaneous tests. For the simultaneous test the powder was evident at the completion of aging. For the sequential test we first observed it on the eighth day of the LOCA simulation during our visual examination in response to the unanticipated cooldown. Upon completion of the accident exposures we removed some of the powder from the sequentially exposed jacket and performed emission spectroscopy and wet chemical analysis. Antimony ($>$ 10 wt %), chlorine ($\sim$ 4.5 wt %) and bromine ($\sim$ 8 wt %) were important constituents of the powder.

Wet chemical analysis was used to determine whether the chlorine or bromine had diffused into or interacted with the EPR D insulation enclosed inside the CPE jacket. For comparison purposes, analysis was also performed on an unaged specimen and on single conductor specimens. The single conductor specimens had been exposed without a jacket to our sequential and simultaneous tests. Neither the single conductors nor the unaged insulation specimens had detectable bromine contents ($<$ .2 wt %). Chlorine contents of 8 to 10 wt % were detected. The EPR D specimens enclosed inside a CPE jacket did have measurable bromine contents (.7 wt % after simultaneous exposure; 2.5 wt % after sequential exposures) and slightly enhanced chlorine contents (10-12 wt %). Additional details are presented in Appendix B.

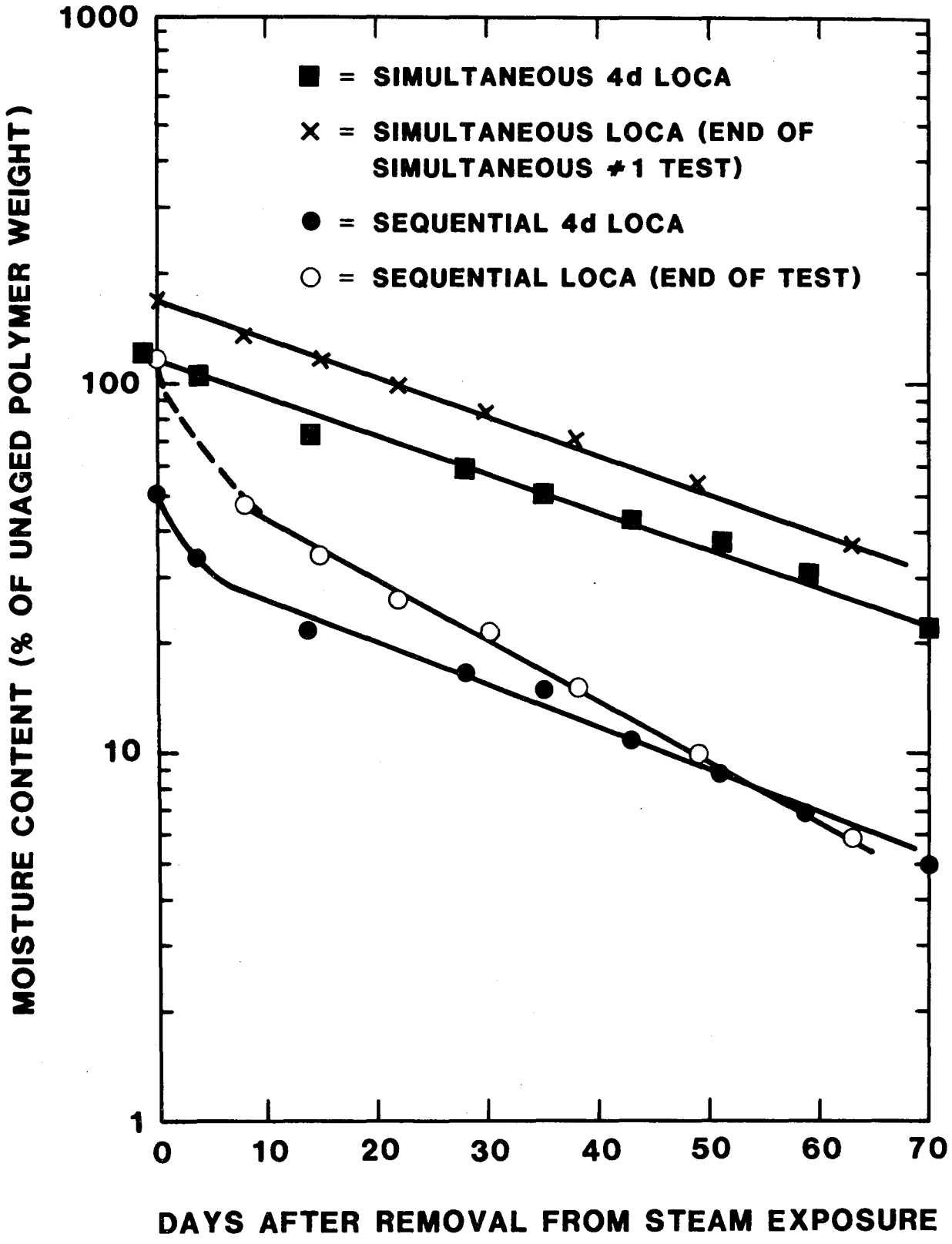

Figure 3.17. EPR D Weight Changes After Removal From Exposures

Condition	Sequential Test Samples Aged Before LOCA		Simultaneous Test #1		Simultaneous #2 Samples Aged before LOCA		Simultaneous #2 Samples Unaged before LOCA	
	e/e_o	T/T_o	e/e_o	T/T_o	e/e_o	T/T_o	e/e_o	T/T_o
Unaged	1.00±.04 (240±10%)	1.00±.04 (8.8± 0.6MPa)	1.00±.04 (240±10%)	1.00±.04 (8.8± 0.6MPa)	1.00±.09 (240±10%)	1.00±.05 (8.8± 0.6MPa)	1.00±.09 (240±10%)	1.00±.05 (8.8± 0.6MPa)
Aged	.41±.04	1.04±.04	.19±.02	.59±.04	.12±.04	.75±.04		
After Sequential $R_{Accident}$	.08±.01	.69±.07						
4 d LOCA	.04 (.09**)	.52±.04* (.4**)	.13±.01 (.16**)	.57±.04* (.4**)	.16±.02	.58±.04*	.33±.07	1.09±.08*
16 d LOCA					.18±.02	.52±.05	.25±.04	.97±10*
End of LOCA	.06±.04 (.09**)	.50±.11* (.23**)	.13±.02 (.09**)	.61±.02* (.23**)				

*Because of the difficulty of measuring changes in cross-sectional area, we normalized T/T_o using the unaged cross-sectional areas.

**These measurements were made within 24 hours after removing samples from steam chamber.

Table 3.15: Ultimate Tensile Properties for EPR D. The LOCA tensile measurements (except those marked by **) were performed after the sample weight had stabilized.

3.5 EPR E

EPR E multiconductor cables, single conductor cables, and insulation tensile specimens were exposed during the sequential test and simultaneous test #1. We generated the single conductor cable by carefully disassembling a multiconductor cable. Because the primary jacket and insulator were bonded together, our single conductor cables actually consisted of a jacket and insulator covering the conductor. We obtained compression molded sheets of the insulation material from the manufacturer and used them to generate our tensile specimens.

Multiconductor Results

Simultaneous test #1 contained one EPR E multiconductor cable with 8.4 m of cable inside the steam chamber. The sequential test contained three EPR E multiconductors with lengths internal to the steam chamber of 6.3, 9.2, and 17.6 m.

Insulation resistance (I.R.) measurements were performed periodically on these cables throughout the aging and accident exposures. These measurements were made between one of the conductors of the multiconductor and the ground wire and ground sheath with the other conductor of the multiconductor guarded. Our megohmmeter had a minimum reading of 1 MΩ at 500 Vdc and 0.1 MΩ at 50 Vdc.

During the first 171°C LOCA steam peak we measured I.R. values of 3.7×10^7 Ω-m for both conductors of the EPR E multiconductor in the simultaneous chamber. For the three EPR E multiconductors exposed to the sequential test profile, the black conductors gave I.R. values between 1.7×10^6 Ω-m and 2.5×10^6 Ω-m at 50 Vdc (readings at 500 Vdc were less than our instrument range.) We did not measure the white conductors at 50 Vdc during the first 171°C steam peak.

Figure 3.18 illustrates the I.R. data for the 9.2 m multiconductor cable (white conductor) during the sequential test as well as the I.R. data for the multiconductor cable (white conductor) during the simultaneous test. Insulation resistance measurements recorded for day 11 were during the unanticipated room temperature cooldown and are several orders of magnitude larger than those recorded during the steam exposure. The simultaneous exposure I.R. values are typically an order of magnitude better than the sequential exposure I.R. values (For the sequential exposure, the normalized I.R. values for the three multiconductor cables rarely varied by more than a factor of two. This suggests that our measurement error is substantially less than the difference between the simultaneous and sequential results.) A similar order of magnitude difference between simultaneous and sequential I.R. values was observed for the black conductors.

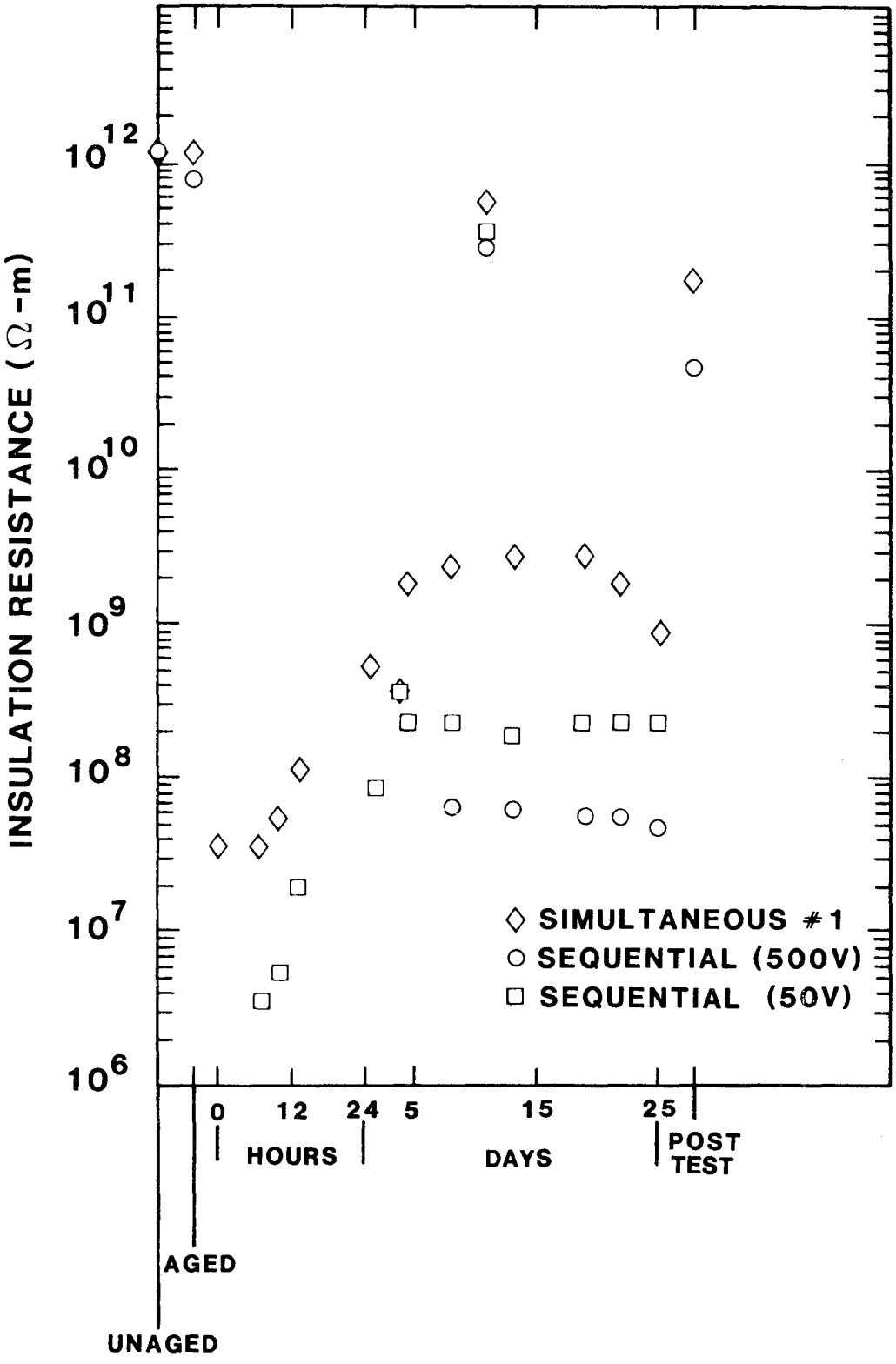

Figure 3.18. Insulation Resistance for EPR E Multiconductors

At completion of our LOCA simulations we performed leakage current measurements for each conductor of our multiconductor cables. During these tests the conductor was connected to the high voltage terminal of the testing unit. The other conductor and the shield and ground wire were grounded. The cable was also immersed into a grounded tap water bath. We summarize in Table 3.16 our results for the black conductors. At 2400 Vac, each conductor had leakage currents greater than 750 mA (the upper measurement range of our instrumentation). A 2400 Vac withstand test voltage was used by the manufacturer during his qualification tests. However, the 30 mil thick composite insulation and jacket contained a 20 mil insulation layer with a 10 mil jacket layer. Therefore a 1600 Vac withstand test more adequately reflects the 80 Vac/mil intent of IEEE Std 383-1974. After a 1 minute 1600 Vac exposure, our measured leakage currents were less than 10 mA for each of the black conductors. (Since the 750 mA leakage currents during the black conductor measurements may have impacted the later white conductor measurements, we do not report the white conductor test results at 1600 Vac.) For multiconductor leakage current testing there is no significant difference between simultaneous and sequential test results.

3.5.2 Single Conductor Results

In contrast to our EPR E multiconductor I.R. results, sequentially exposed EPR E single conductors had a factor of 10 higher I.R. values than did simultaneously exposed EPR E single conductors. Figure 3.19 illustrates this behavior. All I.R. measurements were performed after a one minute 500 Vdc electrification. As for the multiconductor results, insulation resistance measurements recorded on day 11 are several orders of magnitude higher thasn those measured during the steam exposure since they were measured at ambient temperatures.

Table 3.17 summarizes our leakage current data obtained at the completion of the test exposures. These single conductor measurements were between the conductor and a grounded water bath. We do not observe significant differences in leakage current caused by differences between simultaneous and sequential test procedures.

3.5.3 Insulation Specimens

Insulation specimens were used to monitor weight changes, dimensional changes, and tensile properties. We removed specimens after the first four days and at the completion of the steam exposure. There was not appreciable increase in any of these parameters because of the test exposures.

	Leakage Current (mA)			
		Simultaneous Test #1		
Applied Voltage	Sequential Test	Cable 1	Cable 2	Cable 3
600 Vac	1.8	1.6	1.9	3.2
1000 Vac	3.1	3.1	3.7	5<x<10
1600 Vac	5<x<10	5<x<10	5<x<10	5<x<10
2400 Vac	> 750	> 750	> 750	> 750

Table 3.16: Leakage Current Values for EPR E Multiconductors After the Sequential and Simultaneous #1 Exposures. Measurements were made at the completion of one minute electrification for the 600, 1000, and 1600 Vac exposures. At the 2400 Vac the instrument measurement range (750 mA) was exceeded prior to the completion of a 5 minute electrification.

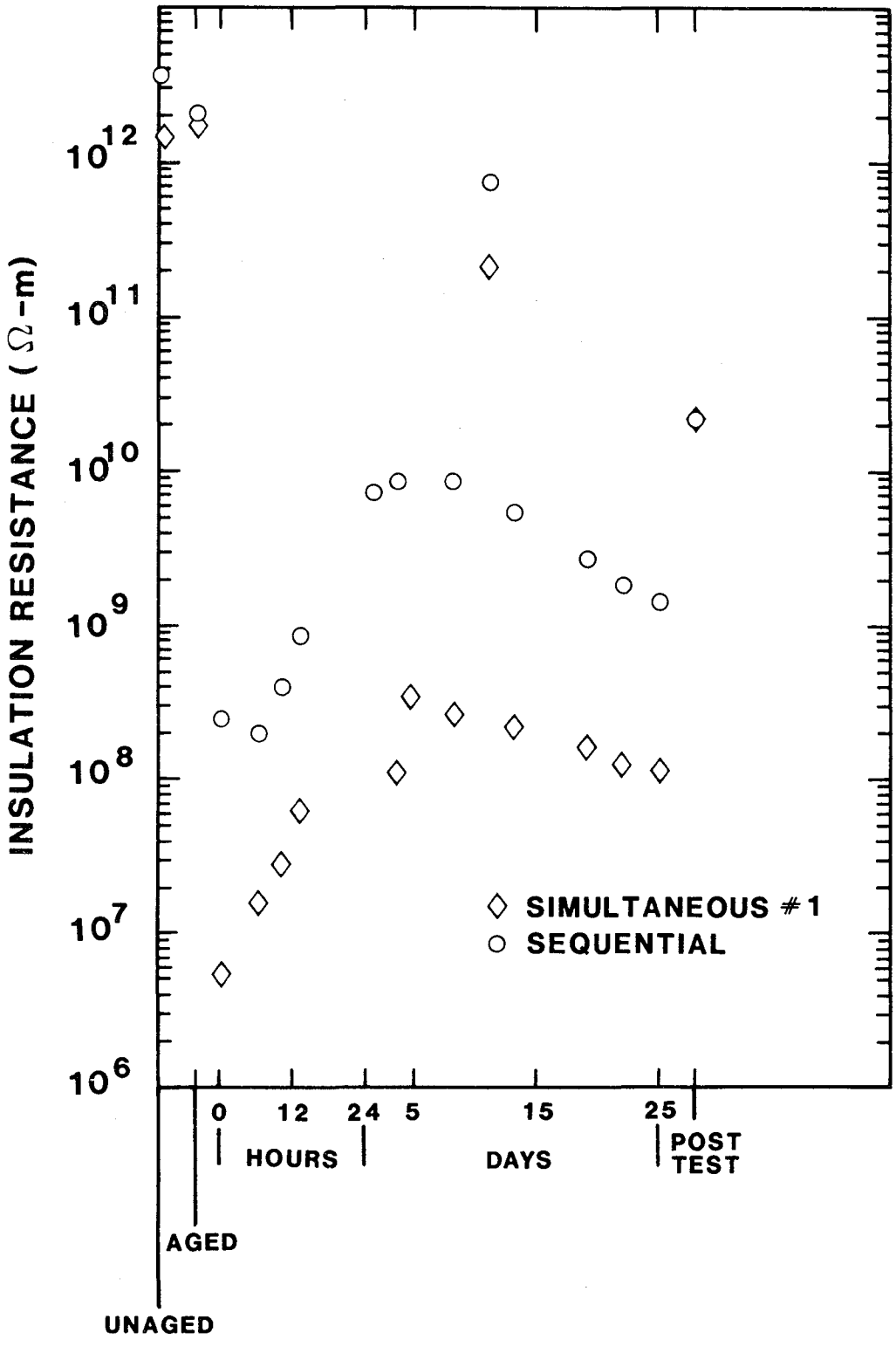

Figure 3.19. Insulation Resistance for EPR E Composite Primary Insulation and Jacket

	Leakage Current (mA)	
Applied Voltage	Sequential Test	Simultaneous Test #1
600 Vac	0.9	1.2
1000 Vac	1.5	2.2
1600 Vac	2.6	5.0
2400 Vac	> 750	> 750

Table 3.17: Leakage Current Values for EPR E Single Conductor Cables After the Sequential and Simultaneous #1 Exposures. Measurements were made at the completion of one minute electrification for the 600, 1000, and 1600 Vac exposures. At the 2400 Vac the instrument measurement range (750 mA) was exceeded prior to the completion of a 5 minute electrification.

Ultimate tensile elongation and ultimate tensile strength were measured prior to aging, after aging, after 4 days of LOCA exposure and at the completion of the LOCA exposure. Tensile measurements were made within 24 hours of removing the tensile specimens from the steam environment and also several months after removing the specimens from the chamber. Results are given in Table 3.18. The sequential test exposures reduce both the ultimate tensile strength and the ultimate tensile elongation more than does the simultaneous test exposure.

3.6 EPR F

Two EPR F single conductor cable and insulation tensile specimens were exposed during simultaneous test #2.

3.6.2 Electrical Results:

Figure 3.20 illustrates the I.R. behavior of both EPR F single conductors. All measurements were performed after a one minute 500 Vdc electrification between the conductor and the grounded steam chamber. (The chamber contained either steam or water during all I.R. measurements. For the unaged, aged, day 18, and post test data ambient temperature tap water was in the chambers. All other measurements were performed in the steam environment.) Table 3.19 summarizes our leakage current data obtained during the test. These single conductor measurements were between the conductor and a grounded tap water bath.

3.6.2 Insulation Specimens:

Insulation specimens were used to monitor weight and dimensional changes during the accident simulation. We removed specimens after the first four days and during the unanticipated cooldown of the steam exposure (simultaneous test #2). We report in Table 3.20 results for two sets of insulation specimens: those that were aged with the cables and those that were unaged prior to the start of the LOCA simulation. Upon removal from the steam environment, the samples desorbed moisture. Tensile properties are reported in Table 3.21.

3.7 EPR G

Two EPR G single conductor cables were exposed during simultaneous test #2. The jacket and insulation were bonded together for these conductors and hence we could not generate any insulation tensile specimens. Figure 3.21 illustrates the I.R. behavior of both EPR G single conductors. All measurements were performed after a one minute 500 Vdc electrification between the conductor and the grounded steam chamber. (The chamber contained either steam or water during all I.R. measurements. For the unaged, aged, day 18, and post test data ambient temperature tap water was used in the chamber. All other measurements were performed in the steam environment.) Table 3.22 summarizes our leakage current data obtained during the test. These single conductor measurements were between the conductor and a grounded tap water bath.

Condition	Sequential Test e/e_o	Sequential Test T/T_o*	Simultaneous Test #1 e/e_o	Simultaneous Test #1 T/T_o*
Unaged	1.00±.12 (380 ± 50)	1.00±.16 (8.4 ± 0.3 MPa)	1.00±.12 (380 ± 50)	1.00±.16 (8.4 ± 0.3 MPa)
Aged	.34±.04	1.38±.29	.49±.07	1.28±.22
After Sequential $R_{Accident}$	.11±.02	1.45±.29		
4 d LOCA	.04±.01 .07±.01**	.68±.14 .77±.14**	.27±.04 .31±.05**	1.22±.25 1.22±.23**
End of LOCA	.05±.01 .07±.01**	.71±.14 .75±.18**	.19±.03 .19±.04**	1.18±.21 .98±.17**

*We normalized T/T_o using the unaged cross-sectional areas.

**These measurements were made within 24 hours after removing samples from the steam chamber.

Table 3.18: Ultimate Tensile Properties for EPR E. The LOCA tensile measurements (except those marked by **) were performed after the sample weight had stabilized.

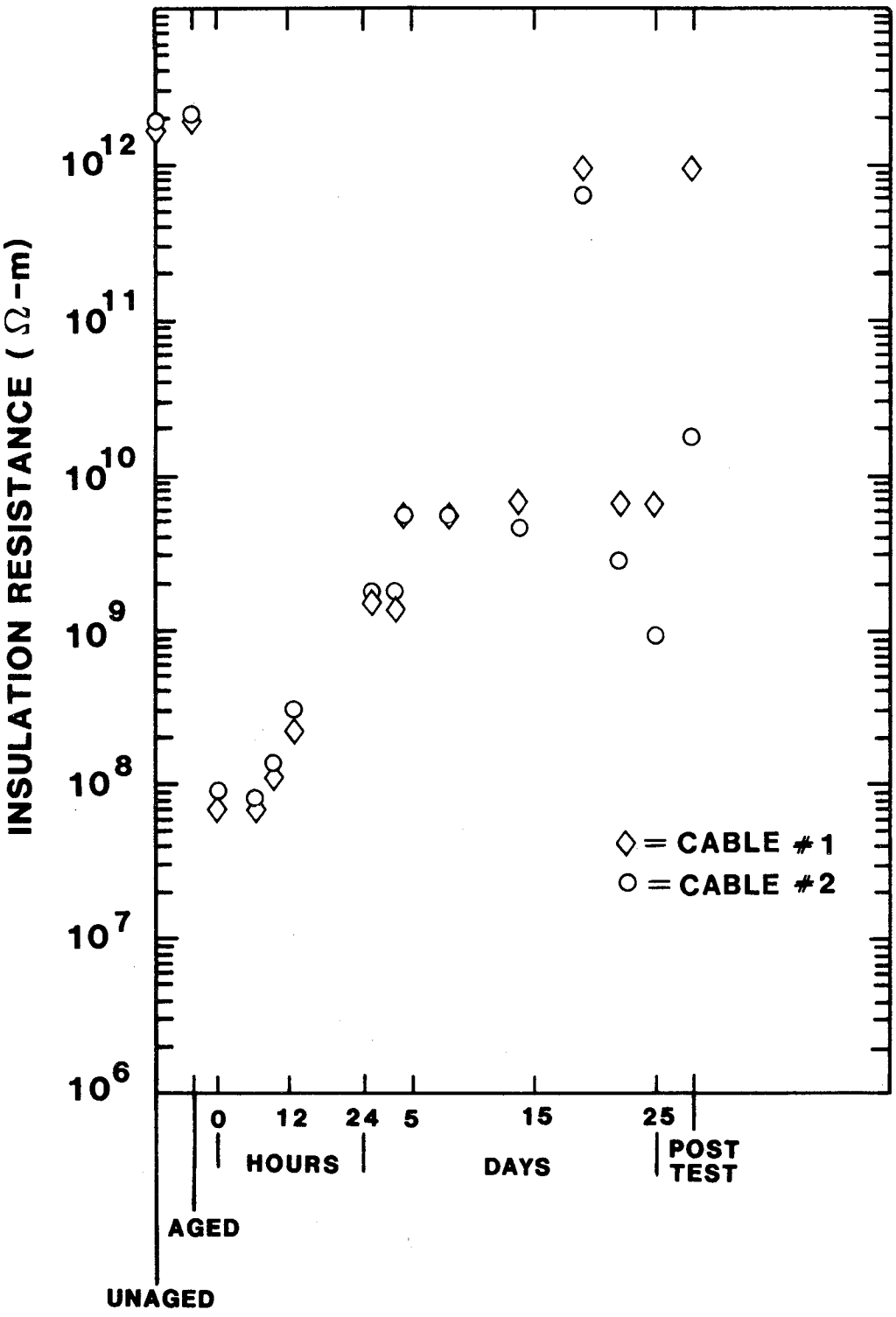

Figure 3.20. Insulation Resistance for EPR F Single Conductor Cables During Simultaneous Test #2

Applied Voltage	Leakage Current (mA)	
	Single Conductor #1	Single Conductor #2
Unaged		
600 Vac	0.4	0.4
Aged		
600 Vac	0.4	0.4
Post Test		
600 Vac	0.7	0.7
1200 Vac	1.3	1.4
1800 Vac	2.0	2.0
2400 Vac	2.7	> 5

Table 3.19: Leakage Currents for EPR F Single Conductors During Simultaneous Test #2. Measurements were made at the completion of a one minute electrification for the 600, 1200, and 1800 Vac exposures and at the completion of a five minute electrification at 2400 Vac. Measurements were between the copper conductor and a grounded water bath.

	Samples Aged before LOCA	Samples Unaged before LOCA
Weight Increase		
4 d LOCA	59 ± 1	8 ± 1
Unanticipated Cooldown	94 ± 2	20 ± 1
Length Increase		
4 d LOCA	9 ± 5	0 ± 5
Unanticipated Cooldown	19 ± 5	2 ± 5
Outer Diameter Increase		
4 d LOCA	23 ± 2	3 ± 2
Unanticipated Cooldown	31 ± 2	6 ± 2

Table 3.20: Percentage Increase for EPR F Insulation Specimen Properties During Simultaneous Test #2.

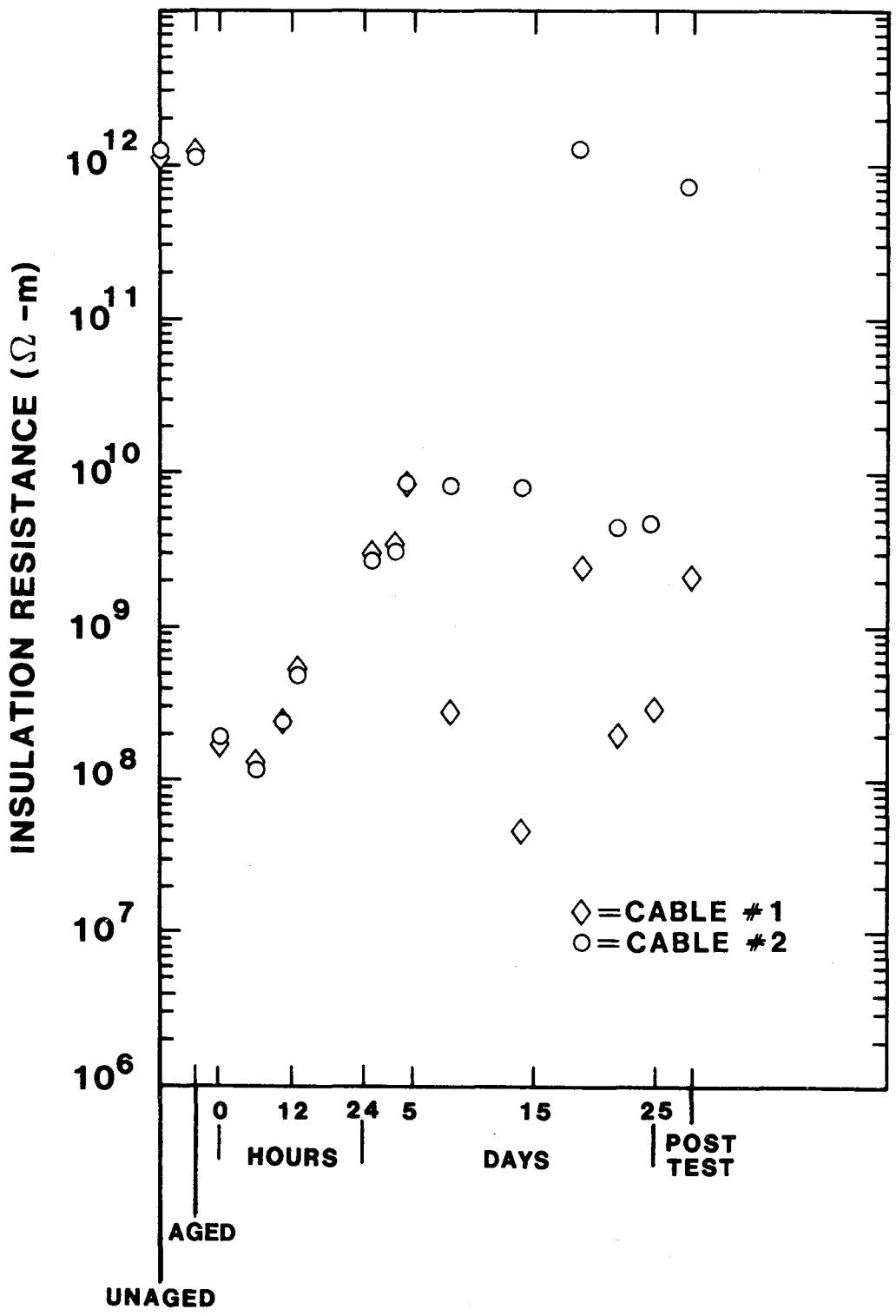

Figure 3.21. Insulation Resistance for EPR G Single Conductors (composite insulation and jacket) During Simultaneous Test #2

Condition	Samples Aged at Start of LOCA e/e_o	Samples Aged at Start of LOCA T/T_o*	Samples Unaged Prior to Start of LOCA e/e_o	Samples Unaged Prior to Start of LOCA T/T_o*
Unaged 1.00 ± .06 (12.4 ± 0.8 MPa)		1.00 ± .05 (288 ± 13%)	1.00 ± .06 (12.4 ± 0.8 MPa)	1.00 ± .05 (288 ± 13%)
Aged	.50 ± .04	.91 ± .06		
After 4d LOCA	.22 ± .01	.77 ± .06	.28 ± .05	.85 ± .08
Unanticipated Cooldown	.10 ± .04	.57 ± .08	.10 ± .01	.58 ± .07

*We normalized $T/_{To}$ using the average unaged cross-sectional area.

Table 3.21: Ultimate Tensile Properties for EPR F During Simultaneous Test #2.

Applied Voltage	Leakage Current (mA)	
	Single Conductor #1	Single Conductor #2
Unaged		
600 Vac	0.5	0.5
Aged		
600 Vac	0.5	0.5
Post Test		
600 Vac	0.7	0.6
1200 Vac	1.7	1.2
1800 Vac	2.2	2.0
2400 Vac	> 5.0	5.0

Table 3.22: Leakage Current for EPR G Single Conductors During Simultaneous Test #2. Measurements were made at the completion of a one minute electrification for the 600, 1200, and 1800 Vac exposures and at the completion of a five minute electrification at 2400 Vac. Measurements were between the copper conductor and a grounded water bath.

3.8 EPR-1483

Compression molded EPR-1483 was cut into tensile specimens and aged by seven different simulations (see Section 2.3.2). At completion of aging the samples were inserted into the HIACA steam chambers at appropriate test points so that for each of the seven aging populations, one-third of the tensile specimens were exposed to one of three accident simulations:

1. sequential accident irradiation than steam exposure (the sequential accident test)

2. simultaneous accident irradiation and steam exposure (simultaneous accident test #1)

3. steam exposure only (the steam exposure of the sequential test)

Unaged tensile specimens were also exposed to these accident simulations. EPR-1483 specimens were removed from the HIACA test chambers after the first four days and at the completion of the steam exposures.

Tables 3.23-3.25 summarize weight and dimensional changes resulting from the different aging and accident combinations. Results for tensile properties are given in Tables 3.26-3.28. Figure 3.22 illustrates that the weight and volume gains are linearly related while Figure 3.23 demonstrates an inverse relationship between the weight gain and the ultimate tensile strength.

3.9 Japanese EPR-5

Prior to the start of simultaneous test #2, Dr. T. Seguchi of the Japan Atomic Energy Research Institute, Takaski, provided some compression molded sheets of EPR-5, a commercial chemically cross-linked fire-retardant EPDM insulation material. The sheets were cut into tensile specimens; half were aged with the cables tested during simultaneous test #2. The other half (unaged) were inserted into the steam chamber prior to the start of the simultaneous #2 accident simulation. Weight gain and dimensional changes during the accident exposure are summarized in Table 3.29. Insulation ultimate tensile properties are summarized in Table 3.30.

Aging Method*	% Weight Increase	% Length Increase	% Width Increase	% Thickness Increase	Calculated % Volume Increase
Unaged	17	5 ± 3	6 ± 1	16 ± 13	29 ± 15
94 h T + R	22	7 ± 3	8 ± 1	21 ± 5	40 ± 7
7 d T + R	67	19 ± 3	20 ± 1	46 ± 9	108 ± 14
30 d T + R	45	16 ± 7	15 ± 3	31 ± 18	75 ± 27
28 d T → 28 d R	22	7 ± 3	9 ± 3	24 ± 11	45 ± 14
28 d R → 28 d T	30	9 ± 4	12 ± 1	20 ± 6	46 ± 9
28 d T → 55 h R	24	7 ± 3	8 ± 1	23 ± 6	42 ± 8
55 h R → 28 d T	30	9 ± 4	10 ± 1	26 ± 5	51 ± 8

Table 3.23: EPR-1483 Properties After the Simultaneous Radiation and Steam Accident Simulation.

*See Section 21.3.2 for aging details.

Aging Method*	% Weight Increase	% Length Increase	% Width Increase	% Thickness Increase	Calculated % Volume Increase
Unaged	-1	0 ± 2	2 ± 2	0 ± 63	2 ± 7
94 h T + R	5	0 ± 2	3 ± 1	8 ± 4	11 ± 5
7 d T + R	46	14 ± 4	17 ± 1	36 ± 5	81 ± 9
30 d T + R	55	16 ± 4	16 ± 3	34 ± 10	80 ± 16
28 d T → 28 d R	5	2 ± 2	4 ± 1	9 ± 4	16 ± 5
28 d R → 28 d T	12	3 ± 3	6 ± 1	12 ± 6	22 ± 8
28 d T → 55 h R	8	2 ± 2	-7 ± 1	7 ± 7	2 ± 7
55 h R → 28 d T	10	2 ± 2	5 ± 2	12 ± 6	20 ± 7

Table 3.24: EPR-1483 Properties After a Steam Only Accident Simulation.

Aging Method*	% Weight Increase	% Length Increase	% Width Increase	% Thickness Increase	Calculated % Volume Increase
Unaged	34	5 ± 3	13 ± 2	29 ± 24	53 ± 39
94 h T + R	39	7 ± 3	14 ± 1	32 ± 5	61 ± 8
7 d T + R	53	9 ± 4	19 ± 4	44 ± 17	87 ± 24
30 d T + R	66	10 ± 3	27 ± 2	58 ± 14	121 ± 21
28 d T → 28 d R	--	5 ± 3	17 ± 2	46 ± 5	79 ± 9
28 d R → 28 d T	63	7 ± 3	18 ± 1	45 ± 5	83 ± 8
28 d T → 55 h R	55	7 ± 3	17 ± 2	43 ± 4	79 ± 8
55 h R → 28 d T	58	7 ± 3	19 ± 3	42 ± 13	81 ± 18

Table 3.25: EPR-1483 Properties After the Sequential Radiation Followed by Steam Accident Simulation.

Aging Method*	After Aging		After 4 d Steam Only LOCA		At End of Steam Only LOCA	
	T/T_o	e/e_o	T/T_o*	e/e_o	T/T_o	e/e_o
Unaged	1.00±.05	1.00±.09	1.06±.07	.96±.09	1.08±.06	1.02±.09
94 h T + R	.99±.05	.93±.08	1.03±.08	.92±.10	1.06±.05	.88±.08
7 d T + R	.83±.06	.41±.05	.70±.04	.36±.05	.64±.04	.32±.04
30 d T + R	.79±.07	.41±.10	.73±.08	.43±.07	.72**	.42**
28 d T → 28 d R	.98±.07	.47±.10	.95±.09	.42±.05	.93±.08	.44±.04
28 d R → 28 d T	1.01±.10	.41±.05	.91**	.43**	.78±.04	.46±.09
28 d T → 55 h R	.97±.08	.35±.04	.99±.14	.40±.07	.98±.05	.38±.06
55 h R → 28 d T	.93±.06	.32±.04	.83**	.31**	1.01±.07	.41±.04

* = We normalized T/T_o using the unaged cross-sectional areas.
** = Only one sample available for measurement.

Table 3.26: EPR-1483 Ultimate Tensile Properties for the Steam Only LOCA Simulation.

Aging Method*	After Aging		After 4 d Sequential LOCA		At End of Sequential LOCA	
	T/T_o	e/e_o	T/T_o*	e/e_o	T/T_o*	e/e_o
Unaged	1.00±.05	1.00±.09	.72±.08	.14±.02	.80±.05	.16±.02
94 h T + R	.99±.05	.93±.08	.80±.05	.17±.02	.72±.08	.15±.02
7 d T + R	.83±.06	.41±.05	.58±.08	.11±.02	.47±.11	.09±.02
30 d T + R	.79±.07	.41±.10	.67±.07	.12±.02	.52±.06	.11±.01
28 d T → 28 d R	.98±.07	.47±.10	.64±.04	.11±.02	--	--
28 d R → 28 d T	1.01±.10	.41±.05	.62±.08	.12±.02	.55±.08	.11±.02
28 d T → 55 h R	.97±.08	.35±.04	.71±.13	.12±.02	.71±.04	.11±.01
55 h R → 28 d T	.93±.06	.32±.04	.51±.04	.09±.01	.63±.13	.12±.01

* = We normalized T/T_o using the unaged cross-sectional areas.

Table 3.27: EPR-1483 Ultimate Tensile Properties for the Sequential Radiation Followed by Steam LOCA Simulation.

Aging Method*	After Aging		After 4 d Simultaneous LOCA		At End of Simultaneous LOCA	
	T/T_o	e/e_o	T/T_o*	e/e_o	T/T_o*	e/e_o
Unaged	1.00±.05	1.00±.09	1.01±.11	.27±.05	.80±.18	.16±.02
94 h T + R	.99±.05	.93±.08	.94±.11	.24±.04	.84±.17	.18±.03
7 d T + R	.83±.06	.41±.05	.68±.07	.21±.03	.33±.05	.08±.01
30 d T + R	.79±.07	.41±.10	.69±.06	.21±.03	.62±.06	.16±.03
28 d T → 28 d R	.98±.07	.47±.10	.90±.06	.23±.04	.74±.10	.16±.02
28 d R → 28 d T	1.01±.10	.41±.05	.89±.16	.22±.04	.77±.12	.16±.02
28 d T → 55 h R	.97±.08	.35±.04	.94±.08	.21±.02	.80±.11	.14±.02
55 h R → 28 d T	.93±.06	.32±.04	.81±.22	.18±.04	.69±.16	.13±.02

* = We normalized T/T_o using the unaged cross-sectional areas.

Table 3.28: EPR-1483 Ultimate Tensile Properties for the Simultaneous Radiation and Steam LOCA Simulation.

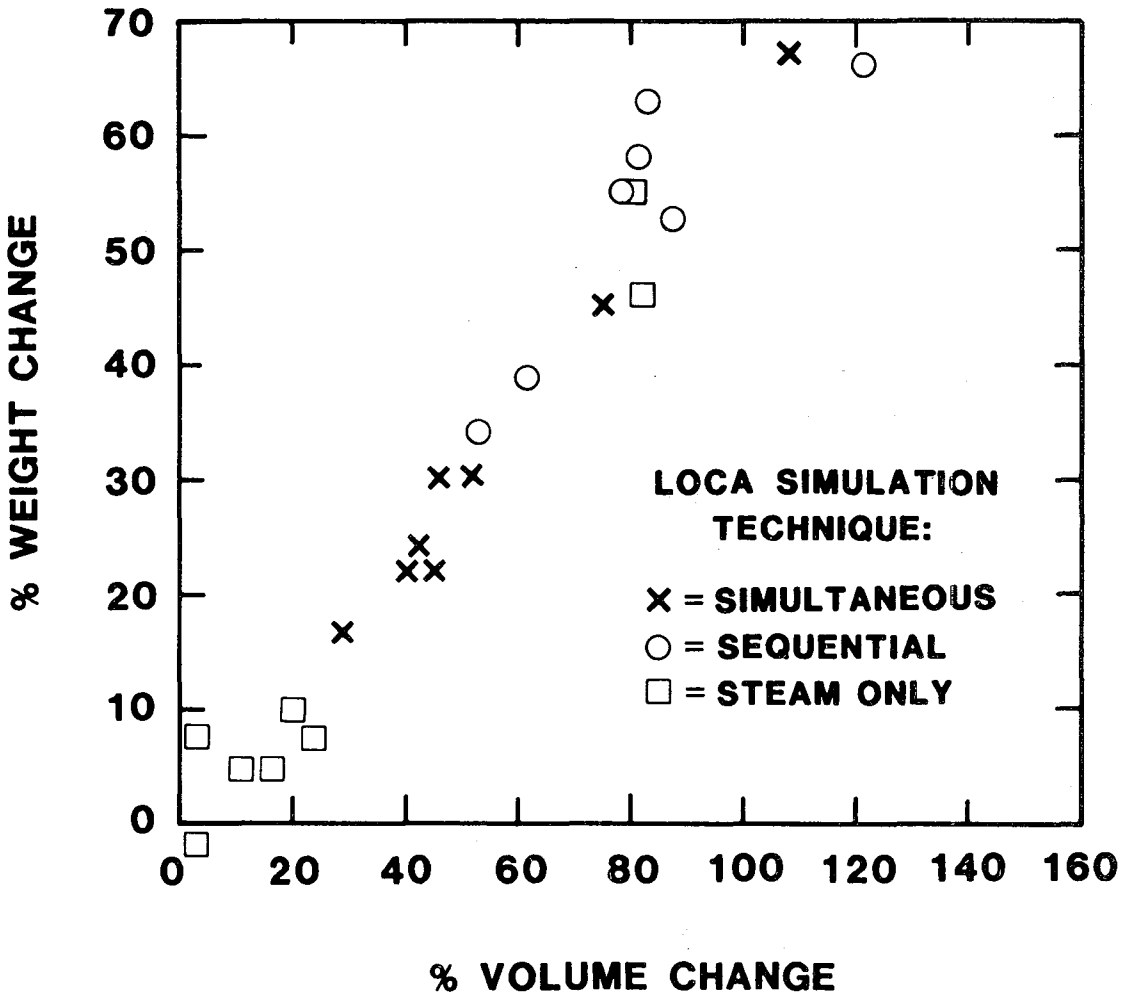

Figure 3.22. Relationship Between Weight and Volume Changes for EPR-1483

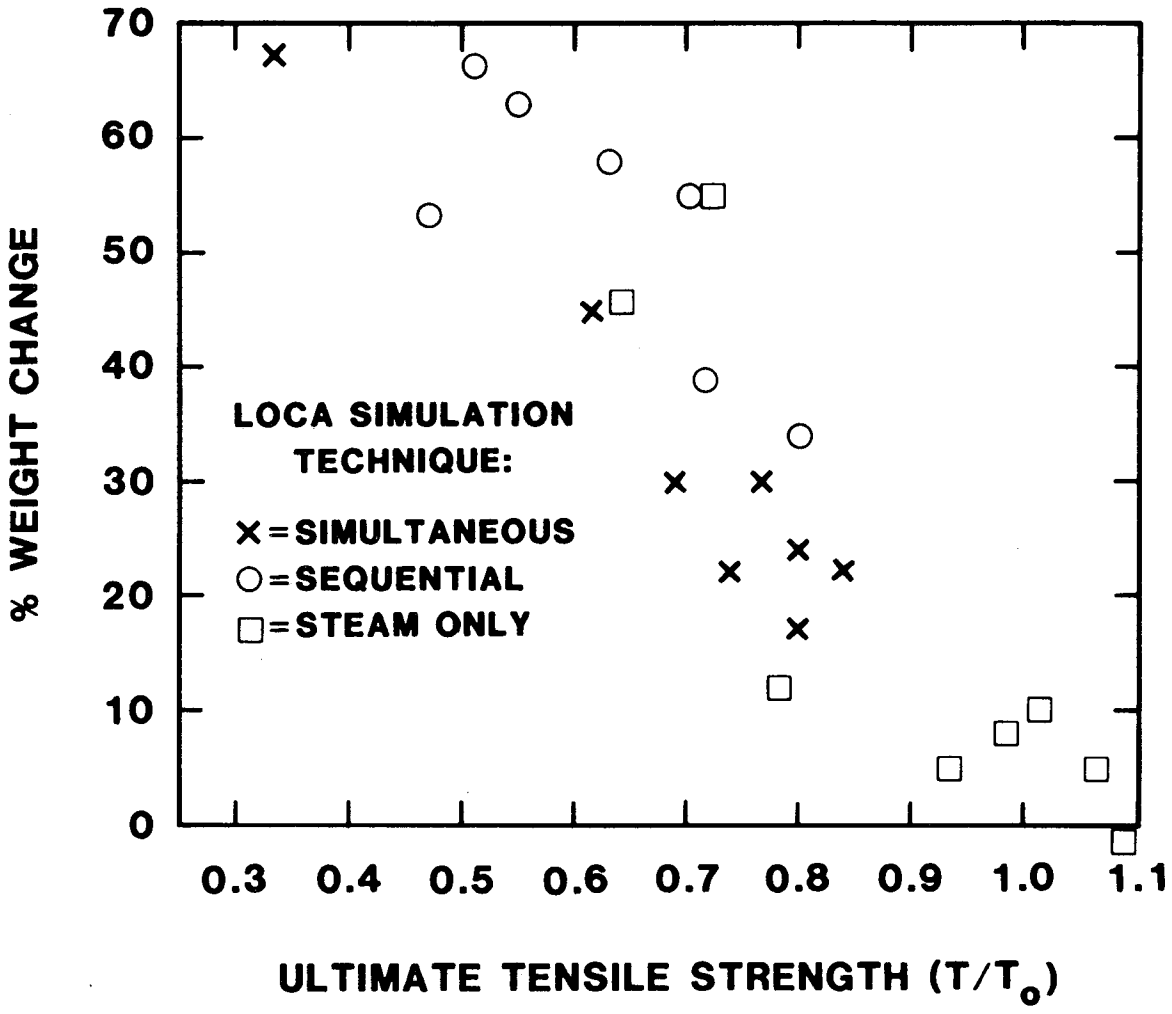

Figure 3.23. Relationship Between Weight Changes for EPR-1483 and the Normalized Ultimate Tensile Strength

	Aged at Start of LOCA	Unaged at Start of LOCA
Weight Increase		
4 d LOCA	44 ± 1	25 ± 1
Unanticipated Cooldown	77 ± 2	49 ± 1
Length Increase		
4 d LOCA	14 ± 5	7 ± 5
Unanticipated Cooldown	21 ± 5	14 ± 5
Width Increase		
4 d LOCA	9 ± 4	4 ± 4
Unanticipated Cooldown	18 ± 5	11 ± 4
Thickness Increase		
4 d LOCA	30 ± 8	18 ± 4
Unanticipated Cooldown	45 ± 4	35 ± 4

Table 3.29: Percentage Increase for Japanese EPR-5 Insulation Specimen Properties

Condition	Samples Aged at Start of LOCA e/e_o	Samples Aged at Start of LOCA T/T_o*	Samples Unaged Prior to Start of LOCA e/e_o	Samples Unaged Prior to Start of LOCA T/T_o*
Condition	Samples Aged at Start of LOCA		Samples Unaged Prior to Start of LOCA	
Unaged 1.00 ± .17 (7.8 ± 1.3 MPa)		1.00 ± /07 (560 ± 37)	1.00 ± .17 (7.8 ± 1.3 MPa)	1.00 ± .07 (560 ± 37)
Aged		.33 ± .05	.97 ± .17	
After 4d LOCA	.13 ± .02	.85 ± .15	.19 ± .02	.83 ± .14
Unanticipated Cooldown	.10 ± .01	.80 ± .14	.11 ± .02	.79 ± .17

*We normalized $T/_{To}$ using the average unaged cross-sectional area.

Table 3.30: Ultimate Tensile Properties for Japanese EPR-5 During Simultaneous Test #2.

4.0 DISCUSSION

For EPR A multiconductor cables we did not observe electrical performance variations caused by differences between our simultaneous and sequential test procedures. Insulation resistance, I.R., was monitored periodically during the test exposures. A voltage withstand test was performed upon completion of the accident simulations. During this latter test the leakage current was measured. An observable electrical performance difference was noted for the EPR E multiconductor cables. For the sequentially exposed EPR E cables we were unable at the start of the LOCA simulation to make I.R. measurements at 500 Vdc. The I.R. values were less than the lowest instrument reading, namely 1 MΩ. After reducing the applied voltage to 50 Vdc we did measure normalized I.R. values of ∿ 2 MΩ-m. In contrast, the simultaneously exposed multiconductor EPR E cable had a normalized I.R. value of 37 MΩ-m at 500 Vdc. The post-test leakage current values were similar for both the simultaneous and sequentially exposed EPR E cables.

An EPR C multiconductor cable was exposed to simultaneous test #1 environmental conditions only. The normalized I.R. values were greater than 3000 MΩ-m throughout the test. The post-test leakage current was less than 5 mA during a voltage withstand test of 80 Vac per mil of insulation thickness.

Electrical performance of our EPR D multiconductors depended strongly on LOCA simulation techniques. Both electrically and visually the simultaneously exposed EPR D multiconductor cables were worse than the sequentially exposed multiconductor cables. An example is provided by the post-LOCA leakage current data obtained after immersing the cables in tap water. At 600 Vac the sequentially exposed multiconductor had leakage currents of ∿ 1 mA. In contrast, the simultaneously exposed multiconductors had leakage currents of several hundred milliamps. Although we do not know exactly why this occurred, we will discuss three possibilities, the first of which we consider the most likely explanation. The remaining two hypotheses are presented for completeness in the discussion.

1) Figure 3.9 illustrates that the EPR D multiconductor jacket split during the simultaneous steam and radiation exposure. In Section 3.4 we also reported that the insulation had swelled dimensionally during the simultaneous accident simulation. Possibly the dimensional swelling of the EPR D insulation caused stress buildup within the multiconductor geometry. When the jacket split to relieve the stress, the sudden release of constrictive force on the insulators may have caused cracking or breakup of the insulation. Alternatively, sections of insulation which adhered to the jacket during the splitting were pulled away from the conductor. The bare copper conductor evident in Figure 3.9b is suggestive of such a process.

Our tensile specimen data (see Table 3.14) indicates that spatial swelling for sequentially exposed specimens is less severe than for simultaneously exposed samples. Thus for the sequential specimens, the initiating stress for jacket "splitting" would be less severe. In addition, the jacket may have had better tensile strength during the sequential steam exposure and hence resisted splitting. We did not measure the jacket tensile strength during our tests but note (see Figure 4.1) that simultaneous radiation and thermal exposures more severely degrade tensile strength for chlorinated polyethylene jacket material than does a thermal followed by radiation sequential set of exposures to the same environmental stresses.

A variation of the above hypothesis is as follows: swelling of the insulation caused splitting of the jacket. This removed a constraint on the insulation and allowed it to crack when its ultimate tensile elongation became less than the strain produced by bends in the cable. The applied strain to the cable consists of two "bend" components: (1) The multiconductor consists of a helical arrangement of single conductors spirally wound around each other. (2) The multiconductor is also wound on a mandrel.

From Thomas and Finney[16] we compute that the radius of curvature, r_e, for a helix with radius a and lay length h is:

$$r_e = a[1 + (h/2\pi a)^2]$$

For EPR D, the lay length, h, is approximately 11 cm while the helical diameter is between one and two thicknesses of each individual conductor. (The diameter of a single conductor was $\sim$ .5 cm by the end of the simultaneous LOCA simulation.) Thus we calculate r_e to be 7-13 cm. We relate this helical radius of curvature to strain by arguing that the outer surface of the insulated conductor must stretch to accommodate the helical wrapping of the inner surface with radius r_e. The elongation, e, at the outer surface will be

$$e = 2a/r_e$$

We predict that the helical component of elongation for the EPR D multiconductor geometry is between 4 and 7%.

In addition to the helical elongation component, during testing our EPR D multiconductor cables were wrapped on a mandrel with a radius of 15 cm. The radius of the

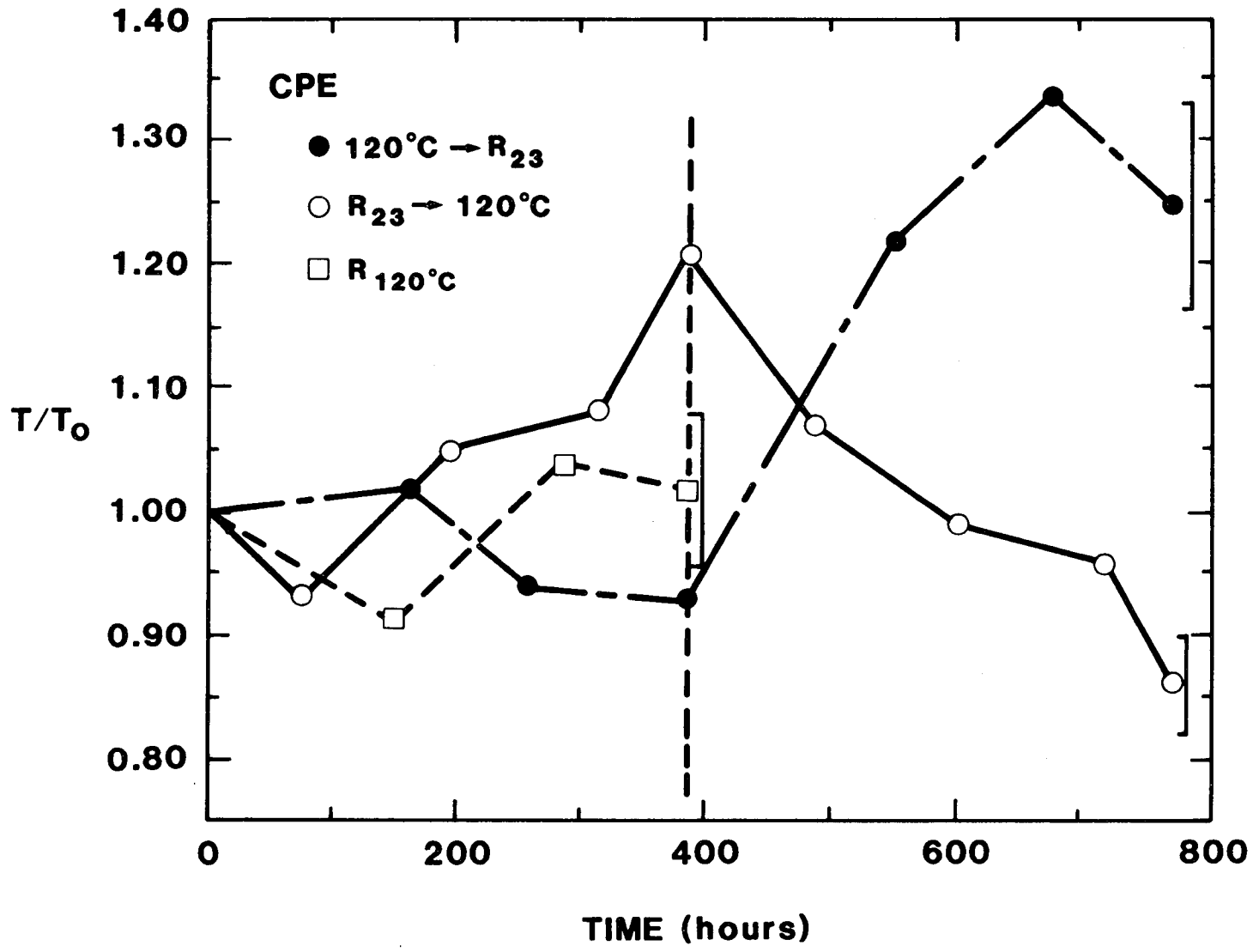

Figure 4.1. Chlorinated Plyethylene Jacket Ultimate Tensile Strength Behavior. Each portion of the sequential exposures lasted ~ 380 h. From reference 22.

multiconductor was ∿ .55 cm. This produces a "mandrel" elongation component of ∿ 7%. We therefore predict a maximum strain for some insulation segments of 10-15%. This maximum strain would occur at the outer surface of mandrel and helical wraps.

Room temperature measurements performed on EPR D tensile specimens within 24 hours of the completion of both the simultaneous and sequential test exposures yielded ultimate tensile elongations of ∿ 20%, comparable to our theoretical strain predictions of 10-15%.

Figure 3.9b illustrates that EPR D insulation "breakup" did occur at maximum strain locations (i.e., the outer surface of both the helical and mandrel wraps). While similar behavior might have been expected for the sequentially exposed multiconductor (its geometry and tensile properties were similar) the jacket did not split; impeding strain relief.

2) The EPR D spatial swelling also could have caused stress buildup for the multiconductor geometry because the three insulated conductors are spirally wound around each other. Hence, one conductor provides restraints against the spatial swelling of its neighboring conductor. For single conductor geometries this stress buildup would not occur. Though plausible, this hypothesis does not explain the degradation visible in Figure 3.9b; namely degradation on the outer surface of the multiconductor bundle.

3) A chemical interaction between jacket and insulation might also help explain our EPR D results. It is known that some chlorinated polymers evolve hydrogen chloride during radiation and/or thermal environments. Salovey[17] reports that "hydrogen chloride is the major volatile product of irradiated polyvinylchloride. The formation of hydrogen chloride during irradiation is sensitive to temperature" and is larger at higher temperatures.[17] Rose and Coffey[18] report that during processing chlorinated polyethylene will undergo rampant catalytic dehydrochlorination above approximately 190°C. Clough[11,19] reports on significant chlorine and antimony losses from chlorosulfonated polyethylene formulations during accelerated aging. He also presents chlorine and antimony loss data for several EPR formulations.

We also observed fire retardant loss during our simultaneous and sequential tests. Section 3.4 provides evidence for antimony, bromine, and chlorine migration from the CPE jacket. This effect was observed earlier in the simultaneous test than for the sequential test.

Possibly the simultaneous exposures generated more HCl and/or HBr than did the sequential exposures. Moreover, since the CPE jacket was not present for the single conductors, the single conductors were exposed to less HCl and or HBr than the multiconductor insulators. The absence of detectable Br in the single conductor insulation supports this hypothesis (see Section 3.4). The evolved acid may have broken chemical bonds between the polymer chain and the reinforcing filler such as calcined clay. Blodgett[20] claims that the water stability of EPR is due to the reinforcing effect of fillers when they are cross-linked into the polymer matrix. He also states that for long life in water, any hydrogen chloride must be neutralized.

Our three hypotheses emphasize insulation and jacket mechanical degradation rather than dielectric degradation. This is consistent with previous studies indicating that permanent changes in the electrical properties of elastomers were minor and that insulation life depends on its resistance to mechanical damage.[21]

During our tests we extensively monitored mechanical properties for several of the EPR insulations. Tensile properties, moisture absorption, and dimensional changes were measured. Our results clearly indicate that EPR cannot be considered to have generic behavior with respect to these parameters. For example, Table 4.1 summarizes moisture absorption data for each of the EPR's we tested. Some EPR's (EPR B and EPR E) experienced small moisture absorption during our tests while other EPR's (EPR D, EPR F, EPR-1483, and the Japanese EPR-5) exhibited substantial moisture absorption. We also observed large dimensional change variations among the different EPR's. Results are summarized in Tables 4.2 and 4.3.

Table 4.4 presents normalized ultimate tensile property data at the completion of accelerated aging. Our simultaneous aging techniques are more severe than our sequential technique for EPR A and EPR D ultimate tensile elongation properties and for EPR A, EPR B, and EPR D ultimate tensile strength properties. Table 4.5 presents normalized tensile results at the completion of the accident exposures. Results for EPR A are uncertain; EPR D and EPR E elongation degradation are worse for the sequential exposure.

Our results clearly show that tensile property degradation should not be used by itself to predict electrical degradation for multiconductor cables. Tensile property results may be useful to establish when insulation is susceptible to damage caused by other factors such as jacket degradation and bend radius. For example, sequentially exposed EPR D multiconductors performed substantially better electrically than did

Table 4.1

Insulation Specimens: Percentage Weight Increases

Cable Material	Sequential Test *	Simultaneous Test #1*	Simultaneous Test #2**
EPR A	+50%	?	
EPR B	+4%	-1%	
EPR C	+9%	+23%	
EPR D	+121%	+173%	+172%
EPR E	+0%	+7%	
EPR F			+94%
EPR-5			+77%***
EPR-1483	+55%****	+45%*****	

*Both the sequential and simultaneous #1 LOCA profiles were interrupted at day 9 by an unanticipated steam cooldown. The test was continued and measurements were made at the end of 21 days of steam exposure

**Measurements made during unanticipated steam cooldown starting at day 16 of LOCA profile

***Data for samples aged before start of LOCA

****Sequential 28 d thermal then 55 h irradiation aging exposure followed by sequential test accident exposure.

*****Simultaneous 7 d radiation and thermal exposure followed by simultaneous test #1 accident exposure.

Table 4.2

Insulation Specimens: Percentage Increase in Length

Cable Material	Sequential Test *	Simultaneous Test #1*	Simultaneous Test #2**
EPR A	+0%	?	
EPR B	+0%	+0%	
EPR C	+0%	+5%	
EPR D	+5%	+35%	+42%
EPR E	+0%	+0%	
EPR F			+19%
EPR-5			+21%***
EPR-1483	+7%****	+16%*****	

*Both the sequential and simultaneous #1 LOCA profiles were interrupted at day 9 by an unanticipated steam cooldown. The test was continued and measurements were made at the end of 21 days of steam exposure

**Measurements made during unanticipated steam cooldown starting at day 16 of LOCA profile

***Data for samples aged before start of LOCA

****Sequential 28 d thermal then 55 h irradiation aging exposure followed by sequential test accident exposure

*****Simultaneous 7 d radiation and thermal exposure followed by simultaneous test #1 accident exposure

Table 4.3

Insulation Specimens: Percentage Increase in Outer Diameter

Cable Material	Sequential Test [1]	Simultaneous Test #1 [1]	Simultaneous Test #2 [2]
EPR A	+19%	?	
EPR B	-18%	-5%	
EPR C [3]	+5% width +20% thickness	+7% width +20% thickness	
EPR D	+38%	+53%	+51%
EPR E [3]	+2% width +0% thickness	+0% width +0% thickness	
EPR F			+31%
EPR 5			+18% width [4] +30% thickness [4]
EPR-1483	17% width [5] +46% thickness [5]	+20% width [6] +46% thickness [6]	

[1] Both the sequential and simultaneous #1 LOCA profiles were interrupted at day 9 by an unanticipated steam cooldown. The test was continued and measurements were made at the end of 21 days of steam exposure

[2] Measurements made during unanticipated steam cooldown starting at day 16 of LOCA profile

[3] The manufacturer provided sheets of insulation material prior to providing actual cable construction. Sheet material was cut to be used as tensile specimens. These specimens were compression molded rather than extrusion molded.

[4] Data for samples before start of LOCA.

[5] Sequential 28 d thermal then 55 h irradiation aging exposure followed by sequential test accident exposure.

[6] Simultaneous 7 d radiation and thermal exposure followed by simultaneous test #1 accident exposure.

Material	Sequential Test		Simultaneous Test #1	
	e/e_o	T/T_o	e/e_o	T/T_o
EPR A	.29 ± .03	.96 ± .09	.05 ± .03	.23 ± .02
EPR B	.37 ± .06	1.21 ± .04	.28 ± .08	.58 ± .10
EPR C	.38 ± .05	.82 ± .06	.58 ± .16	.73 ± .11
EPR D	.41 ± .04	1.04 ± .04	.19 ± .02	.59 ± .04
EPR E	.34 ± .04	1.38 ± .29	.49 ± .07	1.28 ± .22

Table 4.4: Ultimate Tensile Properties at the Completion of Accelerated Aging

Material	Sequential Test		Simultaneous Test #1	
	e/e_o	T/T_o	e/e_o	T/T_o
EPR A	?	?	?	?
EPR B	.20 ± .04	.78 ± .06	.14 ± .03	.74 ± .05
EPR C	.13 ± .03	.66 ± .07	.15 ± .03	.62 ± .07
EPR D	.06 ± .04	.50 ± .11	.13 ± .02	.61 ± .02
EPR E	.05 ± .01	.71 ± 14	.19 ± .03	1.18 ± .21

Table 4.5: Ultimate Tensile Properties at the Completion of the Accident Exposures

simultaneously exposed EPR D multiconductors even though the former's insulation tensile properties were as degraded by the end of the test. This is reasonable since the sequentially exposed EPR D multiconductor experienced less dimensional swelling and not the jacket splitting which we hypothesize initiated mechanical damage for the simultaneously exposed insulation.

It is interesting to note that in our tests the EPR D simultaneously exposed multiconductors uniquely satisfied all the following conditions:

1. The insulation experienced large dimensional changes and substantial moisture absorption.

2. The insulation had low tensile property values at the completion of the test.

3. The jacket split.

4. The cable was tested as a multiconductor.

Other test specimens satisfied some of these conditions, but no other specimen satisfied them all. For example, EPR F also experienced substantial dimensional changes, but EPR F was not tested by us as a multiconductor. Two other features of EPR D separated it from the other EPR's we tested. First, it employed a chlorinated polyethylene jacket; all other jacketed EPR cables in our tests used chlorosulfonated polyethylene jackets (see Appendix C). Second, the initial elongation for EPR D was less than all the other EPR's. This is demonstrated in Table 4.6

For insulated single conductors we do not observe large electrical performance variations caused by differences between our simultaneous and sequential test procedures. EPR A, B, D, and E are examples. EPR C, F, and G insulated single conductors were only exposed to simultaneous testing environmental conditions. For each of these single conductors the I.R. and leakage current behavior was similar to that observed for the EPR A, B, D, and E single conductors.

The simultaneously exposed EPR D single conductors performed substantially better than did their multiconductor counterparts. We hypothesize that the excellent single conductor behavior resulted from (1) the absence of jacket-insulation interaction effects and/or (2) the less severe bending of the single conductor specimens compared to the multiconductor test specimens. The single conductor specimens, unlike the multiconductor insulated conductors, did not have a "helical" bend component associated with the multiconductor geometry. Hence the insulation strain was less. Quantitatively,

Material	e_o(%)	T_o (MPa)
EPR A	420 ± 10	8.8 ± 0.6
EPR B	330 ± 30	7.1 ± 0.4
EPR C*	513 ± 10	12.2 ± .08
EPR D	240 ± 10	15.2 ± .06
EPR E*	380 ± 50	8.4 ± 0.3
EPR F	290 ± 10	12.4 ± .8
EPR-1483*	320 ± 20	9.8 ± 0.4
Japanese EPR-5*	560 ± 40	7.8 ± 1.3

*These EPR specimens were obtained from compression molded EPR sheets.

Table 4.6: Ultimate Tensile Properties for Unaged, Unexposed EPR Tensile Specimens: EPR G values are not reported since the jacket is physically bonded to the insulation.

for our EPR D single conductors we wrapped the cables on a mandrel with a 25 cm diameter (50 x the outer diameter of the single conductor). We predict this caused a strain on the outer insulation surface of ~ 4%; a value less than what we measured for our tensile specimens. Hence cracking of the EPR D single conductors is unexpected and it also was not observed.

More generally, based on our post-test tensile measurements, we predict that our EPR B, EPR C, EPR D, EPR E, and EPR F single conductors would not have insulation cracking at the completion of our accident exposures. This was experimentally verified. Predictions for EPR A and EPR G cannot be made because of the absence of post-exposure tensile data.

Our test facility employed saturated steam conditions for the accident steam simulations. Hence oxygen was swept from the experimental chamber at the start of the accident exposures. Oxygen presence during steam exposures has recently been demonstrated to sometimes strongly affect EPR tensile properties. For example, Gillen, et al.,[23] showed that tensile properties for an EPR material (our EPR A) exhibited a pronounced dependence on the oxygen concentration during accident simulations. More degraded tensile properties were noted for those LOCA simulations with oxygen present. Contrasting this result, for their EPR-S (our EPR-1483) material oxygen concentration was not an important accident parameter. Kusama, et al.[24] also demonstrate that tensile properties for EPR materials are sensitive to the oxygen concentration during PWR LOCA simulations. They noted that elongation values were more degraded when oxygen was present during the LOCA simulations. For neither of these studies, were simultaneous thermal-irradiation aging techniques used prior to the LOCA simulations. We are currently investigating whether the importance of oxygen during LOCA simulations depends on the preconditioning (aging) technique. EPR C and EPR D materials are being studied.[22] Upon completion of these experimental tests, we will be better able to predict whether addition of oxygen during our steam exposures would have more severely degraded our single conductor electrical results.

The electrical behavior differences between our EPR D single and multiconductor cables suggest:

1. Contrary to historical perspective, our results and hypothesis indicate that testing of single conductors may not be more severe than multiconductor testing. It has been suggested that a multiconductor jacket provides additional protection not available to a single conductor. IEEE Std 383-1974[4] in its Table 1 supports this perspective by allowing single conductor test results to be used as a qualification bases for multiconductor control cables. Our results suggest that jacket-insulation interaction effects may be important.

2. Some cable qualification tests may not adequately account for "use" bend conditions. An example is qualification of multiconductors via testing of single conductors. IEEE Std 383-1974[4] does not recommend cable curvature during environmental exposure. It does state in Section 2.4.4:

> Upon completion of the LOCA simulation, the specimens should be straightened and recoiled around a metal mandrel with a diameter of approximately 40 times the overall cable diameter and immersed in tap water at room temperature. While still immersed, these specimens should . . . pass (a) voltage withstand test.

Our calculations for EPR D illustrate that the single conductor "helical" radius of curvature due to the multiconductor geometry is less than 40 times the single conductor's radius.

We also observe that manufacturers' minimum bend radius recommendations are not always correlated to qualification test conditions. For example, EPR C instrumentation cables were qualified to MSLB conditions using a mandrel of radius 14 cm. The manufacturer marketing literature lists a minimum bend radius for this cable of $\sim$ 6 cm. Installation practices are customer specific and are not addressed.

Our single conductor and multiconductor test results suggest an additional conclusion. Insulation resistance is strongly dependent on steam temperature but not very dependent on whether a radiation environment is simultaneously applied. For only EPR A (primary insulation only), EPR D, and EPR E did we notice observable I.R. differences between our sequential and simultaneous test measurements. For EPR D these differences did not occur at the start of the LOCA steam exposure, but rather later after mechanical degradation had presumably started. For EPR A and E we did not observe a consistent effect of radiation on I.R. behavior. For example, sequentially exposed EPR E multiconductors have lower I.R. values than do simultaneously exposed multiconductors while EPR E and EPR A single conductors exhibit the opposite dependence on testing technique.

We recognize that the sequentially exposed cables had experienced much more irradiation at the start of the steam exposure than did the simultaneously exposed cables. Our results reflect the practical difference between simultaneous and sequential qualification techniques.

It should be noted that our test conditions differ from the qualification test parameters used by some manufacturers and utilities. We did not intend our tests to be qualification tests and chose our research test parameters to match our experimental capabilities and to "generally" reflect test procedures used by the cable industry (for example, there is no standard environmental profile). EPR D is an example where our test conditions differed in several respects from those employed by the manufacturer during his qualification tests:

1. We loaded our cables at 0.6 amps while EPR D was loaded by the manufacturer to currents greater than or equal to 10 amps.

2. Our test profile employed two transient steam ramps while EPR D was tested using a steam profile that had only one transient ramp.

3. Our steam profile had saturated steam conditions with maximum temperatures of 172°C and maximum pressures of 106 psig. EPR D was qualified employing superheat conditions to 196°C with pressures of 65 psig or less.

4. Our steam profile did not include chemical spray. EPR D qualification testing included chemical spray during part of the accident simulation.

The major goal of our research was to investigate if test results are sensitive to whether simultaneous or sequential stress exposures are employed. For EPR cable products we cannot provide a generic answer. EPR C provides an example of a cable product for which simultaneous testing procedures are currently not warranted. This product had excellent electrical performance during our simultaneous tests. Insulation tensile degradation and dimensional changes were comparable for sequential and simultaneous testing techniques. Moreover, the residual tensile elongation at the completion of our tests was $\sim$ 60%; large enough to possibly accommodate additional degradation if oxygen presence during accident simulations is important. (We did not include oxygen during our accident simulations.)

EPR D is a cable product for which simultaneous testing techniques were more severe than our sequential procedures. For this product, the simultaneously exposed multiconductor performed electrically worse than did its sequentially exposed counterpart. Dimensional changes during accident simulations did depend on whether simultaneous or sequential techniques were employed. Likewise, jacket degradation was strongly dependent on exposure technique. Finally, the residual insulation tensile elongation at the completion of our tests was $\sim$ 20%; close to our predicted "embrittlement threshold". Thus EPR D may not accommodate additional degradation if oxygen presence during accident simulations is important.

For EPR D we only employed a thermal aging-irradiation-steam exposure sequential test procedure. Possibly, an irradiation-thermal aging-steam sequence would adequately duplicate our simultaneous results. For tensile properties and dimensional changes, the US-French cooperative research program (in progress) will answer whether irradiation followed by thermal aging test sequences are as severe as simultaneous techniques.

In addition to the US-French cooperative research programs, we recommend that research tests be performed to establish why some EPR materials experienced more degradation than others. Without this information we can only report which aging and accident test procedures most severely degrade individual EPR products but cannot begin to understand which test procedures most realistically simulate aging and accident environments. This last research goal may be impossible because proprietary issues associated with cable production and EPR formulations will make progress in this research area difficult.

During its assessment of the safety significance of our research, the USNRC must consider many technical factors. Two additional technical results from our research may be relevant. Both concern the substantial dimensional changes we observed for some EPR materials and which we hypothesize may be responsible for the electrical degradation of our EPR D multiconductor cables. These results are:

1. The large dimensional changes we observed for some of our EPR's did not occur immediately at the start of the accident simulation. For EPR D we did not observe electrical degradation until several days after the start of our accident exposure. Hence, safety systems required to function only at the start of an accident may not be affected by dimensional changes of the cable insulation.

2. Accelerated aging strongly impacted the extent of dimensional swelling and moisture absorption; in agreement with previous results.[23] Tables 3.14 and 3.20 compare test results of EPR D and EPR F for unaged and aged tensile specimens. For example, aged EPR D insulation had a 42% diameter increase during our simultaneous LOCA simulation. Unaged EPR D exposed to the same accident simulation only increased its diameter by 7%. Our aged specimens were accelerated to a 40 year life; far in excess for any current application of EPR D (it was not marketed until late 1976.) Future tests need to establish whether similar results would be obtained for naturally aged cable.

REFERENCES

1. 10CFR50.49 "Environmental Qualification of Electric Equipment Important to Safety for Nuclear Power Plants," Nuclear Regulatory Commission, Federal Register, Vol. 48, No. 15, 2729, 1/21/83.

2. A. J. Szukiewicz, "Interim Staff Position on Environmental Qualification of Safety-Related Electrical Equipment -- Including Staff Responses to Public Comments," NUREG-0588, Rev. 1, U.S. NRC, Washington, DC, July 1981.

3. IEEE Standard for Qualifying Class 1E Equipment for Nuclear Power Generating Stations, IEEE Std 323-1974, New York, NY.

4. IEEE Standard for Type Test of Class 1E Electric Cables, Field Splices, and Connections for Nuclear Power Generating Stations. ANSI/IEEE Std 383-1974 (ANSI N41.1C-1975), New York, NY.

5. F. V. Thome, "Preliminary Data Report: Testing to Evaluate Synergistic Effects from LOCA Environments, Test IX. Simultaneous Mode; Cables, Splice Assemblies, and Electrical Insulation Samples," SAND78-0718, April 1978.

6. K. Yoshida, Y. Nakase, S. Okada, M. Ito, Y. Kusama, S. Tanaka, Y. Kasahara, S. Machi, "Methodology Study for Qualification Testing of Wire and Cable at LOCA Condition," presented at 8th Water Reactor Safety Research Information Meeting, U.S. Nuclear Regulatory Commission, October 1980.

7. T. H. Ling and W. F. Morrison, "Qualification of Power and Control Cable for Class 1E Applications," presented at the IEEE Power Engineering Society Winter Meeting, New York, NY, January 27-February 1, 1974. Conference Paper C74045-1.

8. U. I. Vaidya, "Flame Retarded EPDM Integral Insulation Jacket Compositions With Excellent Heat Resistant and Electrical Stability." Presented at ACS Rubber Division Meeting, October 12, 1978, Boston, MA.

9. L. D. Bustard, "Ethylene Propylene Cable Degradation during LOCA Research Tests: Tensile properties at the Completion of Accelerated Aging," NUREG/CR-2553, SAND82-0346, May 1982.

10. E. A. Salazar, D. A. Bouchard, D. T. Furgal, "Aging with Respect to Flammability and Other Properties in Fire-Retarded Ethylene Propylene Rubber and Chlorosulfonated Polyethylene," NUREG/CR-2314, SAND81-1906, March 1982.

11. R. L. Clough, "Aging Effects on Fire-Retardant Additives in Organic Materials for Nuclear Plant Applications," NUREG/CR-2868, SAND82-0485, August 1982.

12. L. L. Bonzon et al., "Qualification Testing Evaluation Program Light Water Reactor Safety Research Quarterly Report, April-June 1978," SAND78-1452, NUREG/CR-0401, November 1978.

13. K. T. Gillen, R. L. Clough, and L. H. Jones, "Investigation of Cable Deterioration in the Containment Building of the Savannah River Nuclear Reactor," SAND81-2613, August 1981.

14. W. H. Buckalew and F. V. Thome, "Radiation Capabilities of the Sandia High Intensity Adjustable Cobalt Array," SAND81-2655, NUREG/CR-1682, March 1982.

15. E. E. McLlveen, V. L. Garrison, and G. T. Dobrowolski, "Class 1E Cables for Nuclear Power Generating Stations," IE Transactions on Power Apparatus and Systems PAS-03 (4), July/August 1974, pp. 1121-1132. We determined the referenced activation energy for Arrhenius-type plots.

16. G. B. Thomas and R. L. Finney, Calculus and Analytic Geometry, Addison-Wesley, Reading, Massachusetts, 5 ed., 1979.

17. R. Salovey, "Poly(vinyl Chloride)" in The Radiation Chemistry of Macromolecules, Vol. II, M. Dole, ed., Academic Press, 1973, p. 38.

18. J. C. Rose and R. J. Coffey, Rubber World, Vol. 187 (2), p. 28, November 1982.

19. R. L. Clough, "Aging Effects on Fire-Retardant Additives in Polymers," J. Polym. Sci., Polym, Chem. Ed. 21, 767 (1983).

20. R. B. Blodgett, Rubber Chemistry and Technology, 52, 410 (1979).

21. K. T. Gillen, E. A. Salazar, C. W. Frank, "Proposed Research on Class 1 Components to Test a General Approach to Accelerated Aging Under Combined Stress Environments," SAND76-0715, NUREG/CR-0237, April 1977.

22. L. D. Bustard, "QTE LOCA Testing Research," SAND83-1086A. Presented at the EPRI/Sandia/NRC Information Exchange, San Diego, California, May 1983.

23. K. T. Gillen, R. L. Clough, G. Ganouna-Cohen, J. Chenion, and G. Delmas, "The Importance of Oxygen in LOCA Simulation Tests," Nuclear Engineering and Design 74 (1982), 271-285.

24. Y. Kusama, S. Okada, M. Yoshikawa, M. Ito, T. Yagi, Y. Nakase, T. Seguchi, and K. Yoshida, "Methodology Study for Qualification Testing of Wire and Cable at LOCA Conditions," NUREG/CP-0041, Proceedings of the U.S. Nuclear Regulatory Commission Tenth Water Reactor Safety Research Information Meeting, v 5, p 330.

APPENDIX A: Summary of Unanticipated Events During Testing

Our sequential and simultaneous tests did include several unanticipated occurrences. In this appendix we summarize these events and discuss their significance. Our discussion emphasizes EPR D results since this cable product exhibited substantial degradation during our simultaneous tests.

1. Event: During the first four and a half hours of thermal aging for simultaneous test #1, the heater was turned off three times and the chamber opened to allow for adjustment of the heater ducts. Hence the cables and insulation samples were thermally cycled.

   Discussion: We redesigned the heater ducting before performing simultaneous test #2. This latter test did not thermally cycle the cables and insulation samples. Simultaneous test #2 did produce similar EPR D behavior as simultaneous test #1, hence the thermal cycling is considered not important.

2. Event: During thermal aging for simultaneous test #1, the chamber overheated for approximately an hour. The maximum temperature during this transient was 175°C.

   Discussion: During thermal aging for simultaneous test #2 the chamber temperature did not exceed 150°C (see Table 2.14). Moreover, during thermal aging for the sequential test we also momentarily achieved temperatures near 150°C at the start of the thermal exposure. Finally, a seven day 150°C thermal exposure was chosen by the manufacturer of EPR D for qualification tests. For all these reasons, the 175°C exposure during simultaneous test #1 aging does not appear to explain EPR D's behavior.

3. Event: During the first ramp of the sequential test, a penetration leaked excessively and had to be retorqued. The ramp was continued after retorquing the penetration. Since the simultaneous chamber was initially connected in parallel to the sequential chamber, the leak in the sequential chamber affected the steam profile for simultaneous test #1. Upon discovery of the leak, the simultaneous chamber was isolated from the sequential chamber and its ramp continued separately. Table 2.6 summarizes the time-temperature history for these steam exposures.

   Discussion: The penetration that leaked excessively contained only feedthroughs for EPR E multiconductor cables. A post test examination revealed no cracks or flaws for EPR E jackets in the vicinity of this penetration. The differences in sequential and simultaneous test #1 steam profiles do not appear

significant enough to explain EPR D behavior differences between the two tests. This nonconformance definitely cannot explain the differences between EPR D single conductor and multiconductor behavior during simultaneous test #1. This nonconformance did not occur for simultaneous test #2 which had similar EPR D behavior as for simultaneous test #1.

4. Event: Prior to the first ramp of simultaneous test #2 we momentarily passed steam through the chamber (which was open to ambient conditions).

   Discussion: Both the entrance and exit ports for the steam flow were located in the top section of the chamber. EPR D's poor visual appearance and electrical behavior occurred where the cable was wrapped on the mandrel well away from these ports. This nonconformance cannot explain the differences between EPR D single conductor and multiconductor behavior since both types of cable configurations were in the chamber. Moreover, the nonconformance did not occur during simultaneous test #1. Simultaneous test #1 did produce similar EPR D behavior as simultaneous test #2. For all these reasons, this nonconformance is considered unimportant.

5. Event: During the first peak of simultaneous test #2 a Tefzel cable excessively leaked water onto our current and voltage loading circuit causing it to fail. We reconfigured and repaired the loading circuit and resumed current and voltage loading of cables.

   Discussion: Insulation resistance measurements for EPR D made after this nonconformance gave expected values consistent with simultaneous test #1. Thus the nonconformance is considered unimportant.

6. Event: During the first peak of simultaneous test #2 water accumulated in the bottom of the steam chamber and submerged some cables. We estimate the maximum water level as between 67 and 91 cm below the top of the mandrel. We drained the water from the chamber 1-1/2 hours after the start of the 1st steam peak.

   Discussion: Examination of Table 2.16 indicates that water submergence lowered the exposure temperature for those cables submerged. Both EPR D single conductors and multiconductors were submerged. Simultaneous test #1 did produce similar EPR D behavior as simultaneous test #2, but did not include water submergence. Thus the nonconformance is considered unimportant.

7. Events: On day 9 of the simultaneous test #1 steam exposure the steam supply system failed and the steam chamber cooled to ambient temperatures and pressures.

Twenty-one hours later the irradiation was stopped. On day 12, the steam and radiation exposures were resumed. On day 16 of the simultaneous test #2 steam exposure the steam supply system failed and the steam chamber cooled to ambient temperatures and pressures. Eight hours later the irradiation was stopped. On day 21 we resumed the steam and radiation exposures.

Discussion: Insulation resistance measurements made during simultaneous test #2 for EPR D multiconductors clearly show I.R. degradation starting prior to the unanticipated cooldown. Figure 3.1b was photographed during the cooldown and clearly indicates degradation prior to restarting simultaneous test #2. Likewise, high leakage currents were measured during the cooldown (see Table 3.1). This data indicates that for EPR D the cooldown could be considered the end of a 16 day continuous test with poor electrical and visual behavior evident at the completion of the test. Table 2.16 demonstrates that the cooldown was gradual and not abrupt. For all these reasons we discount the cooldown as the cause of EPR D's poor multiconductor behavior during simultaneous test #2. It is therefore also unlikely that the simultaneous test #1 cooldown was important.

Finally a nonconformance that did not occur needs to be discussed. During all our steam exposures we loaded the cables at 480 Vac and 0.6 amp. This load circuit never "tripped out" due to EPR D degradation. The circuit was not designed to "trip out". Current flow was limited by load resistors to 600 mA. In addition, since we did not apply a chemical spray nor water spray during the steam exposure, our test only provided a rather pure steam environment as a path between an insulation failure and ground. This path is not expected to be very conducting and insulation failures would not necessarily be evident until post-test I.R. and leakage current measurements were made using tap water as a conducting medium.

APPENDIX B: Chemical Analysis for EPR D Samples.

Eleven samples were sent to Huffman Laboratories* for analysis. The samples were:

1. EPR D white insulation removed from an unaged cable.

2. EPR D white insulation removed after completion of aging and accident exposures from a simultaneously exposed (simultaneous test #1) single conductor.

3. EPR D white insulation removed after completion of aging and accident exposures from a sequentially exposed single conductor.

4. EPR D insulation removed after completion of aging and accident exposures from a simultaneously exposed multiconductor.

5. EPR D insulation removed after completion of aging and accident exposures from a sequentially exposed multiconductor.

6. CPE jacket removed from an unaged EPR D multiconductor cable.

7. CPE jacket removed from a simultaneously exposed EPR D multiconductor cable. White surface residue was scrapped from the jacket prior to chemical analysis.

8. CPE jacket removed from a sequentially exposed EPR D multiconductor cable. White surface residue was scrapped from the jacket prior to chemical analysis.

9. CPE jacket removed from a sequentially exposed EPR D multiconductor cable.

10. CPE jacket removed from a simultaneously exposed EPR D multiconductor cable.

11. White powder scrapped off the surface of the CPE jacket exposed to the sequential test sequence.

*3830 High Court, P. O. Box 777, West Ridge, Colorado 80034

E.W.D. HUFFMAN, JR., Ph.D.
PRESIDENT

CUSTOMER #:
01175

ESTABLISHED 1936

HUFFMAN LABORATORIES, INC.
3830 HIGH COURT, P.O. Box 777
Wheat Ridge, Colorado 80034
(303) 424-3232

E.W.D. HUFFMAN, SR., Ph.D.
CHAIRMAN

DATE 05/16/83
LAB# 048483
P.O. 52-9761
RECD 04/19/83

ANALYSIS REPORT

L. D. BUSTARD
SANDIA LABORATORIES.
REC. DIV. BLDG. 894
ALBUQUERQUE NM 87185

SEQUENCE/ SAMPLE ID	01 1	02 2	03 3	04 4
CHLORINE------%	9.72	8.43	8.33	11.04
BROMINE-------%	<0.20	<0.20	<0.20	0.66

SEQUENCE/ SAMPLE ID	05 5	06 6	07 7	08 8
CHLORINE------%	10.85	14.22	10.31	11.41
BROMINE-------%	2.58	3.57	3.44	2.91

SEQUENCE/ SAMPLE ID	09 9	10 10	11 11
CARBON-------%			3.60
HYDROGEN------%			0.40
CHLORINE------%	11.07	10.90	4.59
BROMINE-------%	2.71	3.74	8.20
SPECIAL ANAL.			*

* THE EMISSION SPECTROCHEMICAL ANALYSIS IS ENCLOSED ON A SEPARATE PAGE.
THE CARBON HYDROGEN DETERMINATION WAS PERFORMED BY COMBUSTING THE SAMPLE AT 1050 DEGREES C IN OXYGEN, THEN SEPARATING AND MEASURING THE RESULTING CARBON DIOXIDE AND WATER. AFTER COMBUSTION IN A TIN CAPSULE (WHICH RAISES THE TEMPERATURE OF THE SAMPLE TO ABOUT 1600 DEGREES C) THE COMBUSTION GASES WERE SWEPT THRU COMBUSTION CATALYSTS AND THRU A COOLED TUBE CONTAINING CaCl2 WHICH TRAPPED THE WATER BUT ALLOWED THE CARBON DIOXIDE TO BE SWEPT ON THRU A SCRUBBER TO REMOVE NITROGEN OXIDES AND INTO A COULOMETRICS CARBON DIOXIDE COULOMETER WHICH MEASURES THE CARBON DIOXIDE. AFTER SWEEPING ALL OF THE CARBON DIOXIDE FROM THE CaCl2 TUBE, THE COOLING WATER WAS TURNED OFF AND THE TUBE HEATED TO DRIVE OFF THE WATER WHICH WAS SWEPT INTO A HEATED TUBE OF 1,1' CARBONYLDIIMIDAZOLE WHICH QUANTITATIVELY CONVERTS WATER TO CARBON DIOXIDE. THE RESULTING CARBON DIOXIDE WAS THEN SWEPT INTO ANOTHER CARBON DIOXIDE COULOMETER FOR MEASUREMENT. ACETANILIDE FROM THE NBS WAS USED AS A STANDARD.
THE EMISSION SPECTROCHEMICAL ANALYSIS WAS PERFORMED BY FIRST ASHING THE SAMPLE WITH SULFURIC ACID, THEN PLACING IT ON A CARBON ROD, AND PASSING A HIGH

E.W.D. HUFFMAN, JR., Ph.D.
PRESIDENT

ESTABLISHED 1936

HUFFMAN LABORATORIES, INC.
3830 HIGH COURT, P.O. Box 777
Wheat Ridge, Colorado 80034
(303) 424-3232

E.W.D. HUFFMAN, SR., Ph.D
CHAIRMAN

CUSTOMER #:
01175

DATE 05/16/83
LAB# 048483
P.O. 52-9761
RECD 04/19/83
* * (CONT) * *

ANALYSIS REPORT

L. D. BUSTARD
SANDIA LABORATORIES
REC. DIV. BLDG. 894
ALBUQUERQUE NM 87185

VOLTAGE ELECTRIC SPARK BETWEEN THE SAMPLE ROD AND ANOTHER CARBON ROD. THE LIGHT PRODUCED IS THEN SEPARATED BY PASSING THRU A DIFFRACTION GRATING AND RECORDED ON FILM WHICH IS THEN COMPARED TO FILM PRODUCED BY RUNNING INTERNAL STANDARDS. THERE WERE NOT ANY APPROPRIATE NBS STANDARDS AVAILABLE.

THE CHLORINE AND BROMINE DETERMINATIONS WERE PERFORMED BY COMBUSTING THE SAMPLES IN OXYGEN AND ABSORBING THE COMBUSTION GASES IN A BASIC SOLUTION, FOLLOWED BY TWO TYPES OF MEASUREMENT. ONE METHOD INVOLVED ABSORBING THE COMBUSTION GASES IN A SOLUTION OF SODIUM HYDROXIDE AND SODIUM BISULFITE, DESTROYING THE THE BISULFITE WITH H202, ADJUSTING THE pH, THEN TITRATING THE SOLUTION WITH SILVER NITRATE USING POTENTIOMETRIC END POINTS FROM A SILVER SULFIDE ELECTRODE AND DOUBLE JUNCTION REFERENCE ELECTRODE. THE OTHER METHOD USED A KOH AND H202 ABSORBING SOLUTION WHICH WAS THEN RUN THRU A WESCAN ION CHROMATAGRAPH FOR DETERMINATION OF THE BROMIDE AND CHLORIDE CONTENT. A FAIRLY WIDE RANGE OF HALOGEN CONTENT WAS FOUND IN MOST OF THE SAMPLES WHICH IS DUE TO THE NON-HOMOGENIETY OF THE SAMPLES. THE METHODS THEMSELVES SHOULD GIVE REPEATABLE RESULTS WITHIN PLUS OR MINUS 0.3% ABSOLUTE. THE FOLLOWING TABLE GIVES THE RESULTS OBTAINED BY THE TWO DIFFERENT METHODS ALONG WITH SOME REPLICATES. FOR STANDARD MATERIALS WE USED P-CHLOROBENZOIC ACID AND P-BROMOBENZOIC ACID SUPPLIED FROM THE BRITISH DRUG HOUSE.

	ION CHROMATAGRAPH		SILVER NITRATE TITRATION	
SAMPLE #	CHLORINE%	BROMINE%	CHLORINE%	BROMINE%
1	10.09	<0.20	9.72, 10.82	<0.20, <0.20
2	9.12	<0.20	8.67, 8.33	<0.20, <0.20
2	10.51	<0.20	8.64, 8.23	<0.20, <0.20
4	11.60	0.58	10.47	0.74
5	11.65	2.33	10.81, 10.10	2.83, <0.20
6	16.60	3.96	14.15	3.55
7	11.45	3.69	9.17	3.19
8	11.19	3.48	11.62	2.34
9	11.07	2.71	12.10	--
10	11.90	3.74	10.85	--
11	0.62, 4.17	6.72, 8.76	8.76	6.07
11	6.07	8.56		

APR 29 1983

Spectran Laboratories INC.
2310-R KIPLING STREET, 80215
~~6000 W. 10TH AVE.~~ DENVER, COLORADO ~~80214~~
PHONE: AREA CODE 303-232-6304
CHEMICAL ANALYSIS • RESEARCH • CONSULTING

APRIL 27, 1983

HUFFMAN LABORATORIES, INC.,
POST OFFICE BOX 777,
WHEAT RIDGE, COLORADO 80034

ATTENTION: DALE RAINES

SUBJECT: OUR ANALYSIS REPORT, YOUR PURCHASE ORDER NO. 14983.

DEAR DALE:

THE FOLLOWING ARE OUR QUALITATIVE-SEMIQUANTITATIVE EMISSION SPECTROCHEMICAL ANALYSIS RESULTS, OBTAINED IN EXAMINATION OF YOUR SAMPLE. THEY ARE EXPRESSED AS WEIGHT PERCENTAGES, AND ARE ESTIMATES ONLY.

ELEMENT FOUND	NO. 484-83-11
ANTIMONY	MAJOR*
SILICON	0.5 %
IRON	0.1
LEAD	0.1
CHROMIUM	0.005
ALUMINUM	0.001
CALCIUM	0.001
COPPER	0.001
MAGNESIUM	0.0005

(* = CONC'N WELL ABOVE 10%, NOT DETERMINABLE BY SPECTROGRAPH; FILM REFERENCE: 48308-5)

NO OTHER ELEMENTS WERE DETECTED. THE SPECTROGRAPH DOES NOT DETECT: C, H, O, N, S, SE, OR THE HALOGENS. OUR INVOICE IS ENCLOSED. THANK YOU.

SINCERELY

SPECTRAN LABORATORIES, INC.

Leo D. Frederickson

LEO D. FREDERICKSON, JR., DIRECTOR

ENCL. - INV. 6107

APPENDIX C: Jacket Behavior

Chlorosulfonated polyethylene (CSPE) or chlorinated polyethylene (CPE) jackets are employed for all the commercial EPR product constructions which we tested except for EPR F. (The EPR F single conductor does not have a jacket.) In this appendix we describe the jacket behavior observed during our tests. Our data consists mostly of visual descriptions since jacket tensile specimens were not part of the test program.

Figures A.1 and A.2 illustrate the degraded condition of the jackets at the completion of the sequential test and simultaneous test #1, respectively. The simultaneous test was clearly more damaging for both CPE and CSPE jacket materials than was the sequential test. (EPR D's jacket was CPE; all other cables had CSPE jackets.) At the completion of the sequential test, every CSPE and CPE jacket was intact; there was no cracking evident. In contrast, at completion of the simultaneous test, every multiconductor CSPE and CPE outer jacket was substantially cracked and degraded.

The type of jacket degradation depended strongly on both the manufacturer and the jacket material. Figure A.3 illustrates two CSPE jacketed cables produced by different manufacturers. The upper cable in Figure A.3 has many small surface cracks with more gigantic (but localized) rupturing and splintering of the jacket. The lower cable has no evidence of small surface cracking. Rather, localized splitting and splintering of the jacket occurred. In contrast to the localized degradation exhibited by these two CSPE jackets, the CPE outer jacket for EPR D multiconductors had one continuous longitudinal crack (see Figures 3.9a and 3.9b).

EPR A, EPR B, EPR E, and EPR G cables also had CSPE jackets surrounding each single conductor. For EPR E and EPR G, these jackets were initially bonded to the insulation; for EPR A and EPR B the insulation and jacket were not initially bonded together. At completion of simultaneous testing, the EPR G single conductor jackets had longitudinal cracks. The EPR A, EPR B, and EPR E single conductor jackets were intact.

A white powder migrated to the surface of the CPE jacket (the EPR D multiconductor cables) during both the sequential and simultaneous tests. For the simultaneous test the powder was evident at the completion of aging. For the sequential test we first observed it on the eighth day of the LOCA simulation during our visual examination in response to the unanticipated cooldown. Upon completion of the accident exposures we removed some of the powder from the sequentially exposed jacket and performed emission spectroscopy and wet chemical analysis. Antimony (10 wt %), chlorine ($\sim$4.5 wt %) and bromine ($\sim$8 wt%) were important constituents of the powder (see Appendix B).

During thermal aging the jackets also appeared to lose ingredients from their formulations. This was evident as a greasy film that accumulated on the inside surface of the chamber as well as in the blower used to circulate hot air to and from the chamber.

Our thermal exposures also caused mild mechanical damage to the jackets of several cables. For example, during simultaneous test #1 aging, thermocouple wiring caused jacket indentations in EPR D's CPE and EPR A's CSPE jackets. At completion of the simultaneous test #2 aging exposure, the EPR D multiconductor #2 CPE jacket had a circumferential crack ~.5 cm long and ~.15 cm wide. The crack was next to a clip that supported the cable on the mandrel.

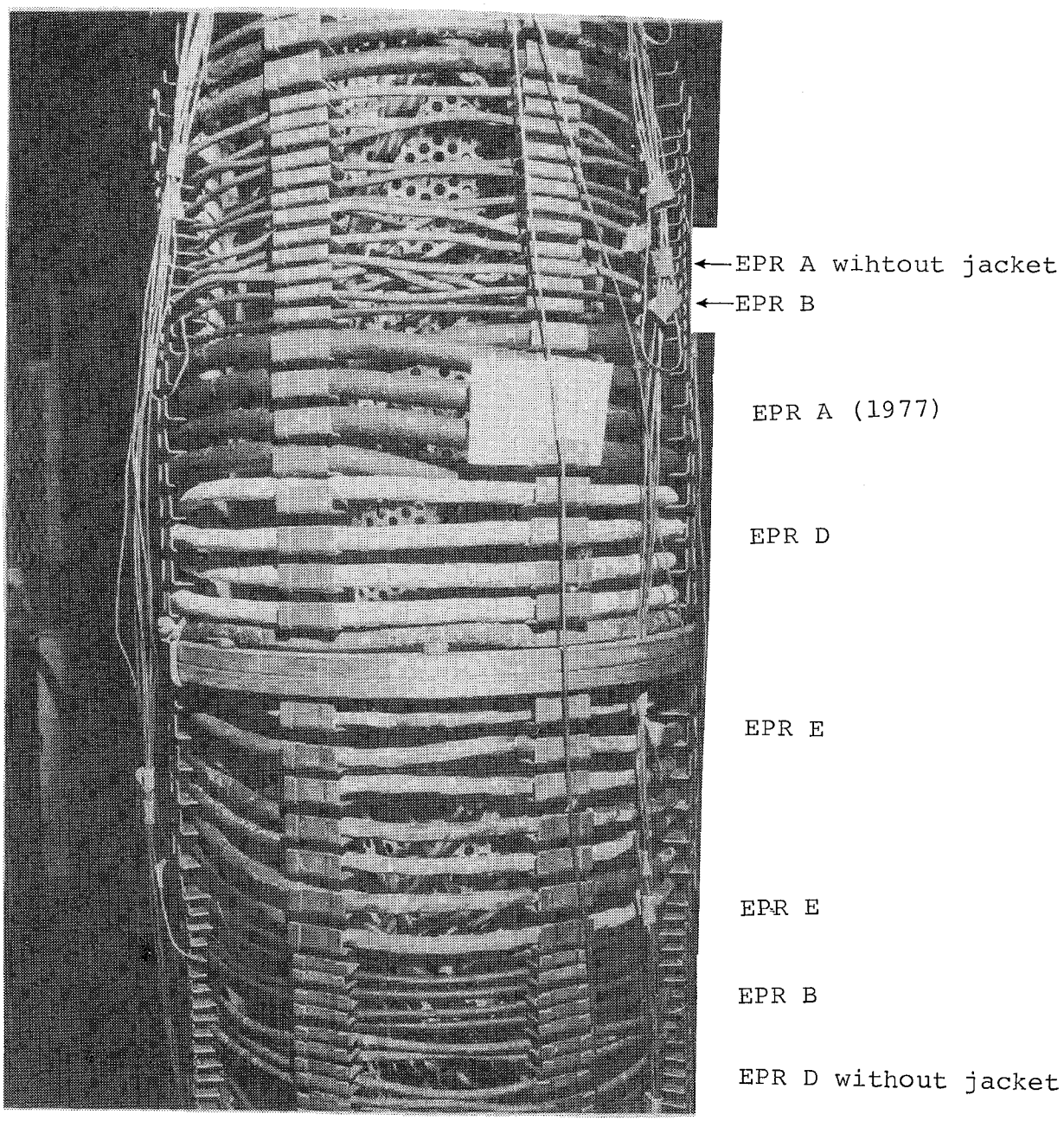

Figure C.1. Jacket Visual Appearance at the Completion of the Sequential Test

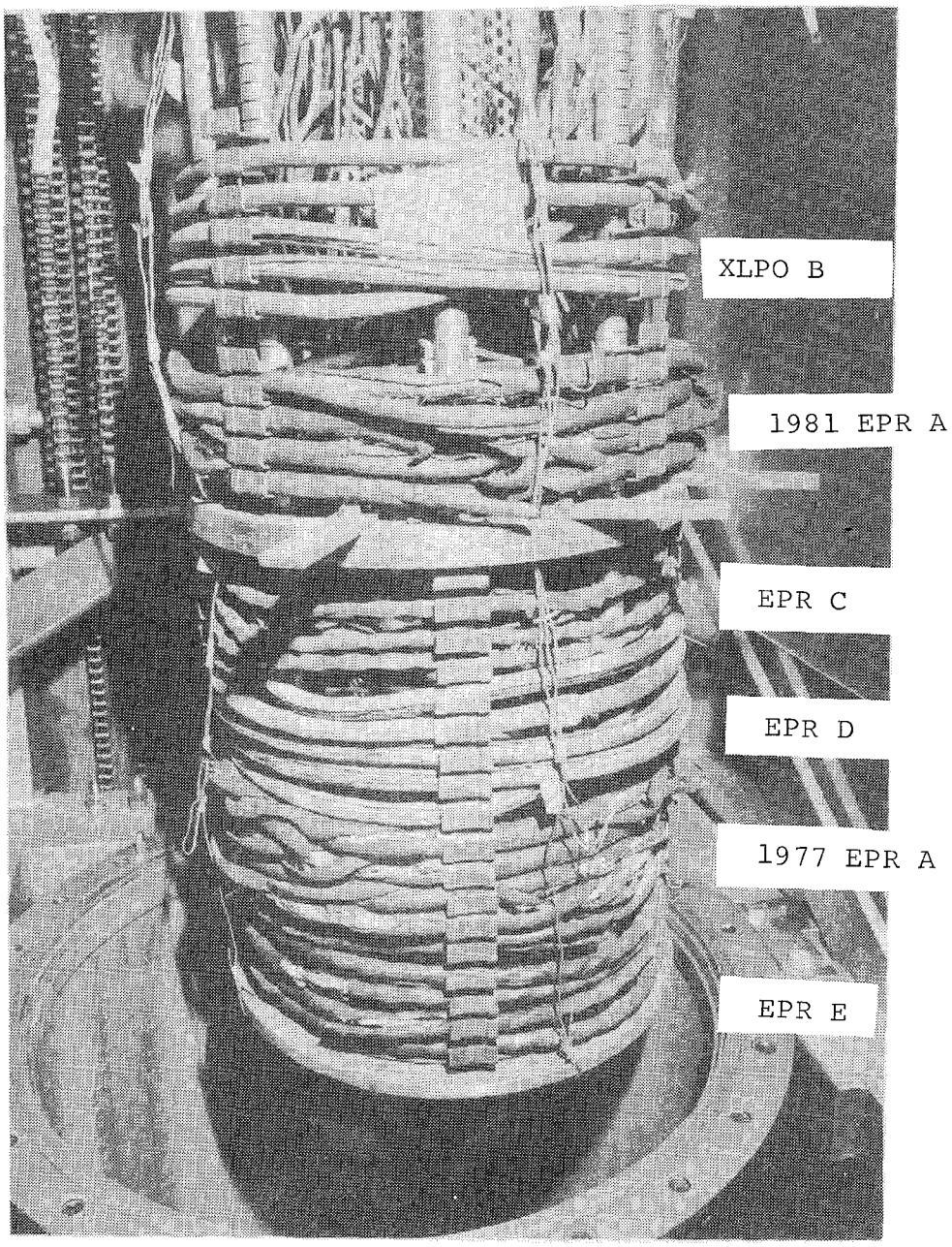

Figure C.2. Jacket Visual Appearance at the Completion of Simultaneous Test #1

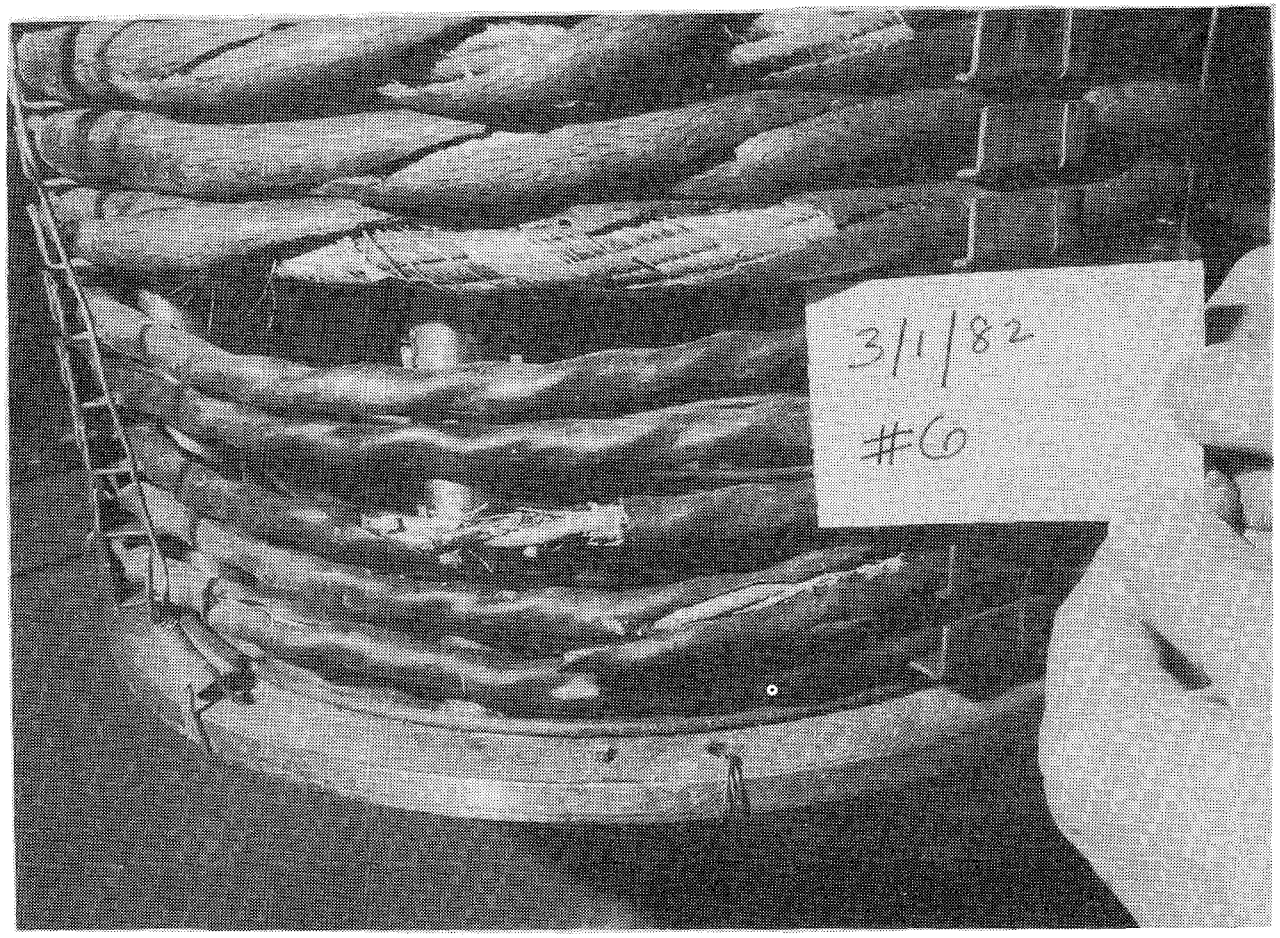

Figure C.3. CSPE Jacket Visual Appearance at the Completion of Simultaneous Test #1 for Two Different Manufacturer's Products

DISTRIBUTION:

U.S. NRC Distribution Contractor
7300 Pearl Street
Bethesda, MD 20014
375 copies for RV

Ansaldo Impianti
Centro Sperimentale del Boschetto
Corso F.M. Perrone, 118
16161 Genova
ITALY
Attn: C. Bozzolo

Ansaldo Impianti
Via Gabriele D'Annunzio, 113
16121 Genova
ITALY
Attn: S. Grifoni

ASEA-ATOM
Department KRD
Box 53
S-721 04
Vasteras
SWEDEN
Attn: A. Kjellberg

ASEA-ATOM
Department TQD
Box 53
S-721 04
Vasteras
SWEDEN
Attn: T. Granberg

ASEA KABEL AB
P.O. Box 42 108
S-126 12
Stockholm
SWEDEN
Attn: B. Dellby

Atomic Energy of Canada, Ltd.
Chalk River Nuclear Laboratories
Chalk River, Ontario K0J 1J0
CANADA
Attn: G. F. Lynch

Atomic Energy of Canada, Ltd.
1600 Dorchester Boulevard West
Montreal, Quebec H3H 1P9
CANADA
Attn: S. Nish

Bhabha Atomic Research Centre
Health Physics Division
BARC
Bombay-85
INDIA
Attn: S. K. Mehta

British Nuclear Fuels Ltd.
Springfields Works
Salwick, Preston
Lancs
ENGLAND
Attn: W. G. Cunliff, Bldg 334

Brown Boveri Reaktor GMBH
Postfach 5143
D-6800 Mannheim 1
WEST GERMANY
Attn: R. Schemmel

Bundesanstalt fur Materialprufung
Unter den Eichen 87
D-1000 Berlin 45
WEST GERMANY
Attn: K. Wundrich

CEA/CEN-FAR
Departement de Surete Nucleaire
Service d'Analyse Fonctionnelle
B.P. 6
92260 Fontenay-aux-Roses
FRANCE
Attn: M. Le Meur
J. Henry

CERN
Laboratorie 1
CH-1211 Geneve 23
SWITZERLAND
Attn: H. Schonbacher

Canada Wire and Cable Limited
Power & Control Products Division
22 Commercial Road
Toronto, Ontario
CANADA M4G 1Z4
Attn: Z. S. Paniri

Commissariat a l'Energie Atomique
ORIS/LABRA
BP N° 21
91190 Gif-Sur-Yvette
FRANCE
Attn: G. Gaussens
J. Chenion
F. Carlin

Commissariat a l'Energie Atomique
CEN Cadarche DRE/STRE
BP N° 1
13115 Saint Paul Lez Durance
FRANCE
Attn: J. Campan

Conductores Monterrey, S. A.
P.O. Box 2039
Monterrey, N. L.
MEXICO
Attn: P. G. Murga

Electricite de France
Direction des Etudes et Recherches
1, Avenue du General de Gaulle
92141 CLAMART CEDEX
FRANCE
Attn: J. Roubault
L. Deschamps

Electricite de France
Direction des Etudes et Recherches
Les Renardieres
Boite Postale n° 1
77250 MORET SUR LORING
FRANCE
Attn: Ph. Roussarie
V. Deglon
J. Ribot

EURATOM
Commission of European Communities
C.E.C. J.R.C.
21020 Ispra (Varese)
ITALY
Attn: G. Mancini

FRAMATOME
Tour Fiat - Cedex 16
92084 Paris La Defense
FRANCE
Attn: G. Chauvin
E. Raimondo

Furukawa Electric Co., Ltd.
Hiratsuka Wire Works
1-9 Higashi Yawata - 5 Chome
Hiratsuka, Kanagawa Pref
JAPAN 254
Attn: E. Oda

Gesellschaft fur Reaktorsicherheit
(GRS) mbH
Glockengasse 2
D-5000 Koln 1
WEST GERMANY
Attn: Library

Health & Safety Executive
Thames House North
Milbank
London SW1P 4QJ
ENGLAND
Attn: W. W. Ascroft-Hutton

ITT Cannon Electric Canada
Four Cannon Court
Whitby, Ontario L1N 5V8
CANADA
Attn: B. D. Vallillee

Imatran Voima Oy
Electrotechn. Department
P.O. Box 138
SF-00101 Helsinki 10
FINLAND
Attn: B. Regnell
K. Koskinen

Institute of Radiation Protection
Department of Reactor Safety
P.O. Box 268
00101 Helsinki 10
FINLAND
Attn: L. Reiman

Instituto de Desarrollo y Diseno
Ingar - Santa Fe
Avellaneda 3657
C.C. 34B
3000 Santa Fe
REPUBLICA ARGENTINA
Attn: N. Labath

Japan Atomic Energy Research Institute
Takasaki Radiation Chemistry
Research Establishment
Watanuki-machi
Takasaki, Gunma-ken
JAPAN
Attn: N. Tamura
K. Yoshida

Japan Atomic Energy Research Institute
Tokai-Mura
Naka-Gun
Ibaraki-Ken
319-11
JAPAN
Attn: Y. Koizumi

Japan Atomic Energy Research Institute
Osaka Laboratory for Radiation Chemistry
25-1 Mii-Minami machi,
Neyagawa-shi
Osaka 572
JAPAN
Attn: Y. Nakase

Kraftwerk Union AG
Department R361
Hammerbacherstrasse 12 + 14
D-8524 Erlangen
WEST GERMANY
Attn: I. Terry

Kraftwerk Union AG
Section R541
Postfach: 1240
D-8757 Karlstein
WEST GERMANY
Attn: W. Siegler

Kraftwerk Union AG
Hammerbacherstrasse 12 + 14
Postfach: 3220
D-8520 Erlangen
WEST GERMANY
Attn: W. Morell

Motor Columbus
Parkstrasse 27
CH-5401
Baden
SWITZERLAND
Attn: H. Fuchs

NOK AG Baden
Beznau Nuclear Power Plant
CH-5312 Doettingen
SWITZERLAND
Attn: O. Tatti

Norsk Kabelfabrik
3000 Drammen
NORWAY
Attn: C. T. Jacobsen

Nuclear Power Engineering Test Center
6-2, Toranomon, 3-Chome
Minato-ku
No. 2 Akiyana Building
Tokyo 105
JAPAN
Attn: S. Maeda

Ontario Hydro
700 University Avenue
Toronto, Ontario M5G 1X6
CANADA
Attn: R. Wong
B. Kukreti

Oy Stromberg Ab
Helsinki Works
Box 118
FI-00101 Helsinki 10
FINLAND
Attn: P. Paloniemi

Rheinisch-Westfallscher
Technischer Uberwachunge-Vereln e.V.
Postfach 10 32 61
D-4300 Essen 1
WEST GERMANY
Attn: R. Sartori

Sydkraft
Southern Sweden Power Supply
21701 Malmo
SWEDEN
Attn: O. Grondalen

UKAEA
Materials Development Division
Building 47
AERE Harwell
OXON OX11 ORA
ENGLAND
Attn: D. C. Phillips

United Kingdom Atomic Energy Authority
Safety & Reliability Directorate
Wigshaw Lane
Culcheth
Warrington WA3 4NE
ENGLAND
Attn: M. A H. G. Alderson

Waseda University
Department of Electrical Engineering
4-1 Ohkubo-3, Shinjuku-ku
Tokyo
JAPAN
Attn: K. Yahagi

1100	F. L. Vook
1120	J. B. Gerardo
1124	A. Owyoung/A. V. Smith
1200	G. Yonas
1234	J. Chang/G. J. Lockwood
1800	R. L. Schwoebel
1810	R. G. Kepler
1811	L. A. Harrah
1811	R. L. Clough
1813	J. G. Curro
1813	K. T. Gillen
1815	R. T. Johnson
2155	J. E. Gover
2155	O. M. Stuetzer
2341	M. B. Murphy
5200	W. C. Myre
6200	V. L. Dugan
6300	R. W. Lynch
6336	D. McKeon
6400	A. W. Snyder
6410	A. W. Snyder, Acting
6420	J. V. Walker
6440	D. A. Dahlgren
6441	M. Berman
6442	W. A. Von Riesemann
6443	D. D. Carlson
6444	S. L. Thompson
6445	B. E. Bader
6445	L. D. Bustard (3)
6445	C. M. Craft
6445	E. A. Salazar
6446	L. L. Bonzon
6446	W. H. Buckalew
6446	J. W. Grossman
6446	D. B. Hente
6446	F. V. Thome
6446	F. J. Wyant
6447	D. L. Berry
6450	J. A. Reuscher
6450A	J. Bryson
6452	M. Aker/J. S. Philbin
8214	M. A. Pound
3141	L. J. Erickson (5)
3151	W. L. Garner